



Argonne National Laboratory

TECHNICAL REVIEW OF ZPR-1 ACCIDENTAL TRANSIENT— THE POWER EXCURSION, EXPOSURES, AND CLINICAL DATA

by

R. O. Brittan, R. J. Hasterlik,
L. D. Marinelli and F. W. Thalgott



manier to an un-



UNCLASSIFIED



ANL-4971

Reactors-Research and Power

This document consists of 143 page

No. 36 of 143 copies. Series A.

ARGONNE NATIONAL LABORATORY
P. O. Box 299
Lemont, Illinois

TECHNICAL REVIEW OF ZPR-I ACCIDENTAL TRANSIENT --
THE POWER EXCURSION, EXPOSURES, AND CLINICAL DATA

by

R. O. Brittan, R. J. Hasterlik,
L. D. Marinelli and F. W. Thalgott

Classification changed to UNCLASSIFIED
by authority of the U. S. Atomic Energy Commission,

Per ACR-220-1199 6/30/5

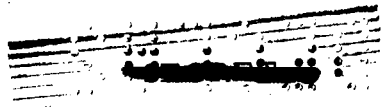
By REPORT LIBRARY M. Placke 5/18/5

January 26, 1953

Operated by The University of Chicago

under

Contract, W-31-109-eng-38



UNCLASSIFIED

ANL-4971

Reactors-Research and Power

<u>Distribution</u>	<u>Copy No.</u>
Argonne National Laboratory	1- 35
Armed Forces Special Weapons Project (Sandia)	36
Atomic Energy Commission, Washington	37- 41
Battelle Memorial Institute	42
Brookhaven National Laboratory	43- 45
Bureau of Ships	46
California Research and Development Company	47- 48
Carbide and Carbon Chemicals Company (ORNL)	49- 60
Carbide and Carbon Chemicals Company (Y-12 Plant)	61- 66
Chicago Patent Group	67
Chief of Naval Research	68
Department of the Navy - Op 36	69
du Pont Company	70- 74
General Electric Company (ANPP)	75- 77
General Electric Company, Richland	78- 81
Hanford Operations Office	82
Idaho Operations Office	83- 89
Iowa State College	90
Knolls Atomic Power Laboratory	91- 94
Los Alamos Scientific Laboratory	95- 96
Massachusetts Institute of Technology (Kaufmann)	97
Mound Laboratory	98-100
National Advisory Committee for Aeronautics, Cleveland	101
National Advisory Committee for Aeronautics, Washington	102
New York Operations Office	103-104
North American Aviation, Inc.	105-106
Nuclear Development Associates, Inc.	107
Patent Branch, Washington	108
RAND Corporation	109
San Francisco Operations Office	110
Savannah River Operations Office, Augusta	111
Savannah River Operations Office, Wilmington	112
University of California Radiation Laboratory	113-114
Vitro Corporation of America	115
Walter Kidde Nuclear Laboratories, Inc.	116
Westinghouse Electric Corporation	117-120
Wright Air Development Center	121-128
Technical Information Service, Oak Ridge	129-143
TOTAL	143

TABLE OF CONTENTS

	Page
INTRODUCTION.	7
SECTION I - R. O. Brittan	9
DESCRIPTION OF INCIDENT	11
THE EXCURSION	22
SUMMARY OF UPPER LIMIT OF DOSES	28
MEASUREMENTS WITH THE ACCIDENT CORE	29
ASSEMBLY AREA - CORE IN PLACE	30
FUEL ELEMENTS	32
Examination of Fuel Elements	35
Residual activity of Fuel Elements	44
Fission Product Analyses	44
CONTROL RODS	49
MEASUREMENTS WITH RECONSTRUCTED CORE.	49
ROD CALIBRATIONS	49
POWER LEVEL	52
FAST NEUTRONS.	52
THERMAL NEUTRONS	56
PROMPT GAMMAS.	56
DECAY GAMMAS.	56
CALIBRATION OF P-V GAMMA MONITOR.	56
GAMMA FLUX FIELD.	61
WATER DUMP	62

TABLE OF CONTENTS

	Page
SECTION II - F. W. Thalgott	65
SOME PHYSICS CONSIDERATIONS	
CONDITIONS PRIOR TO EXCURSION.	67
REACTIVITY AND REACTOR PERIOD.	67
TOTAL ENERGY GENERATED.	69
FISSION PRODUCT ANALYSIS	72
CONTROL ROD RUBBING SHOE ACTIVATION ANALYSIS .	72
RESIDUAL GAMMA ACTIVITY ANALYSIS	73
SUMMARY - TOTAL ENERGY	75
MECHANISM OF REACTOR SHUTDOWN	76
DURATION OF BURST	84
DELAYED NEUTRON ESTIMATES	84
SECTION III - L. D. Marinelli	91
ESTIMATE OF THE RADIATION EXPOSURES	
MEASUREMENT OF GAMMA RADIATION INCIDENT UPON THE FILM BADGES	93
ESTIMATE OF THE GAMMA RAY EXPOSURE IN ROENTGENS	94
ENERGY RELEASE COMPARISONS.	102
THE NEUTRON DOSE	104
PROMPT FAST NEUTRON DOSE ESTIMATES.	104
DELAYED NEUTRON DOSE.	106
THERMAL NEUTRON DOSE.	107
DISCUSSION	107

TABLE OF CONTENTS

	Page
SECTION IV - R. J. Hasterlik, M.D.	109
CLINICAL REPORT	
CASE HISTORIES	112
LABORATORY DATA	114
HEMATOLOGICAL STUDIES	115
BONE MARROW BIOPSIES.	124
AMINO ACID EXCRETION.	124
OPHTHALMOSCOPY.	126
PSYCHOMETRIC STUDIES.	126
SEMEN STUDIES	126
SUMMARY AND CONCLUSIONS	126
APPENDICES	129
A. FUEL COMPONENT DESCRIPTION.	131
B. RADIOACTIVITY MEASUREMENTS ON WHOLE BLOOD.	135
C. IN VIVO MEASUREMENTS OF GAMMA RAY ACTIVITY	137
D. FILM BADGE DOSES	139
REFERENCES	142

TECHNICAL REVIEW OF ZPR-I ACCIDENTAL TRANSIENT -- THE POWER EXCURSION, EXPOSURES, AND CLINICAL DATA

by

R. O. Brittan, R. J. Hasterlik,
L. D. Marinelli and F. W. Thalgott

INTRODUCTION

On June 2, 1952, 15:52 hours, a large reactivity change was made manually in a ZPR-I assembly causing a power excursion of about one kwh, which resulted in damage to the reactor core components and radiation exposure of some of the operating personnel to perhaps several hundred rep.

None of the contributing causes is reviewed here nor are the measures which were taken to reduce the probability of a recurrence discussed since these are considered administrative matters beyond the scope of this technical report. It is intended only to describe the incident, estimate the exposures, and present available clinical data.

In Section I, prepared by R. O. Brittan, appears a general account of the incident, leading chronologically from the experiment in progress through the cleanup and restoration of the reactor. This is followed by a detailed description of the power excursion, the shutdown mechanism, and a summary estimate of the upper limits of exposures. Finally, the pertinent measurements are presented, first those made with the accident core and its components and, subsequently, those made with the reconstructed core. Section II has been prepared by F. W. Thalgott to present calculations and considerations which lead to the energy estimates and support the contended shutdown mechanism. In addition, the analyses used to fill some gaps in the experimental estimates of the space-time variation of the radiation fields are presented. The radiation exposure doses are estimated in Section III by L. D. Marinelli. Doses from prompt and delayed neutrons and prompt and decay gammas are covered. Section IV, prepared by Dr. R. J. Hasterlik, is a clinical report on the four persons exposed. The exposed individuals are identified throughout by the names Art, Bill, Carl, and Don in decreasing order of relative exposures.

SECTION I

R. O. Brittan

DESCRIPTION OF THE INCIDENT

THE EXCURSION

SUMMARY OF UPPER LIMITS OF DOSES

MEASUREMENTS WITH ACCIDENT CORE

MEASUREMENTS WITH RECONSTRUCTED CORE

SECTION I

R. O. Brittan

In this section and generally throughout the report, zero time is taken to be the time at the end of the burst (15:52:00, 6/2/52) and will be noted by t_0 . Space coordinates are rectangular with the origin on the core centerline in the core midplane (z positive upward, x positive East, y positive North). In some instances, cylindrical coordinates having the same origin are used (θ positive from the $+x$ - to the $+y$ -axis, z positive upward). For convenience, the origin of coordinates is sometimes translated vertically to the core bottom or top. General orientation is afforded by the layout showing the significant section of Bldg. 316 (Figure 1). For background data on ZPR-I design and experiments, the reader is referred to reports ANL-4684¹ and ANL-4770.²

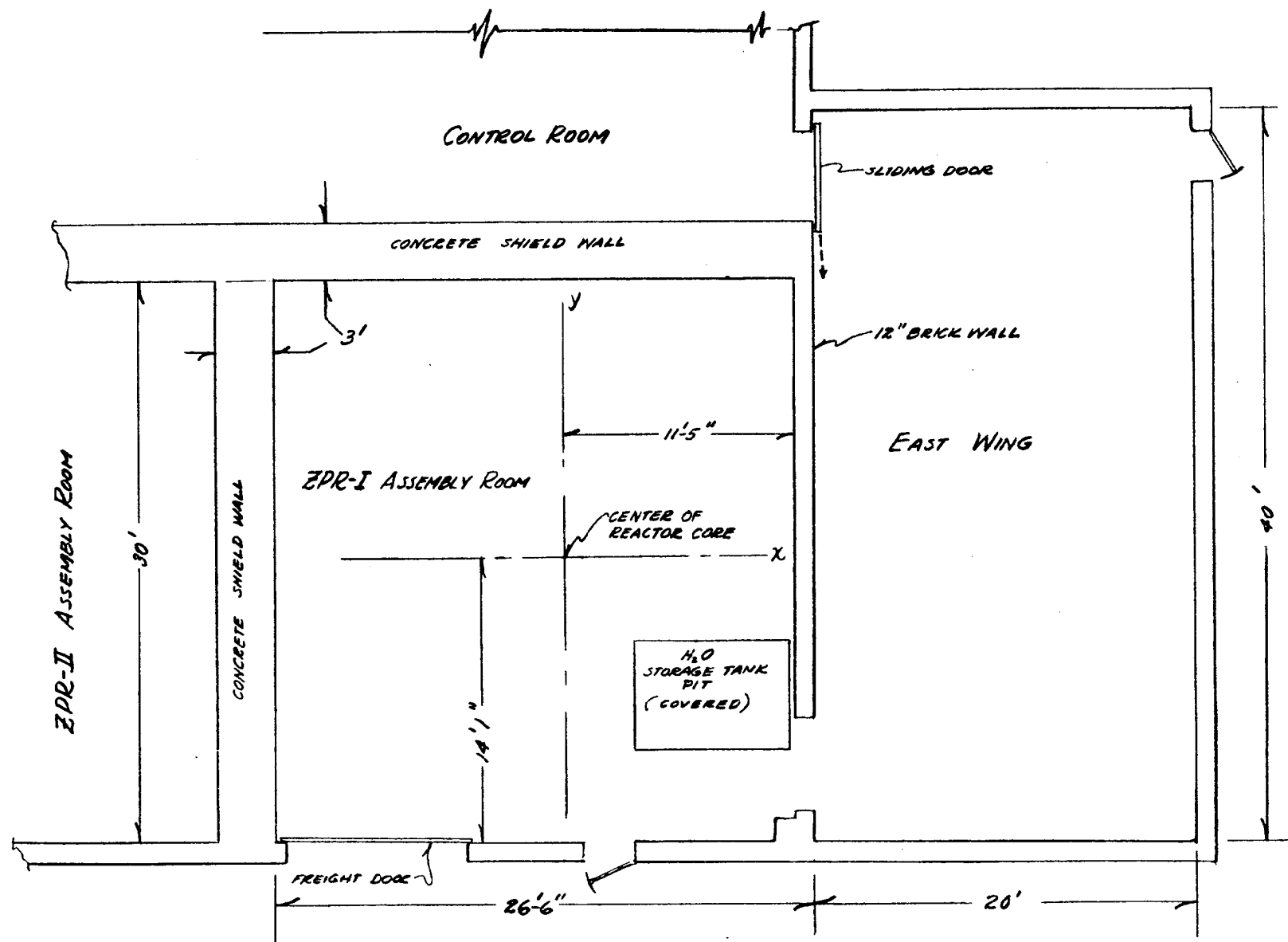
The accounts in this section are supported directly or indirectly by the work in Sections II and III and in the Appendices. The measurements made with the accident core or its components and with the reconstructed reactor have been collected and presented here as a source to be drawn on by the authors of subsequent sections.

DESCRIPTION OF THE INCIDENT

This description first presents some information on the experiments being run, then leads into an account of the experimental procedures leading up to the accidental burst, the phenomena observed during the burst, and the actions of the experimental crew. There follows information on the emergency procedures, the cleanup, and the restoration.

The experiment in progress consisted of an attempt to compare the reactivity of the 3" cross control rod used in ZPR-I experiments with 3" cross regulating rods fabricated for use in the Mark I core of STR. The information was to be used in relating experimental data previously obtained to conditions as they would exist in the actual reactor. This would, incidentally, constitute an absorption proof test of STR rods. Previous calibrations of 3" cross rods in ZPR-I could not be used because the core composition had just been altered.*

*Much of the previous information relating to the 3" cross rod was obtained from a core having 50% zirconium by volume and a U^{235} concentration of 0.0318 g/cc. Only as recently as six weeks before the incident the fuel elements had all been converted to contain 20% more zirconium by addition of one standard size zirconium plate to each. The zirconium had thereby been increased to 60% by volume and the space available for the light water moderator correspondingly reduced. Experi-



ORIENTATION PLAN
FIG. 1

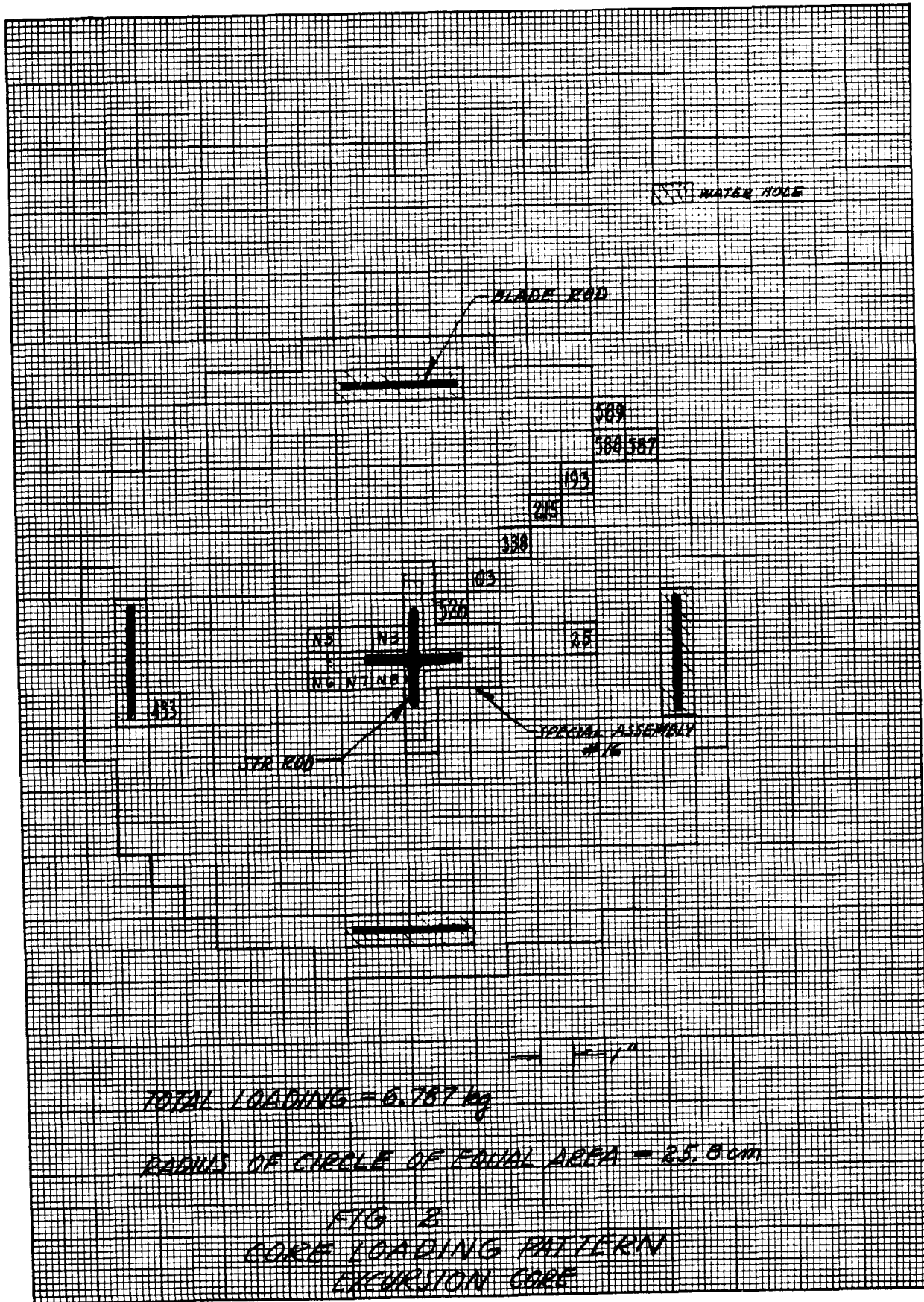
A cylindrical core approximating a circular cross section was assembled with four blade type rods acting as safeties near the periphery and the ZPR-I 3" cross rod at the center. The core components are described in detail in Appendix A. The loading requirements of 5261 grams were estimated on the basis of earlier experiments. A criticality check was started at about $t = -5.5$ hours to determine whether an adequate core had been assembled. By $t = -5$ hours the reaction was made self-sustaining with all four blade safety rods withdrawn from the core and the central ZPR 3" cross rod withdrawn to a height of 74.1 cm (origin at bottom of active core, which is 109.2 cm high). Since it was desired to compare ZPR and STR rods at other lower positions, additional fuel was needed to maintain criticality with the central rod inserted as low as $z = 20$ cm. Estimates of requirements led to the addition of 1526 grams bringing the total to 6787 grams of U^{235} . The core then consisted of 324 standard fuel elements, the special elements associated with cross-control rod assembly type #7M, the control and safety rods and guide tubes, and the dummy elements in the reflector region used to fill the area between the clamps and the core element end caps. The core loading diagram is shown in Figure 2.

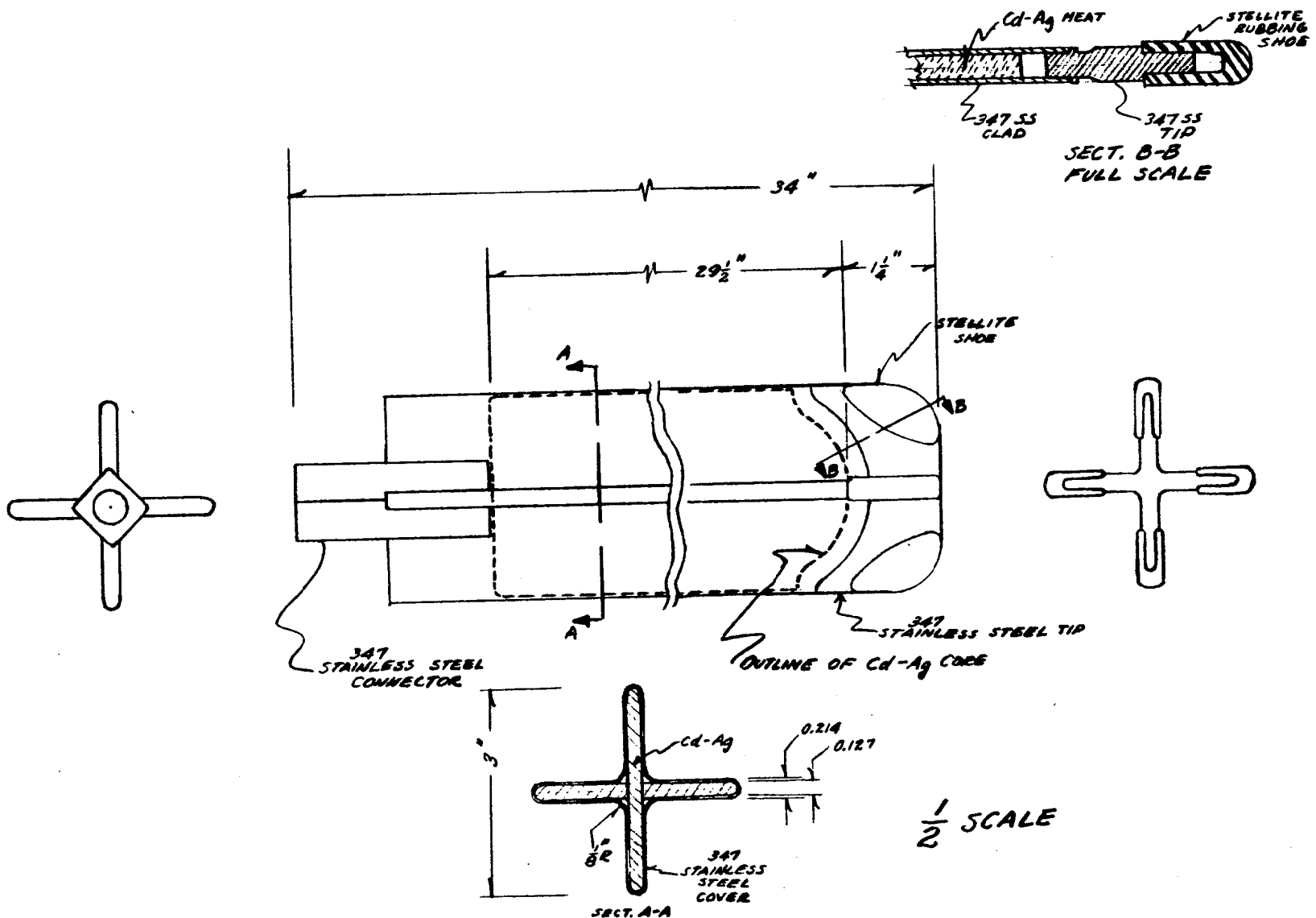
A second criticality check was made, this time with the ZPR cross rod withdrawn to 20 cm. At critical, one of the blade safety rods had to be fully inserted, one inserted to 48 cm, the other two remaining fully withdrawn. Since these blade rods were thought to be worth about 400 inhours apiece, a margin of about 1000 inhours of safeties remained.

Following this check, the ZPR cross rod was replaced with the STR 3" cross rod shown in Figure 3. The rod was clamped in position (not attached to the drive as the ZPR rod was) by the use of triangular wood filler blocks and C-clamps, using the rod guide tube for support. The active tip of the rod was 49.2 cm above the core bottom. At $t = -0.5$ hours the criticality check for this configuration was started. At about $t = -0.1$ hour the position of the safety rods for criticality had been determined to be three blades fully inserted and one blade inserted to 32.5 cm above the core bottom.

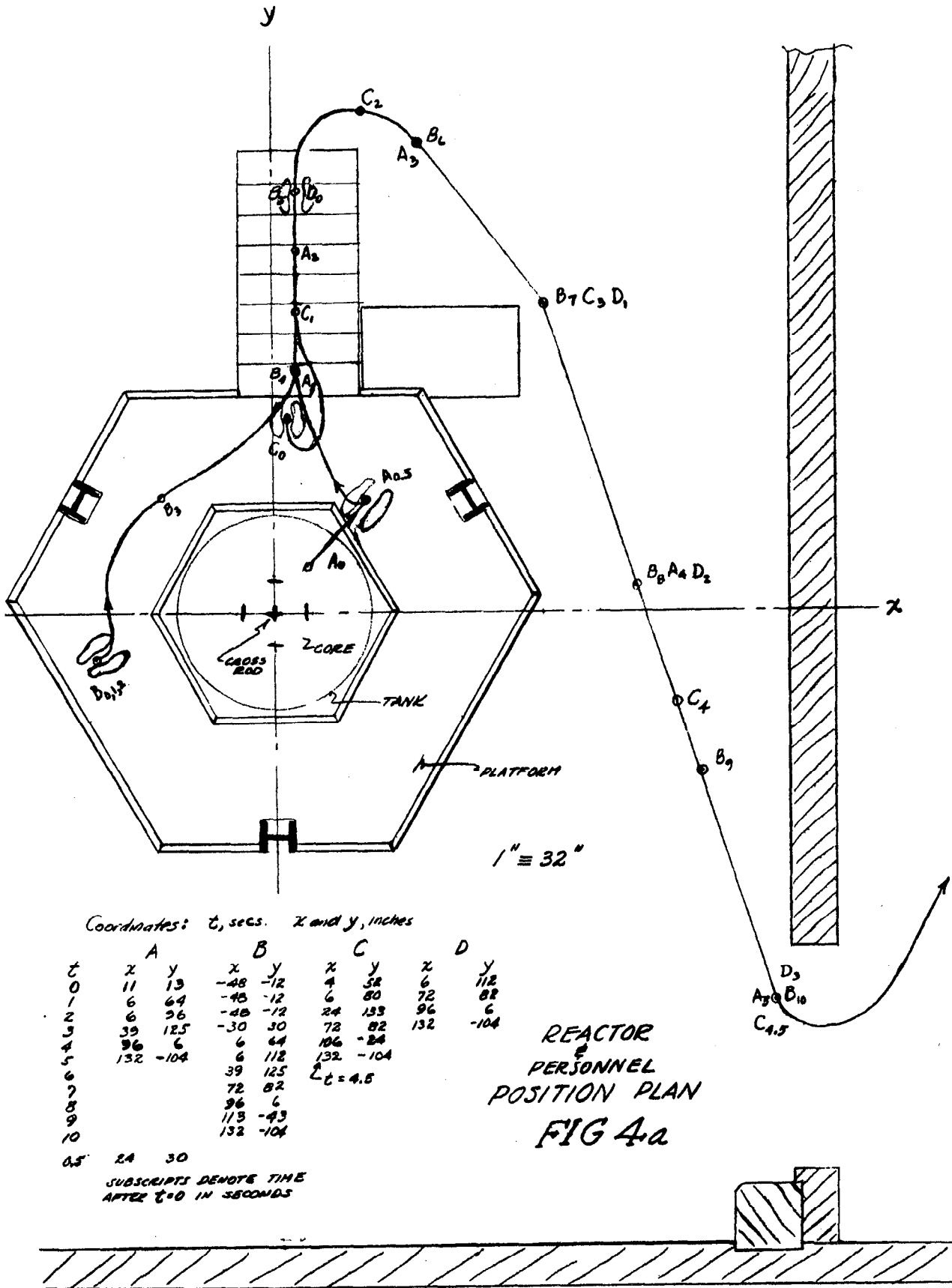
The withdrawn blade rod was inserted to make the assembly subcritical and, with the water still in the reactor tank, the assembly room was entered by Art, Bill, Carl, and Don. With Art, Bill, and Carl on the platform surrounding the reactor tank, and Don on the steps leading up to the platform at the positions indicated by $A_{0.5}$, B_0 , C_0 , and D_0 in Figures 4a and 4b, Art leaned over the assembly, unclamped the central rod, and began to withdraw it.

ments with the new Zr:H₂O ratio showed that cores built with it were less reactive than cores of the same size having the lower Zr:H₂O ratio. Thus, additions or subtractions of fuel elements, and motions of poisons in the core result in smaller reactivity changes than could have been expected in earlier experiments with lower Zr:H₂O ratio.





STR 3-INCH CROSS REGULATING ROD
 FIG. 3



Coordinates: t , secs. x and y , inches

t	A		B		C		D	
	x	y	x	y	x	y	x	y
0	11	13	-48	-12	4	52	6	112
1	6	64	-45	-12	6	80	72	82
2	6	26	-48	-12	24	133	96	6
3	39	12.5	-30	30	72	82	132	-104
4	96	6	6	64	106	-24		
5	132	-104	6	112	132	-104		
6			39	125	$t = 4.5$			
7			72	82				
8			96	6				
9			113	-43				
10			132	-104				
0.5	24	30						

SUBSCRIPTS DENOTE TIME
AFTER $t=0$ IN SECONDS

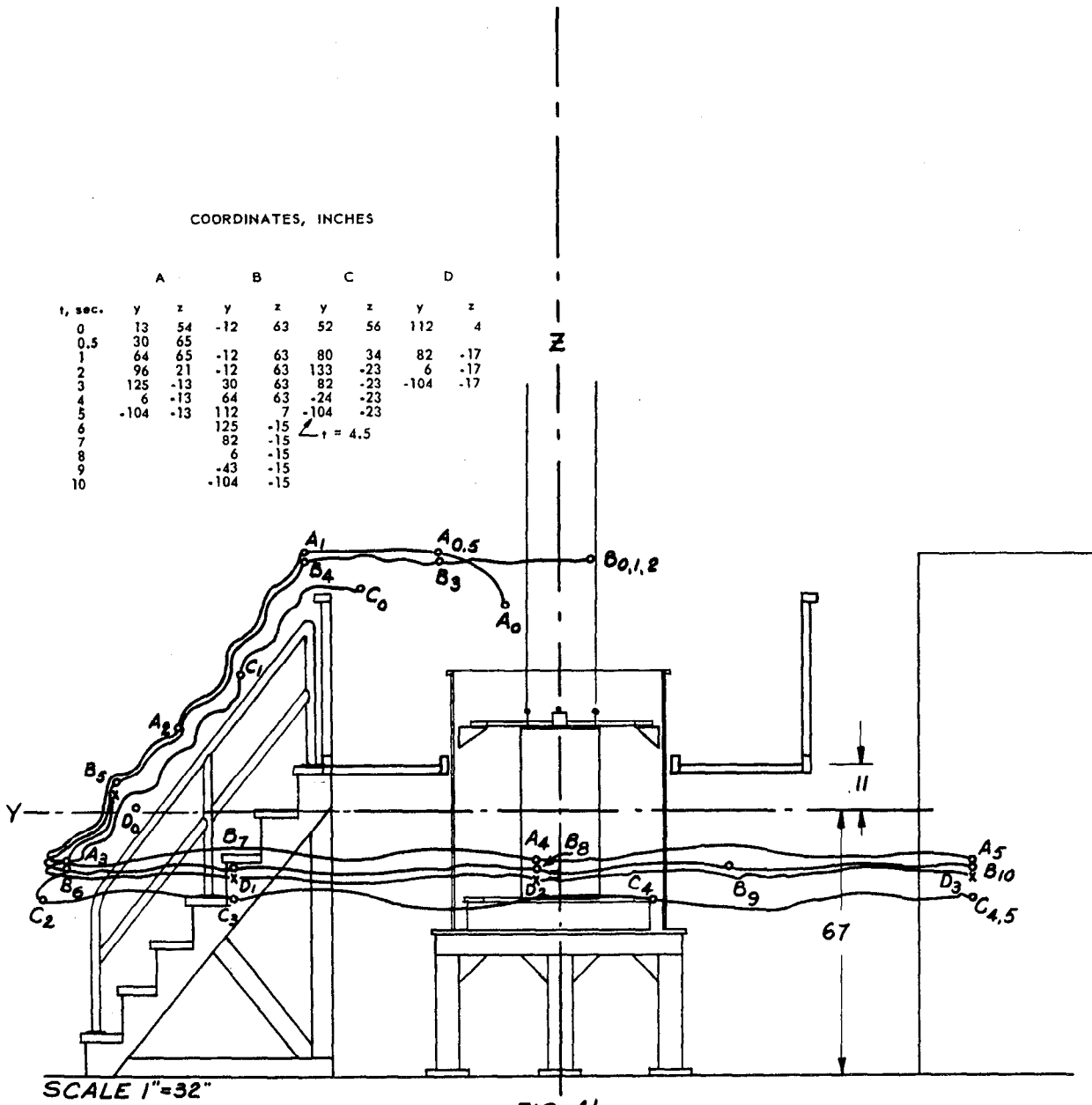


FIG. 4b
 REACTOR & PERSONNEL POSITION
 ELEVATION

By the time the rod had been withdrawn about a foot, a dull thud characterized as an underwater shock was heard and a blue light emanation persisting for a fraction of a second was observed from the top. At the same time the upper clamped surface formed by dummy element end caps buckled, allowing outward lateral displacements of the tops of the core elements. The water displaced from the core rose suddenly, as a bubble, with some gas evolution to a height of about 20 cm before spreading to the sides of the tank. Probably a few hundred milliseconds after sensory perception, Art dropped the cross rod back down its guide tube into the core, straightened up, then followed Carl and Don rapidly out of the assembly room. Bill followed at a more leisurely pace. The paths are shown in Figures 4a and 4b, times being denoted by subscripts are in seconds after $t = 0$.

The water dump valve had been opened by one of the instrument trip circuits very shortly after the burst, and the water began to leave the tank, exposing the core. Just as Art left the assembly room he observed the tank to be half full. Bill observed the water to be at the bottom of the core from the same vantage point. After leaving the assembly room, the group were shielded by the 12" brick wall separating the East wing from the assembly room. On entering the control room from the wing, the group became shielded by the 3' concrete wall.

ZPR-II was in operation at the time and a scram was induced by the sudden increase in neutron and γ background. The two reactors are separate by a 3' concrete wall, with core centerlines about 25 feet apart. No useful data were obtained from ZPR-II chart records and it does not enter further in the analysis here.

Shortly after entering the control room, the sliding door between the control room and the East wing was closed, Health Physics and Medical staffs were notified, and monitoring and preliminary clinical examinations began. The forced ventilation of the assembly room ceased when the sliding door was closed.

Some immediate information regarding the assembly was available since three recording detectors were in operation at the time of the burst. Examination of the records indicated that indeed the reactor was not operating, and that the radioactivity of the exposed core was decaying in a reasonable manner. Attention was immediately directed to caring for the group involved and to monitoring the control room and other parts of the building. At about $t = 2$ hours, the exposed personnel were removed to Albert Merritt Billings Hospital.

An accumulation of fission products occurred in the control room air so that the room was evacuated at about $t = 1$ hour when the level was determined to be above tolerance. The fission products were entering through cracks around the sliding door. Transport by air was halted when the 7000 cf air make-up fan in the control room was turned on, raising the pressure above

that existing in the assembly area. The control room purging was begun by turning on the 2000 cfm exhaust fan in the vault work room. An external survey of the building at about $t = 1$ hour indicated γ activity of several roentgens per hour through the freight door in the South wall of the assembly area.

A plenum chamber containing CWS filters was constructed and installed in the assembly room exhaust system in the penthouse ahead of the blower by $t = 9$ hours. At this time, a predicted light rain began to fall, and purging of the assembly room air was begun by turning on the 5000 cfm exhaust blowers. Entry to the blower room and control room was made only by personnel equipped with assault masks and protective clothing.

Air samples taken through a hole cut in the freight door indicated that purging was adequate by $t = 13$ hours to allow entry with the precaution of wearing assault masks and protective clothing. Several γ measurements were made in the assembly room using Zeus survey meters. The steps to the platform were mounted and Zeus readings six inches above the core showed between one and two roentgens per hour of γ rays. The appearance of the core was as shown in the photographs, Figures 5a and 5b. The water deionizer was found to be still turned on, and water from the drum which was being filled had overflowed to the floor and out the back door or into the dump tank pit. The tap water source was shut off and the assembly area was evacuated until the next day.

Outside contamination was obscured by fallout of radioactive particles which resulted from a bomb test in Nevada earlier. The levels on the ground were not greater than elsewhere on the site or in the general Chicago area. Levels in the rest of the building were well below established tolerances. Checks on the other personnel in the building indicated that a few had picked up radioactive iodine which had deposited in the thyroid. This short-lived fission product rapidly decayed, so that no significant exposures were detectable a few hours later.

The next day (June 3) additional measurements of γ activity around the core were made to provide data for closer estimates of the magnitude of the burst and exposure, since first estimates indicated a possible exposure of several hundred roentgens, close to a possibly lethal dose, although the personnel involved showed none of the expected early symptoms. The γ activity of the core indicated that it must be removed before the area could be decontaminated because determination of degree of contamination would be obscured by the γ -flux field surrounding the core. Several of the fuel elements were removed for inspection, survey, and fission product analysis. However, the decay scheme indicated that it would be about $t = 100$ hours before the core removal could be accomplished without undue exposure. On the fifth day (June 6) the core elements were removed, placed in groups of four in capped iron pipes, and transported to vault storage to await future inspection and disposition. With the core gone, it was possible to survey the assembly room and East wing preparatory to cleanup.

Figure 5a

Core after Incident

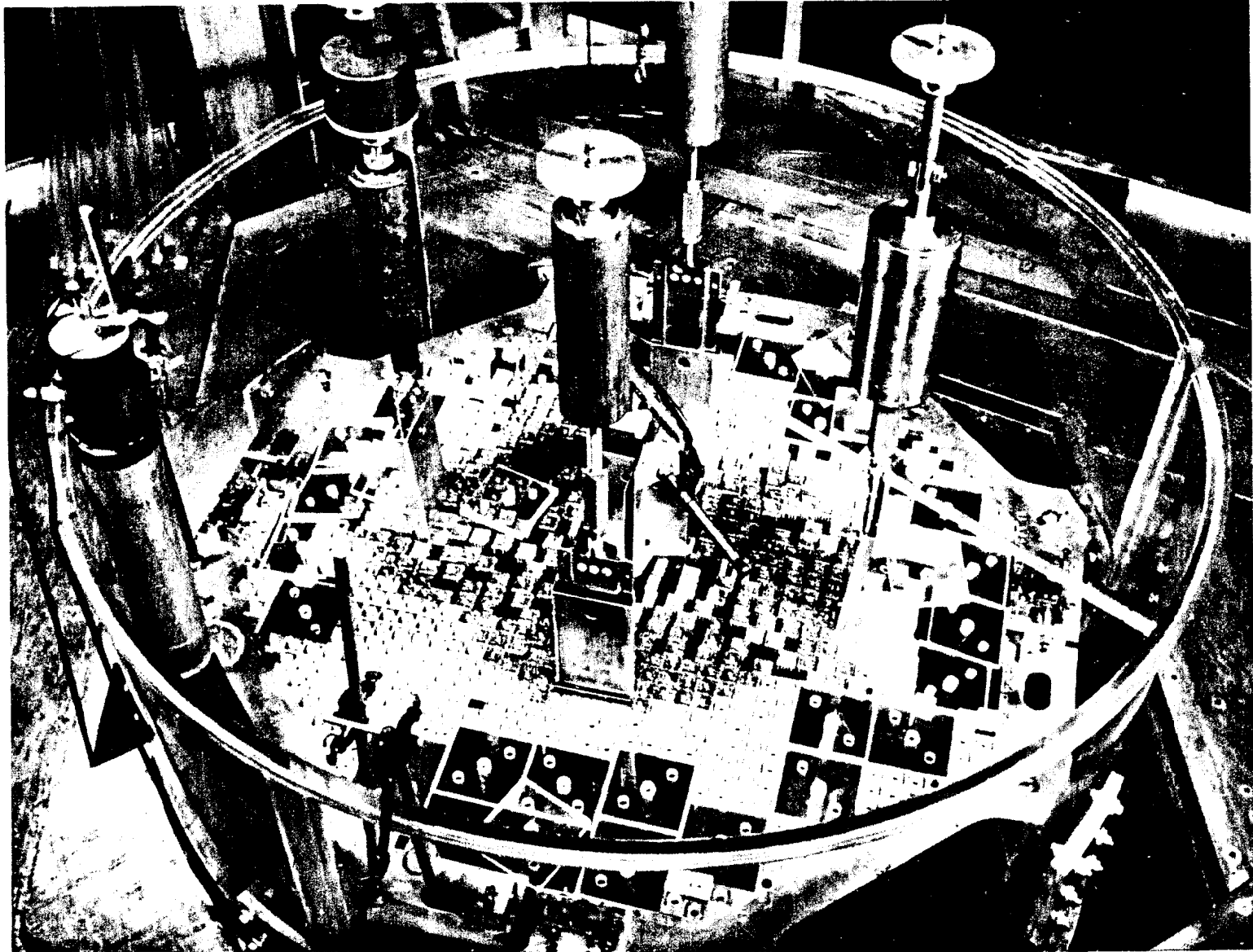
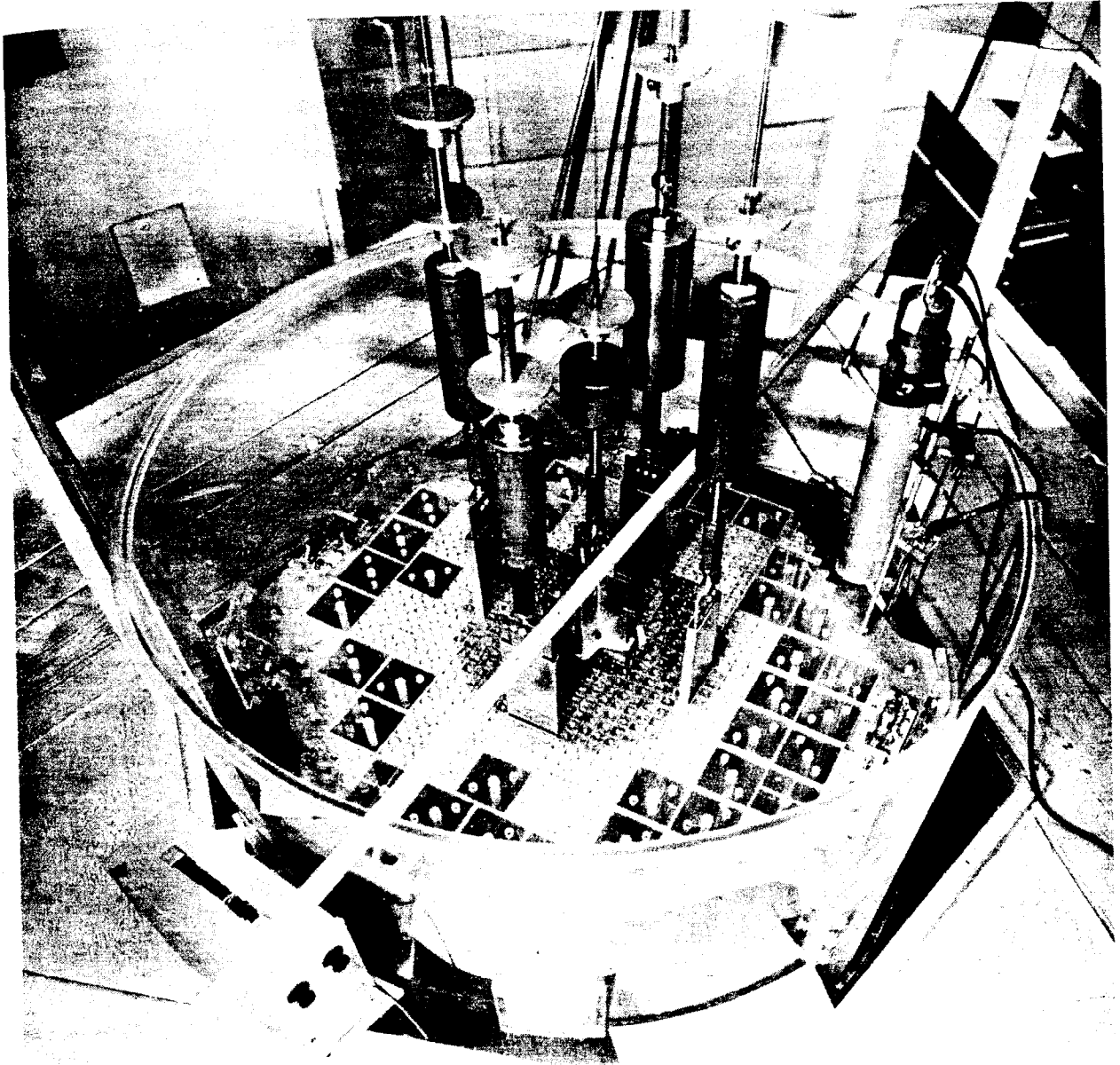


Figure 5b
Reconstructed Core



Cleanup to general background levels was accomplished during the five day interval beginning on the eighth day. The water which had been in the reactor tank was removed from the storage tank to a mobile retention tank, then transported to reclamation site. During its short contact with the core it had picked up some fission products and a small quantity of α emitters. If all the activity in the 700 gallons were attributed to U^{235} not more than 18 milligrams were present. Assays indicated that about 1/2% of the fission product activity was in the water. The water was retained for three months. By this time the activity had decayed enough to dump the water down the drain. Room contamination was due to fall out and deposition of fission products. Decontamination was effected by a single application of detergent and warm water everywhere in the Assembly Room and East wing.

Subsequently, the accident core was reconstructed (with modifications) and experiments were run to augment data for a detailed analysis of the incident.

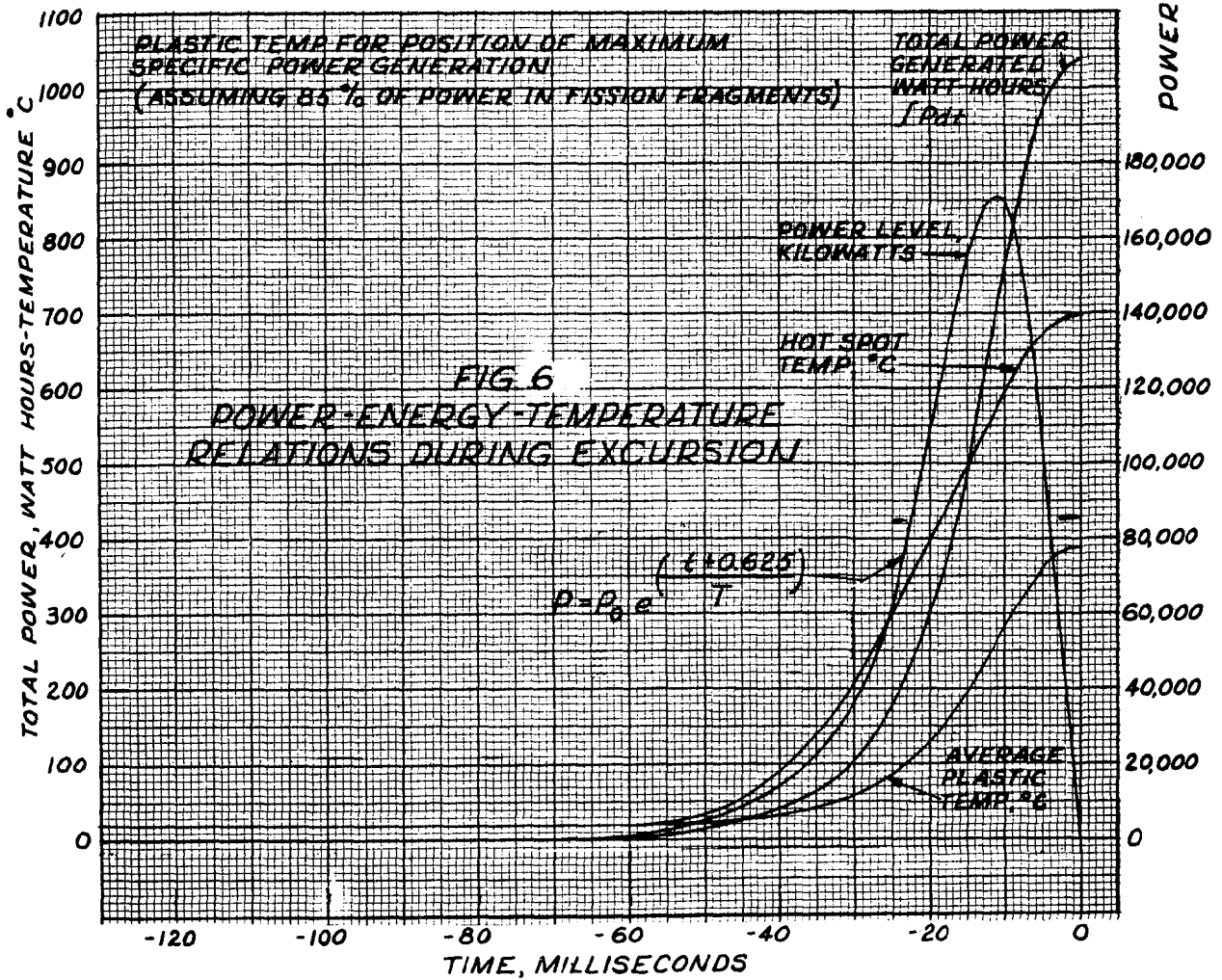
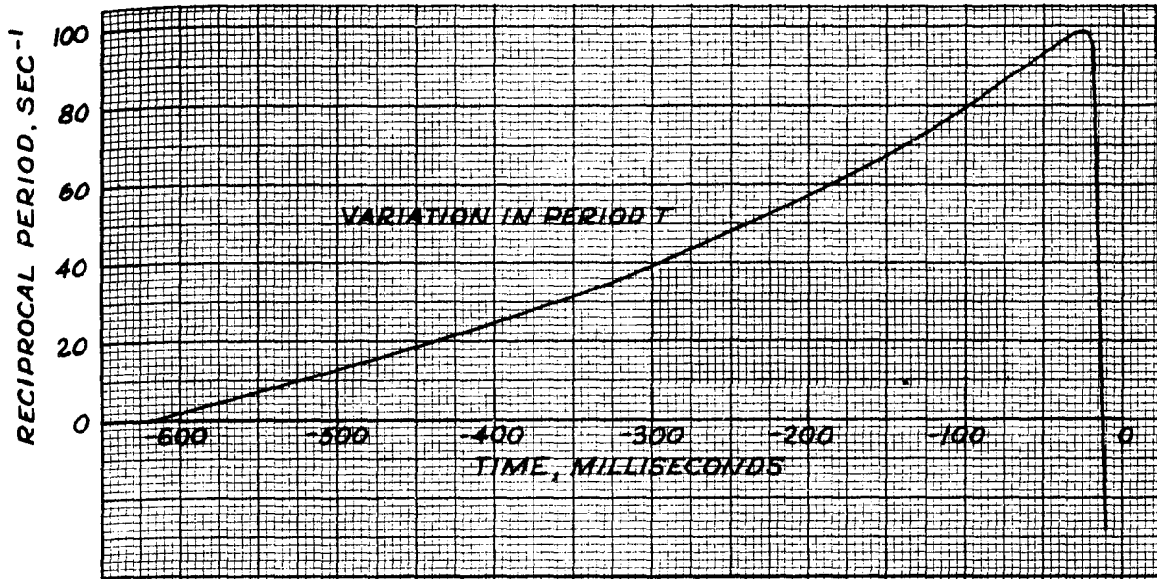
THE EXCURSION

The measurements and examinations made, along with calculations and estimates presented in some detail in Section II make it possible to reconstruct quite closely the physical processes in the core during and shortly after the excursion. The following discussion covers the power excursion, the shutdown mechanism, and the decay. A summary of some significant numbers is included.

The loading pattern of the core (Figure 2) shows the four blade safety rods which were fully inserted. With the cross rod in its clamped position the previous experiment established that the assembly could be made critical by withdrawing one safety rod 32.5 cm. Calibration of the safety rod in the reconstructed core indicated that the reactor was subcritical by 100 inhours (or 0.25 per cent $\delta k/k$) when withdrawal of the central 3 in. cross from its clamped position 49.2 cm above the core bottom began at $t = 700$ ms. By the time the central rod had been withdrawn only a few cm then, the assembly was critical and reactivity was being added at a decreasing rate assuming constant rod withdrawal speed. The variations of reactivity, power, and associated quantities with time are as represented in the following table. It is assumed that the reactor was initially at a power level corresponding to 1 fission per gram of U^{235} .

The position of rod at shutdown was determined by comparison of residual activity in the fuel elements of the accident core with the flux distribution of the reconstructed core and calculated flux distributions near the tip of a partially inserted rod. Estimated variation of total fission energy power level, and fuel strip temperatures is given in Figure 6.

4.8/200



TIME - REACTIVITY - POWER RELATIONS DURING EXCURSION

Time, t milli- seconds	Rod Position, z cm above core midplane	Total Reactivity Introduced by Rod		Rate of Reactivity Change in hours/sec	Total Fission Energy watt-hours	Power Level kw	
		in hours	% $\delta k/k$				
-700	-5.4	-100	-0.25	1350			rod starts out
-625	-2.6	0	0	1290			delayed critical
-545	0.4	100	0.25	1220			
-460	3.6	200	0.51	1140			
-370	7.0	300	0.76	1070			prompt critical
-280	10.4	394	1.00	990			
-165	14.6	500	1.27	890		0.05	normal operating power level
-70	18.2	580	1.48	810	2	680	total power significant
-25	19.9	620	1.57	770	175	61000	plastic at softening temperature
-10	20.4	630	1.60	760	260	165000	net reactivity reduced to zero
0	20.8	635	1.62	750	1040	0	power level zero (shutdown)

Prompt critical was reached at about $t = 370$ milliseconds and the flux had increased to normal operating levels by $t = -165$ milliseconds. The total power developed did not become significant until $t = -70$ milliseconds, by which time the flux was increasing with a period of $\sim 10^{-2}$ seconds, and the power level was several hundred kilowatts. By this time the plastic strip was beginning to heat sensibly in the region of maximum power generation. With all but $1/2\%$ of the oxide distributed in particles of 10 micron diameter or less, the plastic was heated in a uniform manner considering a piece of say one centimeter square, so that the over-all plastic temperature rose in proportion to the fission fragment fraction of total power generated, reaching about 25°C at $t = -45$ milliseconds, and the softening point (80°C) at about $t = -25$ milliseconds. Coincidentally, the large particles of about 40 micron diameter were heating up with a volume to surface ratio eight times that of the smaller particles on the average. The surface temperatures of the large particles then were much higher than for the small particles at the same time, resulting in hot spots or temperature perturbations in the plastic. By the time the general temperature of the plastic had reached 80°C , the softening point, the temperature of the plastic locally in the region of the large particles had reached temperatures of several hundred degrees and conditions existed for the start of bubble formation with the particles as nuclei.

As time went on, the average plastic temperature increased so that it had reached several hundred degrees by $t = -5$ milliseconds. The hotter the average temperature, the softer became the plastic, the hotter the region near large particles, and the more rapid the growth of bubbles.

These plastic vapor bubbles, whether vaporized polystyrene, vaporized monomer, or destructive distillation products, caused the plastic strip to grow in volume, effecting a decrease in density. Since this decrease was exponential, and since reactivity varies nearly as the square of the density, the positive reactivity introduced by the continuing rod withdrawal rapidly became very small in comparison to the negative reactivity caused by the density change. Since it only required a change in strip thickness of $1/2\%$ to reduce the reactivity by 1% , the reactor was made subcritical within a few milliseconds after bubble formation began, and rapidly became subcritical by many percent. It is estimated that by $t = -10$ milliseconds the reactor was subcritical and the power level began to drop. Thus by $t = 0$ there were relatively no fissions occurring and the reaction had stopped, except for delayed neutrons.

Even after the reaction had ceased the bubbles grew, displacing all the water and expanding the fuel elements laterally. The heat transfer to the water was negligible since the water was driven out very rapidly, and since the temperature at the interface even at $t = 0$ was only a few degrees above boiling. Thus expansion of the plastic due to bubble formation around large oxide particles being heated exponentially in a plastic field also being heated exponentially and displacement of water was the mechanism of shutdown. Since to the observer this shutdown was simultaneous with manifestations of the runaway, the dropping in of the cross rod by Art several hundred milliseconds later was of no importance. The fact that the water was permanently displaced by the foamed plastic giving an assembly with 75% voids would have prevented recurrence up to the time the water was dumped.

The plastic expansion took place essentially in the last 10 milliseconds, filling the space formerly occupied by the water and forcing zirconium strips laterally. The slap of zirconium strips from adjacent elements would account for most of the noise heard by the personnel. Bulging of the assemblies at their centers greatly increased the lateral loads at the clamping planes. The pressures developed and transmitted to the water which was being ejected augmented these. Since the upper clamping surface had no appreciable normal restraint it buckled, breaking some of the plastic tubes connecting the upper and lower caps and allowing the tops of the fuel elements to be displaced radially. Buckling of the surface and radial spreading of the core element tops provided a water escape route which allowed the water to slug upwards, producing the bubble.

Very little steam formation could have occurred by conduction of heat from the plastic. This is true first because the temperature at the fuel strip-water interface never got more than a few degrees above 100°C , second because the water was rapidly ejected and contact was lost. It is unlikely that more than a fraction of a liter was vaporized. Most of this would condense before escaping from the water, some of it would come off with the water bubble. The fact that the personnel were not contaminated makes it unlikely that significant amounts of vapor or splashed water left the tank. The total power generated would be enough to raise all the water in the tank about $1/4^{\circ}\text{C}$.

Of the total power generated (1040 watt hours) based on 190 Mev/fission only about 900 watt hours representing the energy in the fission fragments went to heating the strips, an additional 25 watt hours came off as prompt gammas. The remaining power excepting ~~neutrons~~ ^{neutrons} comes off after $t = 0$ as delayed neutrons, decay γ 's and β 's. Following a sudden burst of this nature where 90% of the fissions occur in 30 milliseconds before shutdown, it can be assumed with small error that all the delayed neutrons come off after $t = 0$ according to their regular decay scheme. With a total of 1.22×10^{17} fissions, 3×10^{17} neutrons will be produced of which 2.2×10^{15} neutrons are delayed. These appear after $t = 0$ according to their delay schemes, 25% coming off prior to $t = 1$ second, 50% prior to $t = 3$ seconds. Hence the delayed neutron production reduces from $4 \times 10^{14}/\text{sec}$ at $t = 1$ second to $10^{14}/\text{sec}$ at $t = 5$ seconds and to 4×10^{13} at $t = 10$ seconds. A fraction of these ($\sim 90\%$) leak out of the core. The fraction is estimated to be 2% for the top of the core and 86% for the sides. Before water dump those leaking out of the top are attenuated by a factor of 30 between core face and water surface. It takes about a second for the water level to reach the top of the core. Personnel seeing the core top receive the leakage delayed neutrons without attenuation other than geometrical after this. The water continues to drop, so that after 10 seconds the core is completely exposed and all the delayed neutrons leaking out are unattenuated by water.

By $t = 5$ minutes all the delayed neutrons but 0.1% have come off, and after this they need not be considered. The fission products have associated decay gammas and betas. The energy of these decay radiations falls off slowly right after fission, gradually decreasing at an increasing rate until

$t = 10$ seconds, when the decay rate becomes proportional to $t^{-1.21}$. This decay scheme is followed for about 75 hours, then gradually drops off so that the exponent of t changes to -1 by $t = 200$ hours. At this time the intensity is down by a factor of more than 10^6 over its value at $t = 0$.

Pertinent data relating to the excursion is presented in the table which follows.

SUMMARY TABLE OF EXCURSION

(Most Probable Values)

δ k/k subcritical at start	-0.25%
δ k/k added before shutdown	1.87%
δ k/k maximum	1.62%
δ k/k subcritical after shutdown	-46%
Shortest period	0.01 seconds
Maximum power level	165 megawatts
Total number of fissions	1.22×10^{17} fissions
Duration of burst $\sim 99\%$ of fissions occurred in	50 milliseconds
Total fission energy release (190 Mev/fission)	1040 watt-hours
Duration of excursion	700 milliseconds
Average temperature reached in plastic at position of peak flux	390°C
Mechanism of shutdown	Introduction of voids by bubble formation in plastic around large uranium oxide particles as nuclei
Prompt gamma burst	150r at water surface 8" above core
Fast neutron burst	39r at water surface 8" above core
Decay gamma intensity	200r/second at top of core one second after shutdown (water down)

SUMMARY OF UPPER LIMIT OF DOSES

A summary of exposures is included here for the convenience of the reader. Only the upper limits are given, and it should be pointed out that it is equally probable that the fast neutron contributions might be only 40% of those shown. If such were the case, some of the doses would be materially smaller. For example, those given for the eyes would be reduced by 30%

Some of the measurements of fast neutron doses are not in agreement. The various counters which must be biased to eliminate gammas seem to give consistent results among themselves which are several times higher than the results obtained by the use of NTA plates or by the subtraction method. This latter method uses differences between tissue-equivalent ionization chambers sensitive to both gammas and fast neutrons and gamma dosimeters which are insensitive to neutrons. The first scheme is said to have disadvantages, among them being the difficulty of determining whether adequate discrimination has been achieved. The second scheme has a disadvantage in this particular case of operating in a mixed fast neutron-gamma field where the relative gamma ionization is more than ten times greater than the fast neutron ionization, resulting in small differences between large numbers. These differences sometimes are smaller than the experimental error as was the case here. Rather than decide which measurements are correct, it seems that the best thing to do is include all the evidence and possible errors when estimating the upper limits. The average doses to the trunk are based on the dose at the badge position, where most of the measurements are taken. Doses at the eyes, at the groin, and at the feet may be inferred from the various surveys that were made. The following tabular summary then is that of the upper limits of dose at the various positions. The numbers represent rep (unidirectional in air), not badge rep, in the case of the components and rem in the case of the totals. Because of the difference in biological effectiveness of fast neutron type ionization and gamma induced ionization, the gammas and fast neutrons must be separated to determine the equivalent doses. After separation, a biological effectiveness factor must be applied to the fast neutron dose. This factor is assumed to be 3, generally, but in the case of cataract formation it is considered to be 10. Thermal neutron doses are not included since these were less than 1 rep

TABLE OF UPPER LIMITS OF FAST NEUTRON-GAMMA EXPOSURES
(Unidirectional in Air)^(a)

Badge Position (Av. for trunk)	prompt gammas rep	decay gammas rep	total gammas ^(b) rep	fast neutrons ^(c)		total neutrons ^(c)		total dose ^(e) rem
				prompt rep	delayed rep	rep	rem ^(d)	
Art	120	25	145	12.0	2.2	14.2	43	189
Bill	50	66	116	5.0	4.6	9.6	29	146
Carl	44	11	55	4.4	1.1	5.5	16	71
Don	1	9	10	0.6	0.2	0.8	2.4	12
Eyes								
Art			165			16.2	162	327
Bill			111			9.1	91	202
Carl			51			5.1	51	102
Don			11			0.8	8	19
Groin								
Art			154			13	39	193
Bill			163			19	57	220
Carl			77			10	30	107
Don			8			0.5	1.5	10
Feet								
Art			220			14	42	192
Bill			308			29	87	303
Carl			209			12	36	180
Don			4			0.2	1	3

(a) Gamma rep equivalent unidirectional in air = badge rep/1.39 plus dose missed by badge because of body shielding.

(b) Accuracy: + 0
- 20%

(c) (Lower limit, based on subtraction method and NTA Plates, is 40% of these values.)

Accuracy: + 0
- 18%

(d) Rem = 3 x rep except in case of eyes where rem = 10 x rep

(e) Total dose = total gamma rep + total neutron rem.

MEASUREMENTS WITH THE ACCIDENT CORE

Here are presented and discussed, first, measurements made in the assembly room following the burst with the core in place and, second, survey, observation, and analysis of core components.

ASSEMBLY AREA - CORE IN PLACE

Measurements made in the assembly room after the burst were, of course, limited to those of delay γ -flux variation in space and time. There were a series of measurements made with the three recording instruments in operation at the time of the burst. These indicated variation with time only. Other measurements were made at various times and various positions with Victoreen chambers and Zeus survey meters. Consider first the recording instruments.

Three recording instruments were turned on at the time of the burst. These are designated P-V, P-VI, and P-VII and described as follows:

P-V Argon filled pressure chamber giving a current proportional to the γ -flux. Active length = 12"; active diameter = 10"; active volume = 930 cm³; pressure = 40 atmospheres. (Range: 6 decades to 10⁻⁷ amp full scale.)

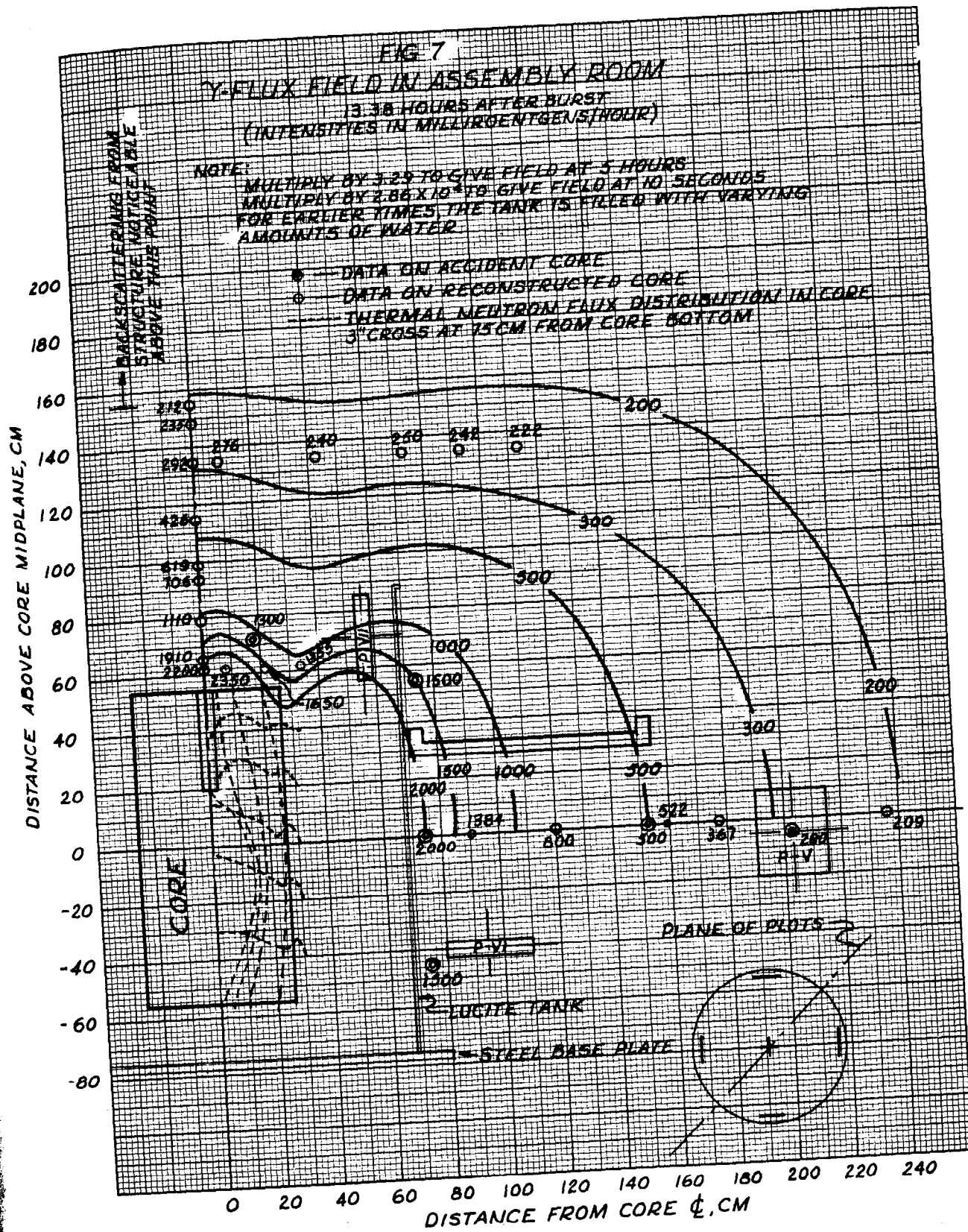
P-VI B¹⁰F₃-filled ion chamber detector, giving an amplified current reading proportional to the thermal neutron flux, but sensitive also to ionization by γ 's. Active length = 12"; active diameter = 2"; pressure = 760 mm. (Range: 3 decades to 10⁻⁷ amp full scale.)

P-VII B¹⁰F₃-filled ion chamber detector designed to give a reading proportional to the logarithm of its current. The chamber is of the same design as P-VI.

The relative locations of these instruments are shown rotated into the x - z plane in Figure 7. The coordinates of the centers of the active volumes of these detectors for z = 0 at midcore height are, in cm,

	x	y	z	R	θ
P-V	-143	+143	-5	202	135°
P-VI	93	16	-40	94	10°
P-VII	53	-19	+71	56	340°

Because of slow response time, lack of range, and/or intermittent operation, the records are imperfect. In all cases, the pen traveling at a rate of 1/2 full scale/second was unable to keep up with the rise in power level during the burst and showed an initial peak at 4/10 full scale. This was where the pen reversed direction as the shutdown power decreased from its true peak. The pen then followed the decrease, reaching a minimum as the initial removal of the water shield allowed an increase in flux. As soon as P-V and P-VI saw the bare core they went off scale. P-VII however,



which records proportional to the logarithm of the current, rose only to the level commensurate with the ionization current from γ 's and delayed neutrons, then followed their decay. P-VI remained off scale for several minutes, then returned and followed the decay. P-V, however, stayed off scale for several hours because of malfunctioning of a resistance changer switch.

Unfortunately, the recorders were turned on and off at various times without record, so that the early decay curves could not be accurately reconstructed. To offset this, a number of readings of the ammeters of P-V, P-VI, and P-VII were recorded along with the time of day. The best reconstruction of chart data possible is shown in Figure 8 using the observed individual points. During the first few minutes after $t = 0$, the chart records include contributions of delayed neutrons. This contribution has certainly vanished after ten minutes. Superimposed on the data are the straight line curves proportional to $t^{-1.21}$. It is evident then that the burst is of short enough duration to assume that the gammas decay proportional to $t^{-1.21}$. The γ intensity was determined for P-V using the conversion factor of 2.63×10^{10} mr/hr/amp established in later measurements on the reconstructed core.

The attempts at determining the γ flux at several points in the assembly room with Victoreen chambers inserted through a small hole in the freight door introduced errors of such magnitude that the results are in question and are discounted. Partial shielding by structural members, back-scattering at the door, and presence of fission products in the air contributed to the questionable observations. These observations are listed for record, however. At various times after access, readings were taken with a Zeus survey meter. One seems to be out of line by a factor of 2, which has been ascribed to an error in applying the scale factor. To compare the readings, the data has been adjusted to $t = 5$ hours assuming the decay proportioned to $t^{-1.21}$. The space and time coordinates are given with the readings as well. All readings taken at core midheight have been adjusted to the position of P-V in the last column of the table (radial distance from core centerline = 202 cm). The average value at this position for $t = 5$ hours is $928 \pm 5\%$ (mr/hr). The point γ -flux measurements at approximately midcore height are summarized in the table on the following page.

FUEL ELEMENTS

Fuel elements were removed from the core between the third and fifth day for examination, survey measurements and fission product analysis. Each standard element is identified by a serial number. Each special element making up the control rod sub-assembly is identified by a letter-number combination. Locations in the core of the elements removed for inspection are shown in Figure 2. The elements are N-3, N-5, N-6, N-7, N-8, 25, 103, 193, 215, 338, 433, 526, 587, 588, and 589.

Instrument	Time After Burst, hr	Distance from Core, cm	γ Inten- sity mr/hr	Corrected to 202 cm from Axis 5 hr After Burst
Victoreen Thimble	7.38	144	1560	1270
Victoreen Thimble	7.63	280	430	1367
Victoreen Thimble	8.13	462	176	1658
Zeus	1.63	466	1500	2060
Zeus	3.97	466	250	1010
Zeus	12.88	151	500	875
Zeus	13.38	75	2000	910
P-V	6.80	202	658	955
P-V	9.80	202	421	951
P-V	21.88	202	150	892
P-V	25.63	202	121	875
P-V	5.00	202	908	908

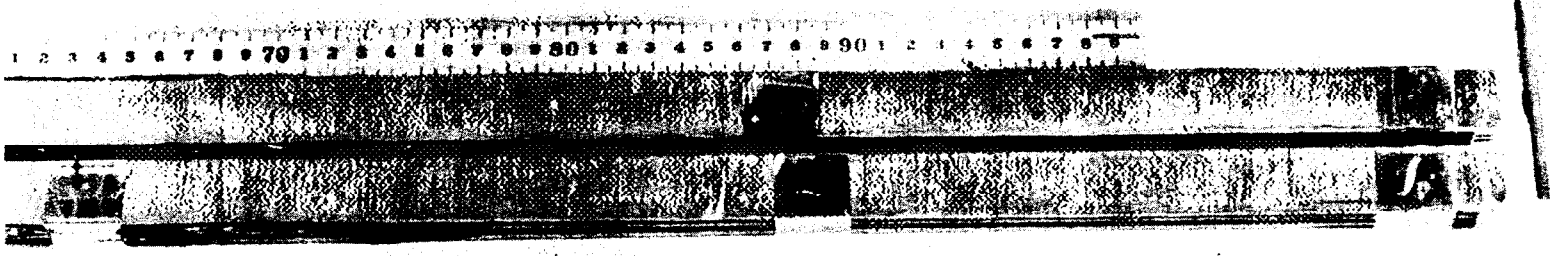
Examination of Fuel Elements

Photographs of elements N-6, N-7, N-8, and 587 were made and are shown in Figures 9 to 14. The typical appearance can be described for the central section of an element as follows: The plastic fuel strips had expanded to fill all of the space between zirconium plates. Where two fuel strips existed between plates (in two spaces, since there are seven strips per assembly) the space was expanded by bowing the zirconium out. The plastic had also extruded in a direction parallel to the plates, contacting and fusing with extruded plastic from the adjacent assembly to the extent that elements stuck together, requiring some force to separate them. As the extruding plastic reached the edge of the plate it appears to have flowed normal to the plate thus filling all free space. The plastic is filled with small voids in the form of bubbles which equal the original free space in volume. The appearance might be characterized as "foamed plastic." This description is of the most altered section. The extent of "foaming" was less toward the ends of the elements and in elements farther from the center of the core. This latter characteristic may be seen by comparing the photographs for elements N-6 and 587, located 6.6 and 25 cm from the core centerline, respectively. Elements adjacent to a fully inserted safety rod showed little or no foaming.

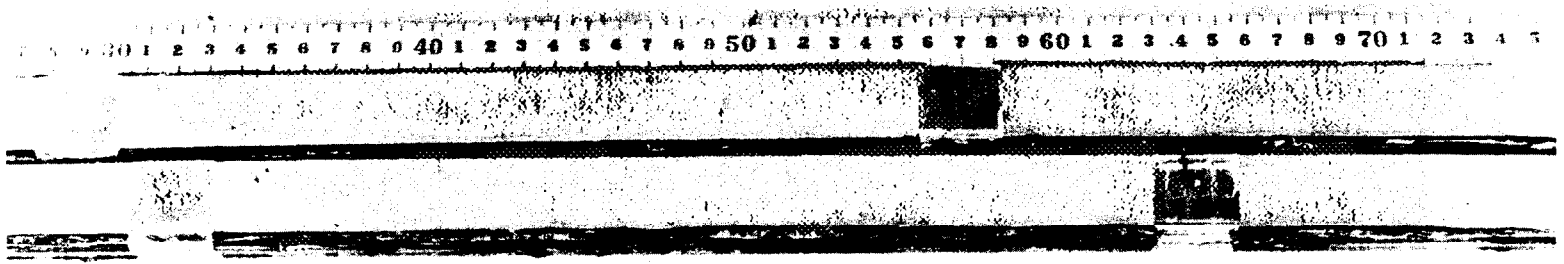
If two elements are stacked with their end caps together at the lower end as in Figure 10, the upper caps are well separated as a result of the bulging in the central sections where the zirconium plates are bowed out. It is evident then that the expanded plastic occupies more than the original free space, at least in the central region.

To assist in the examination, some experiments were run on samples of unused fuel strip to indicate gross behavior on heating. The samples were placed for one minute between metal blocks heated to controlled temperatures of 250, 300, 350, and 430°C and then quenched in water. Photographs of three of the samples are shown in Figure 15. Below 300°C the plastic shows deformation or plastic flow, but no foaming. At 350°C the plastic exhibits considerable gross foaming, and at 430°C is completely vaporized. Polystyrene transition temperatures lie between 80°C and 85°C. At this temperature it becomes very soft and can flow markedly under moderate pressures. Depolymerization begins to occur rapidly above 250°C and the monomer is attained above 300°C. The monomer is in the gaseous state above 146°C (stp). Destructive distillation becomes evident when the polystyrene reaches 330°C and is quite rapid above 360°C. Distillation products can be identified as toluene, isopropenylbenzene and others. Analysis of foamed strip showed presence of free carbon, and the elements had characteristic odors associated with distillation products.

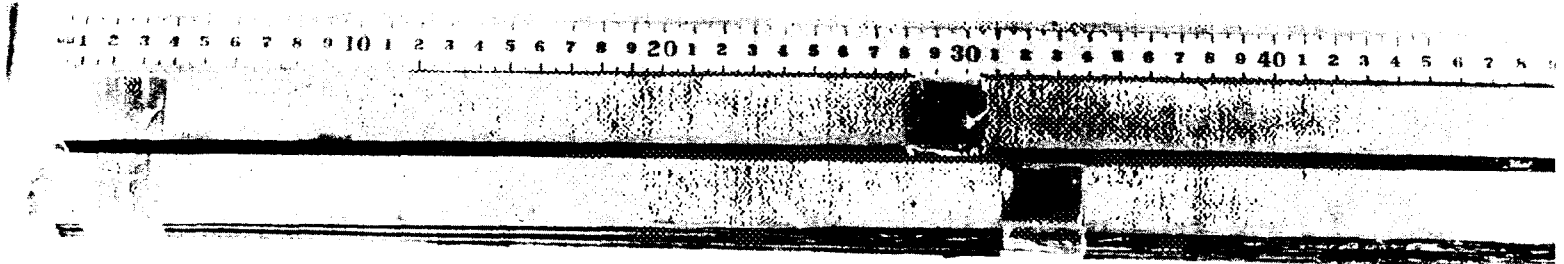
About six weeks after the accident, the core fuel elements were examined to establish salvage possibilities. In making the examination it was assumed that only peripheral elements could be of further use. Hence, 15 peripheral elements of one quadrant, including some from both sides of the safety rods were chosen.



9-a

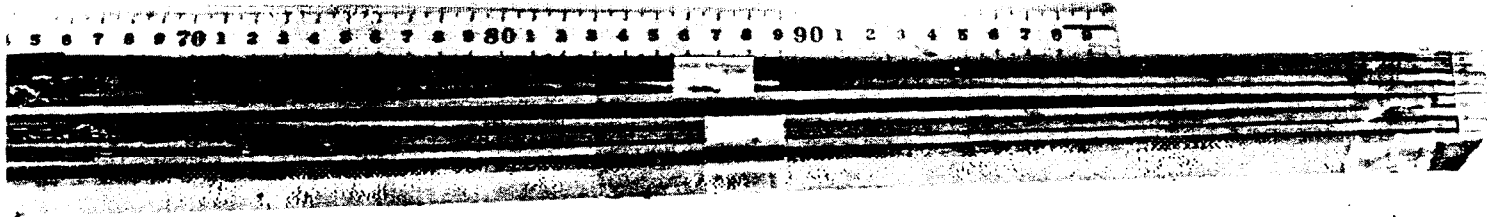


9-b

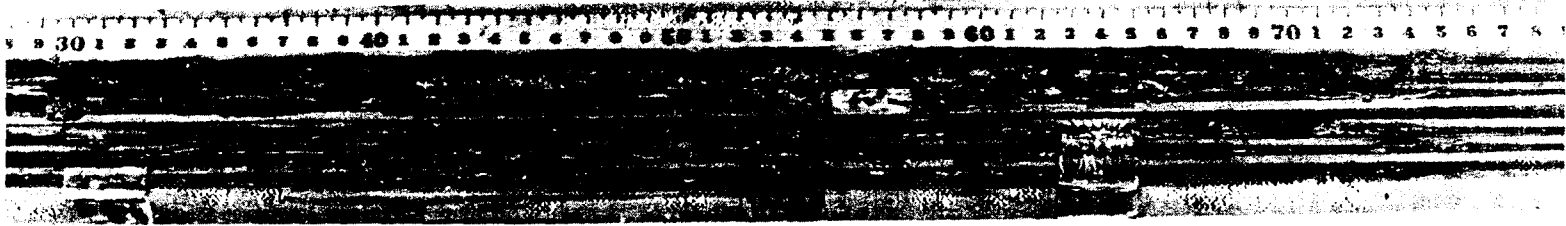


9-c

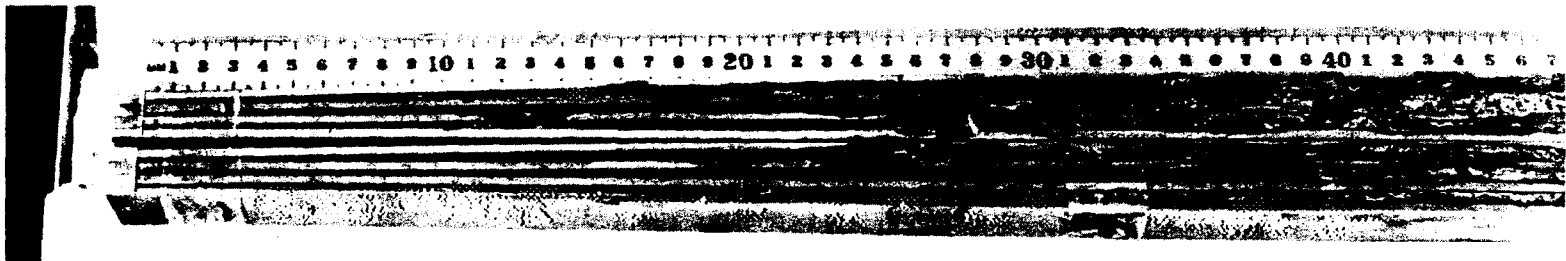
Figure 9



10-a

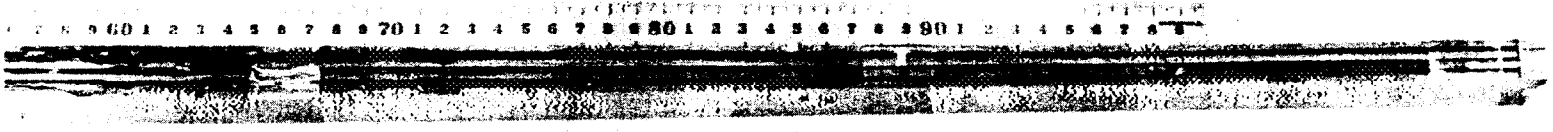


10-b

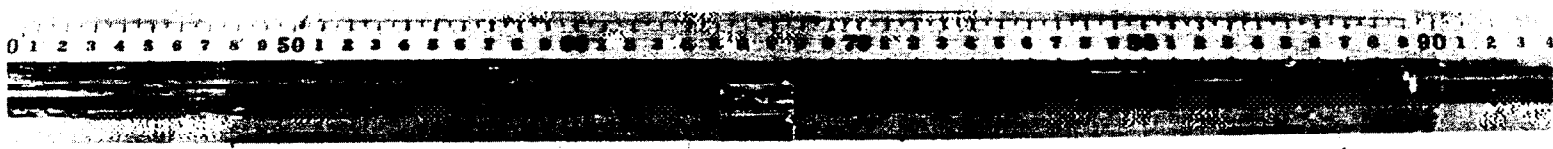


10-c

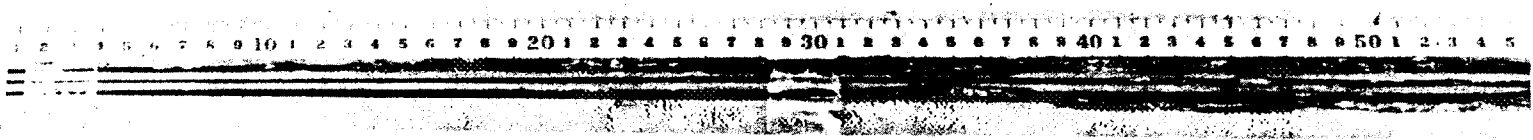
Figure 10



11-a



11-b



11-c

Figure 11

Figure 12

12-a

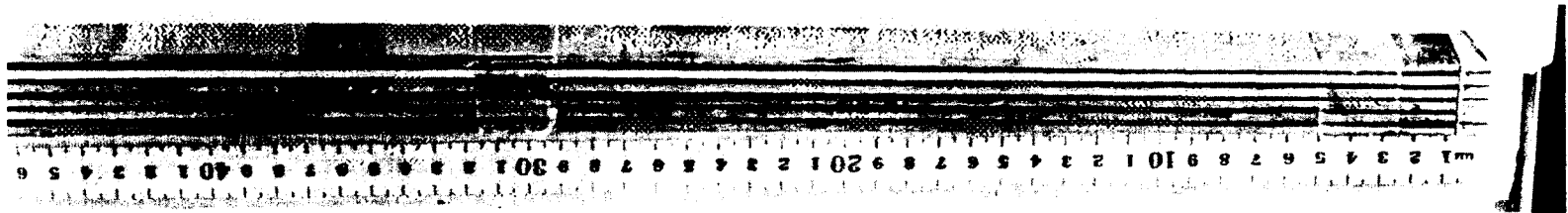


12-b

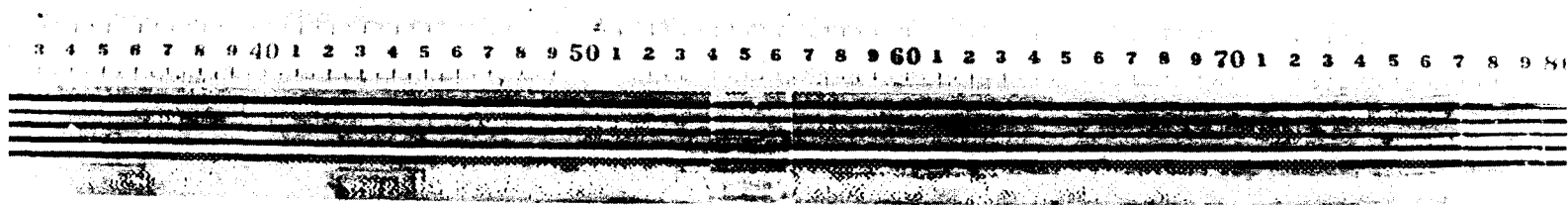


12-c

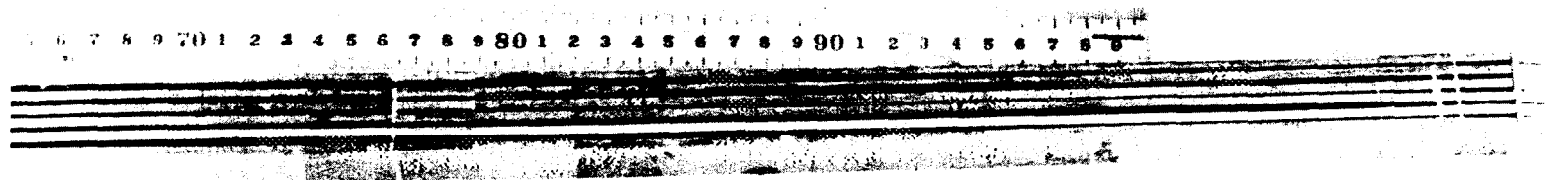




13-a



13-b



13-c

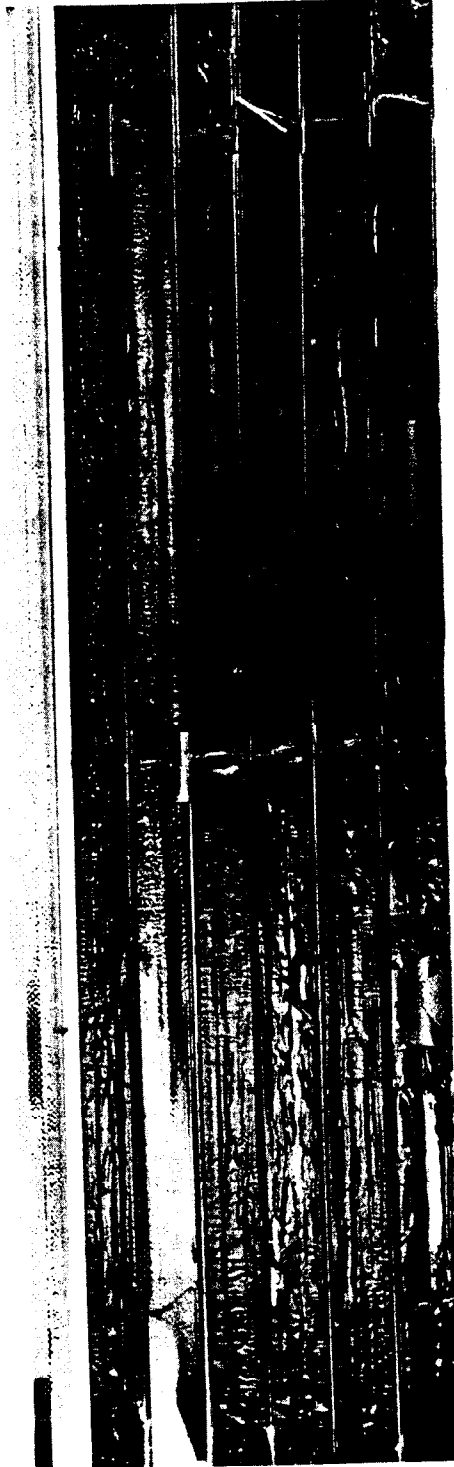
Figure 13

Figure 14

14-a



14-b



14-c



Figure 15



The method of examination consisted of removing the bottom plastic end cap and three of the five strips of polyethylene tape which holds the element together. By spreading the zirconium strips apart, it was possible to examine approximately 30 inches of the fuel strip.

Extensive damage was noted on all fuel strips which were cemented to zirconium. The damage consisted of swelling, bubbling, or an apparent increase in thickness of the fuel strip. On fuel strips which had earlier required extensive repairs, it was noted that in areas where a great deal of cement had been used, the amount of swelling or bubbling was greater than in other areas. It is probable that all the solvent (xylene) in the cement had not evaporated and the heat generated at the time of the accident caused the solvent to volatilize with the resulting swelling in the fuel strip. Wherever plastic spacers were used in the elements, deep indentations had been formed in the fuel strips. It will not be possible to reuse any of the fuel strips which were cemented to zirconium.

The extra fuel strips -- those not cemented to zirconium -- are in better condition. It is possible to salvage some of the extra fuel strips from each element that was examined. The amount that can be saved ranges from the entire strip down to pieces approximately six inches long from each end of the strip. The type of damage to the extra strips was similar to that of the strip cemented to zirconium. However, it was not as severe. The thickness of one strip was checked and it was 0.020 inches, an increase of 0.007 inches.

On the basis of the examination it was estimated that not more than 2700 inches of strip, in pieces, could be reused. These strips would correspond to nine fuel elements, about 3% of the total.

A microscopic examination of unirradiated sections of fuel strip was undertaken to obtain information on uranium oxide particle size and distribution. Originally the strip was fabricated using -325 mesh oxide which excludes particles greater than 40 microns in diameter. The microscope could penetrate about 20 microns into the plastic. Nearly all (~100%) of the particles observed were about 10 microns in diameter. Maximum observed particle size was 40 microns, with 20 such particles found on the average per cm^2 of surface examined. There appeared to be no gradation between these sizes. It was estimated that with each 20 micron layer containing 20 of the 40 micron diameter particles/ cm^2 , there would be found 10^4 such particles/ cm^3 of plastic or 300 particles per cm^2 of fuel strip. The associated particle volume is 3.4×10^{-4} cm^3/cm^3 of fuel strip.

In fabrication of the strip, 705 gm of plastic were mixed with 379 gm of mixed oxide (nearly 100% U_3O_8). If the density of the plastic is taken as 1.05 gm/cc and that of the oxide at 7 gm/cc, the specific volume of all the oxide is

$$\frac{7.46 \text{ cm}^3/\text{cm}^3 \text{ of strip}}{0.0746}$$

Residual Activity of Fuel Elements

A survey of gross residual activities of each of fuel assemblies N-3, N-5, N-7, N-8, 526, 103, 338, 215, 193, 588, 589, 25, and 433 was made with a Geiger counter located 220 cm from the elements. The relative activities were normalized to the uranium density and size of standard element 338 and corrected for decay during the survey on the basis of a control element decay scheme. Finally, this survey contributed a mean radial residual activity plot averaged over the core height, as shown in Figure 16. Determination of the axial distribution of residual activity in each of these fuel assemblies was accomplished by a survey with a β - γ detector, using a 7/8" slotted shield which traversed the assembly. These distributions were normalized by applying the integral values obtained in the gross survey to the integrated curves. The axial distributions are shown in Figures 17a, 17b, and 17c.

The decay scheme of the core elements was studied. Gross activity of element 338 was measured from $t = 25.6$ hours through $t = 72$ hours. Later, the gross activities of elements 338 and 588 were measured in the interval from $t = 93$ hours to $t = 334$ hours. The variation of activity with time is plotted for these elements in Figure 8 along with the records on the whole core. The early activities decay proportional to $t^{-1.21}$ with the exponent of t decreasing to about -1 for the activities in the later tests. Evidently very little error will be entailed in assuming the decay proportional to $t^{-1.21}$ for measurements made before the core was removed on the fifth day.

Fission Product Analyses

Segments of fuel elements N-6 and 587 were removed for fission product analysis by the Chemistry Division. Two segments from N-6 were used, and one from 587. Their extent and location in the core are given by the following coordinates, with $z = 0$ at core midplane:

	z			x	y
	top of segment cm	bottom of segment cm	center of segment cm	cm	cm
N6(A)	+45.6	+50.6	+48.1	-6.4	-1.7
N6(B)	-3.4	-1.4	-2.4	-6.4	-1.7
587	-5.4	+6.6	+0.6	+19.0	+16.5

Assays were made to isolate the fission product Mo^{99} . From the activity, known yields, and concentration of U^{235} the number of fissions per gram were determined for the three samples to be

FIG 16
RADIAL DISTRIBUTION OF FLUX
IN ZPR-I
from scan of activation

Flux - arbitrary scale

$$\bar{\phi}(r) = .560$$

Radius - inches

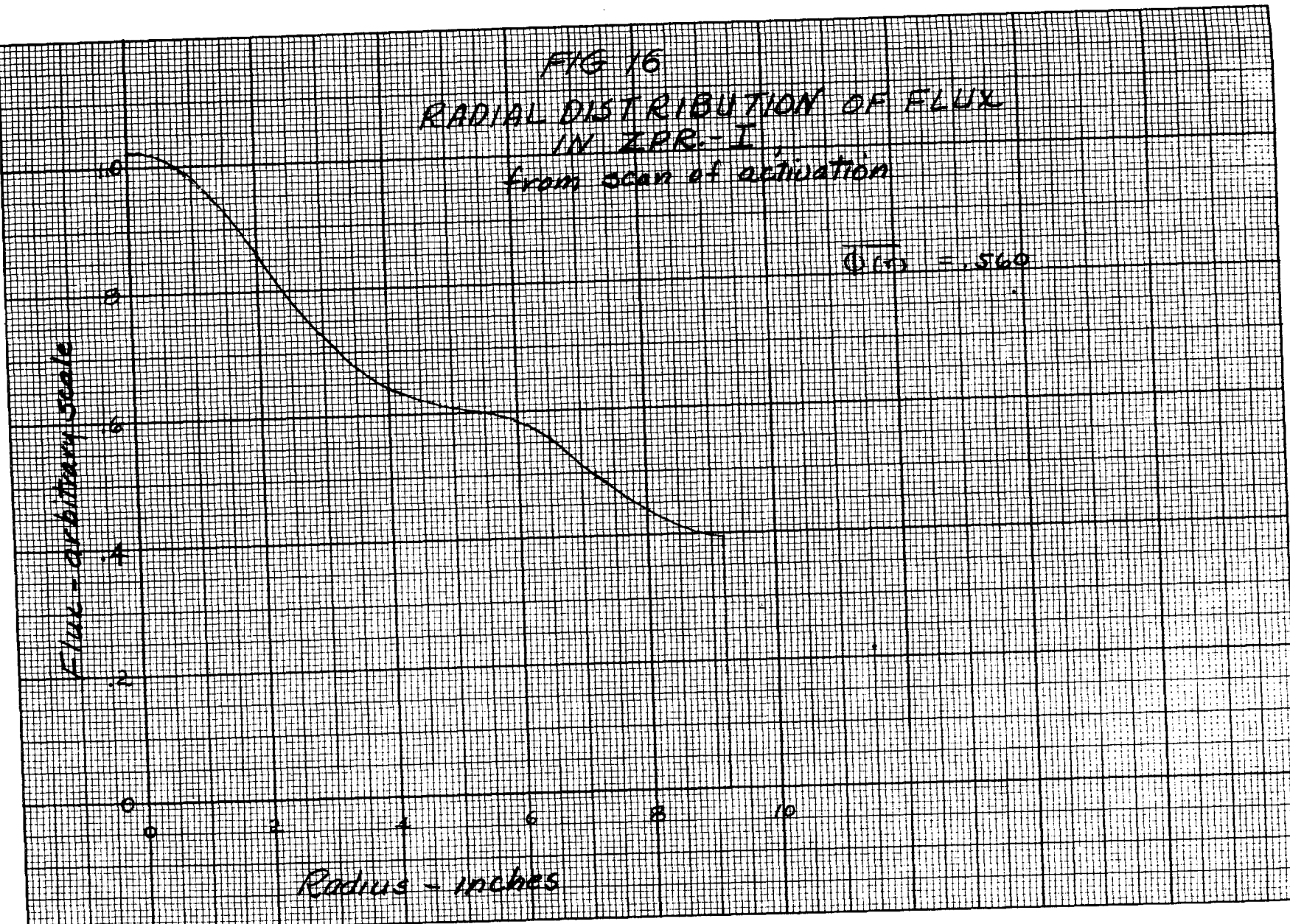


FIG 17a
 NORMALIZED DISTRIBUTIONS OF
 FISSION PRODUCT ACTIVITY
 ALONG FUEL ELEMENTS

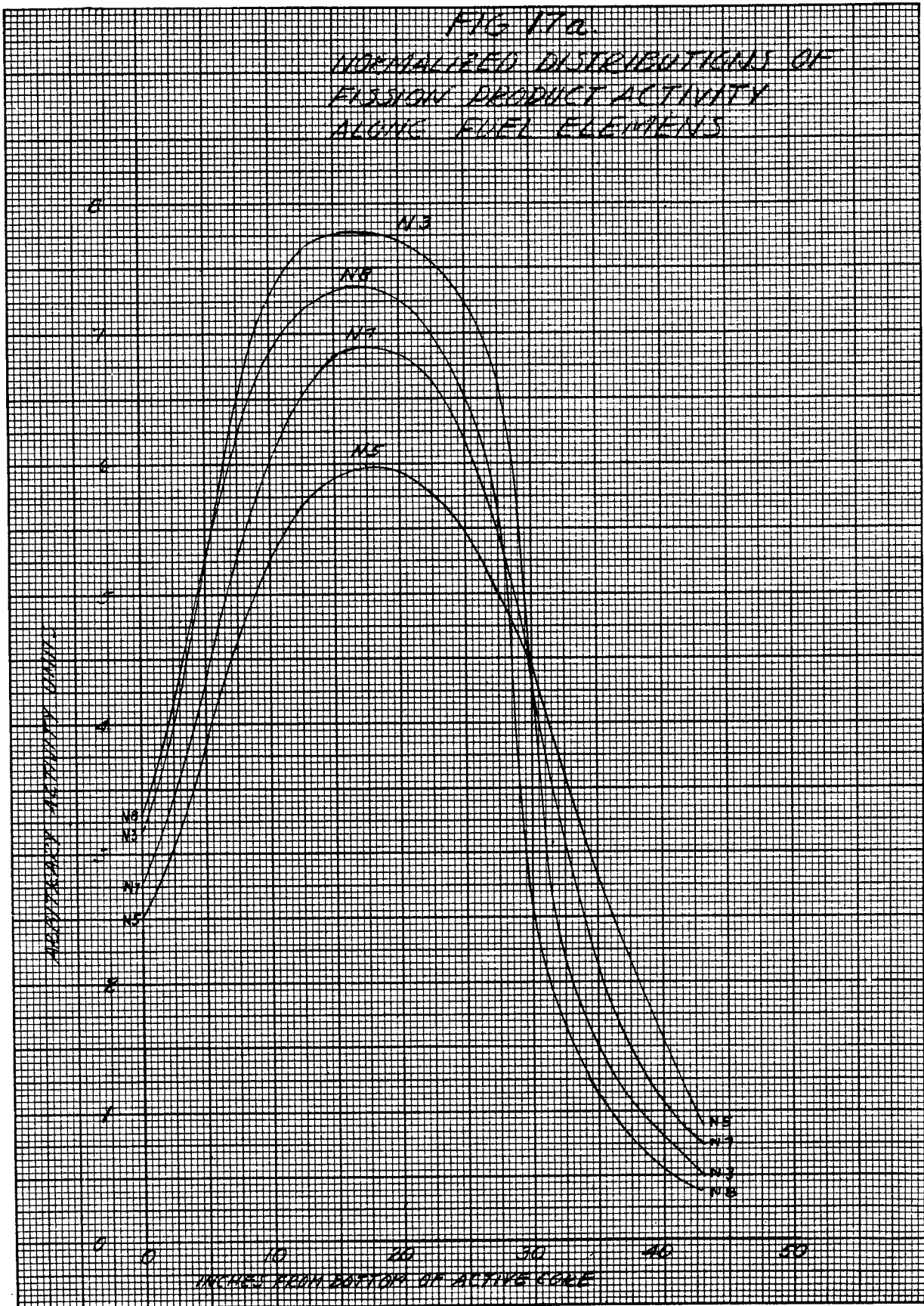


FIG 17b
NORMALIZED DISTRIBUTIONS OF
FISSION PRODUCT ACTIVITY
ALONG FUEL ELEMENTS

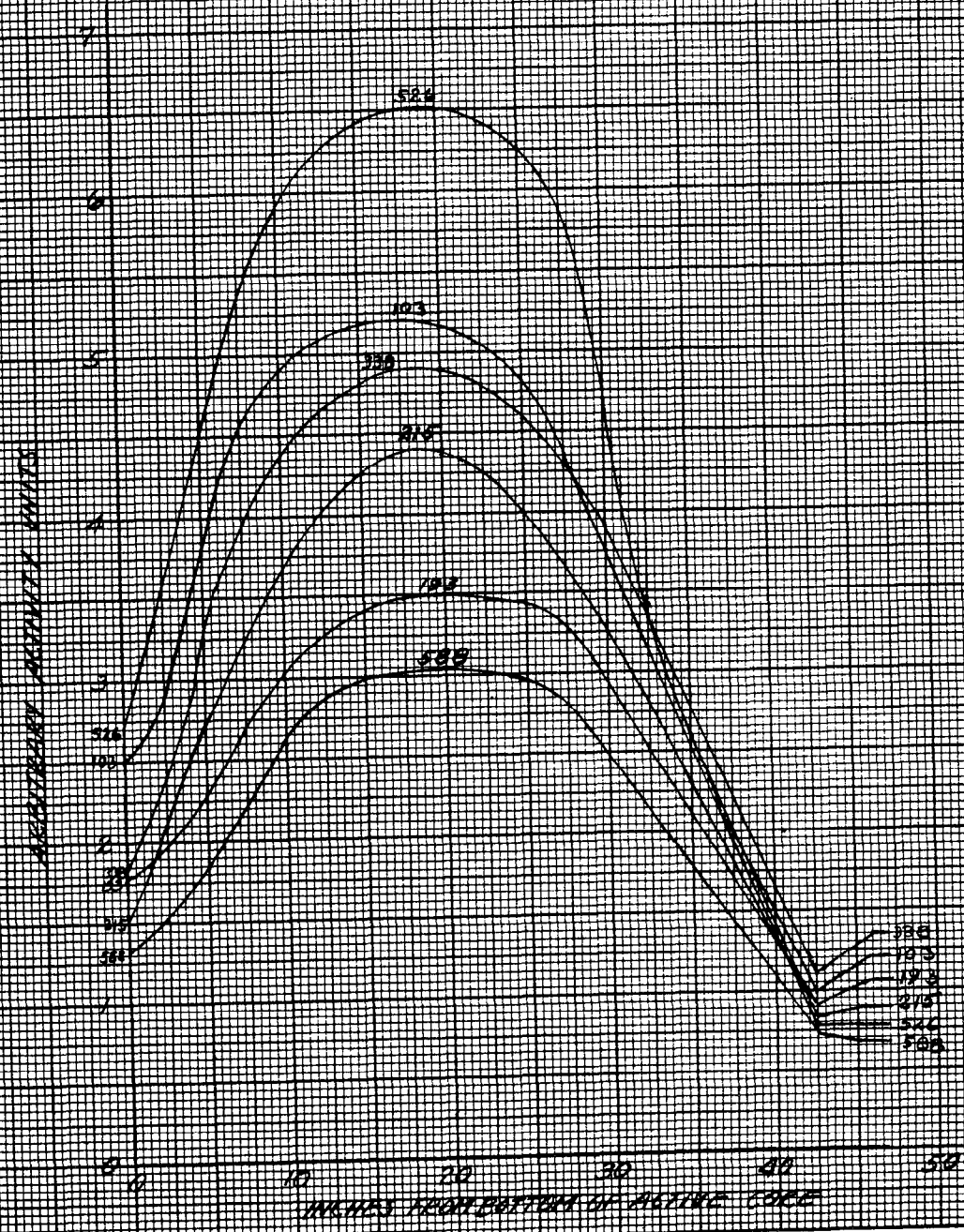
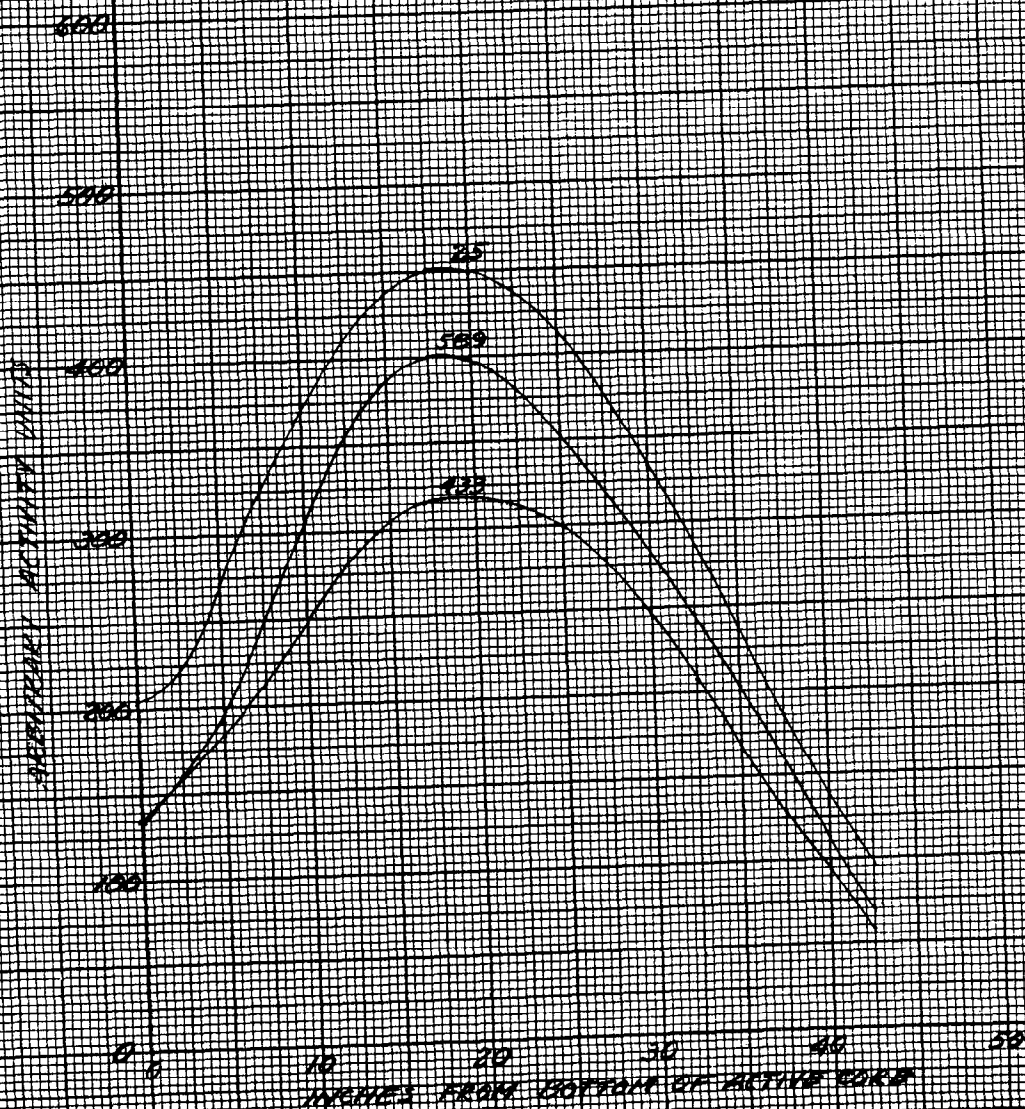


FIG 17c
NORMALIZED DISTRIBUTIONS OF
FISSION PRODUCT ACTIVITY
ALONG FUEL ELEMENTS



N6(A)	1.01×10^{13} fissions/gram of U^{235}
N6(B)	3.33×10^{13} fissions/gram of U^{235}
587	2.13×10^{13} fissions/gram of U^{235}

CONTROL RODS

The cross control rod was undamaged, as were the blade rods and their guide tubes. An axial survey of the 3" STR cross rod (Figure 3) of the accident core yielded the activation curve shown in Figure 18. The stellite rubbing shoe of the rod was examined to determine the activation of Co^{60} . A similar shoe was activated by a known thermal flux in the CP-2 thermal column. The total integrated flux of thermal neutrons for the CP-2 activation was determined to be 1.55×10^{12} neutrons/cm². The measured activation for this experimental irradiation was less than that of the stellite shoe which was subjected to the accidental burst by a factor of 31.6 after suitable decay corrections. The CP-2 irradiation was carried out with the axis of the rod parallel to the thermal column beam so that the neutron path was roughly parallel to the shoe face. Experimental scans of the tip indicate an attenuation of 1.4 for the beam to the position of activation measurements.

MEASUREMENTS WITH THE RECONSTRUCTED CORE

To assist in establishing the physics of the incident, and the doses received by the personnel involved, the reactor core was reconstructed, with modifications, so that conditions at the time of the accident could be fairly represented. Principal modification was a reduction in the number of fuel elements required to increase the subcriticality with safety rods to greater than 1.5%k. To achieve similarity with less excess reactivity, 24 peripheral fuel elements were eliminated so that 6.248 kg of U^{235} instead of 6.787 kg were present. Work on the reconstructed reactor was under the direction of F. H. Martens.

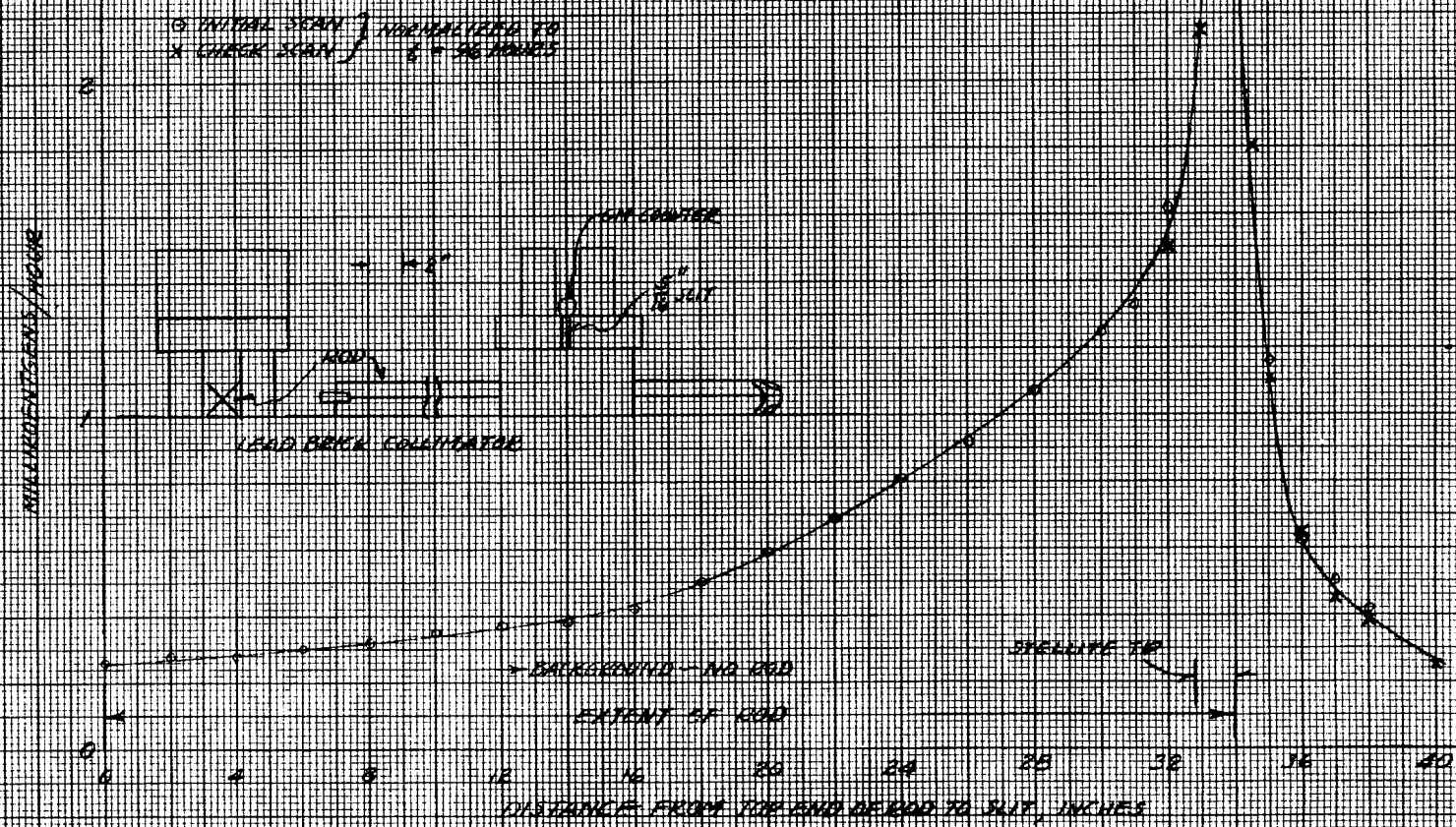
ROD CALIBRATIONS

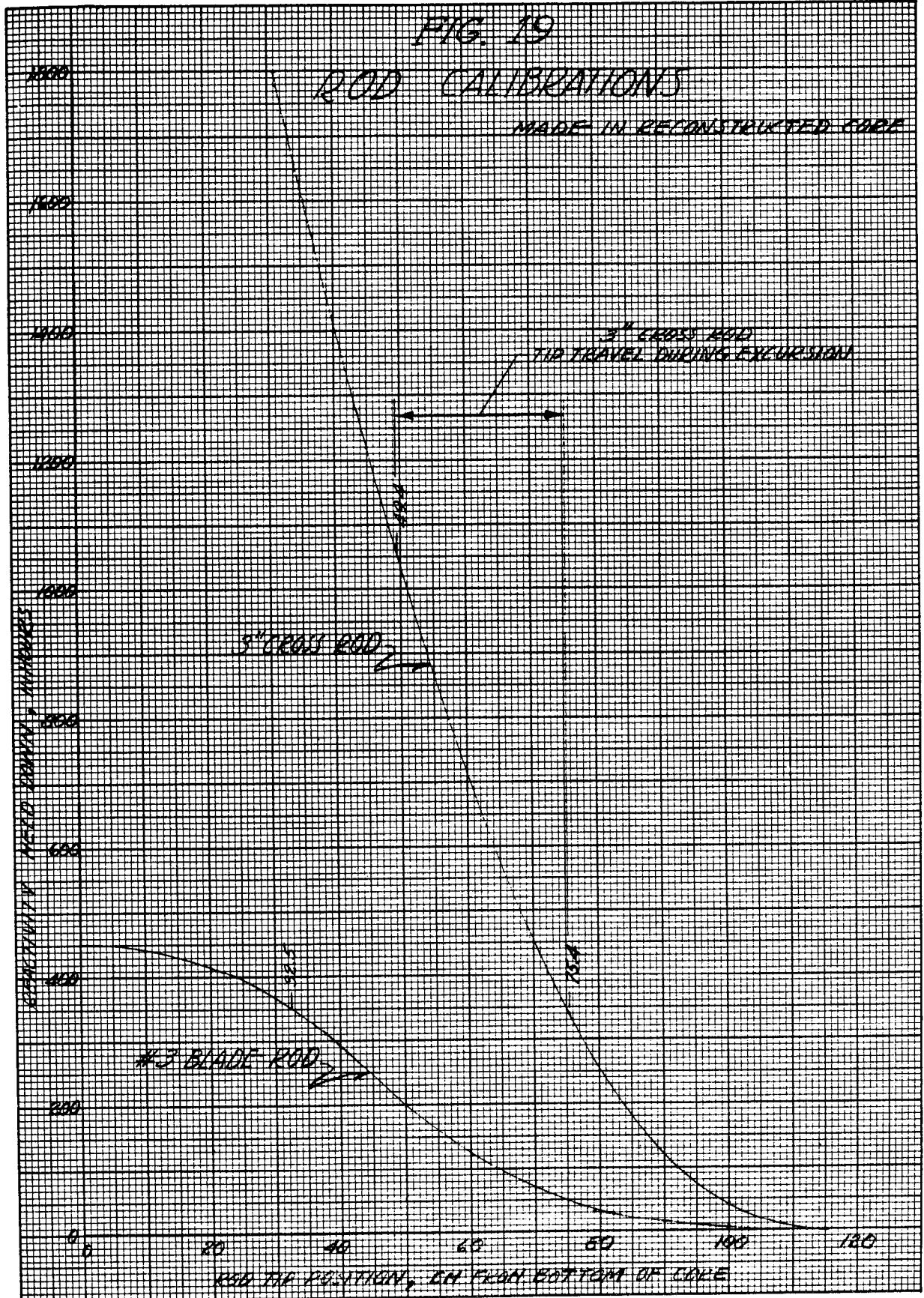
The four blade type safety rods near the periphery were separately calibrated over the entire distance of their travel ($z' = 0$ to $z' = 113.8$ cm, origin at core bottom). The three-inch cross-rod was calibrated in the interval from $z' = 29.8$ to 113.8 cm. The data are obtained in terms of inhours/cm at various withdrawal distances, integrated starting at position of maximum withdrawal, and presented for the # 3 blade rod and the three-inch cross-rod in Figure 19. These curves then represent the reactivity being held down by the rod. The reactivity resulting from a motion of a rod can be determined by ordinate differences over the interval of motion.

ACTIVITY ALONG 3" CROSS ROD

ACTIVITY INDICED DURING EXCURSION
3" REGULATING ROD
(SEE FIGURE 3)

FIG. 13





POWER LEVEL

In order to relate the experiments in the reconstructed core to the accidental burst, it was necessary to determine the energy release or power production in the reconstructed core. In turn, this had to be related to the current developed in a monitoring circuit for normalization of all the experiments. To do this, the thermal neutron flux distribution was measured at many points in the core by activation of manganin wire. The wire was calibrated in a known flux to give the relation between activity and activating flux. Cadmium ratios for manganese and U^{235} gave the relation between fission and manganese activation. The average flux density in the core was determined by volume integration of measured flux densities. Then the power level was found to be 22.6 watts. The current induced in the selected monitoring instrument (P-VI) was used to normalize various runs, it being proportional to the power level.

FAST NEUTRONS

Fast neutron flux surveys were made with three instruments. One survey was made using the fast neutron dosimeter known as "Rednose" developed by Hurst and Ritchi.⁵ This survey was along the centerline above the core and out along a radius 80 cm above the core. The axial distribution is shown in Figure 20. The radial measurements were made at only three positions, $R = 0$, $R = 23$ cm and $R = 43$ cm. These results are not plotted, but the relative readings were in the ratio 1:0.93:0.65.

The fast neutron flux variation with z at $x = 7''$, $y = 7''$ was measured by T. V. Blosser of ORNL with a proton recoil counter²¹ for a power level of 0.049 watts. These data were used to obtain the distribution at the time of the burst by normalizing to an energy release of 3.75×10^6 watt-seconds. The resulting distribution is shown in Figure 20. The estimated rms error is $\pm 9\%$ for these data. A long counter as described by Rossi and Staub³ was used in a separate fast flux variation determination along the same line above the core. The power level for this run is not known but the count data are included in Figure 20 as confirmation of the distribution shape.

Additional fast neutron dose measurements were made at $x = 11''$, $y = 13''$, $z = 54''$ using tissue⁴ and graphite air ionization chambers. It was found for these measurements that the ratio of ionizations recorded was tissue/graphite = 0.651 ± 0.006 . To obtain the average γ energy a γ spectrum was obtained with a scintillation spectrometer at the same point, as shown in Figure 21. Other measurements of the prompt fast neutron dose were made at this point with the proton recoil counter by T. B. Blosser with the fast neutron dosimeter "Rednose," and with NTA plates. These gave 10.2 rep, 11 rep, and 2.4 rep, respectively.

FIG. 10

INTEGRATED FAST NEUTRON FLUX DISTRIBUTION ABOVE CORE

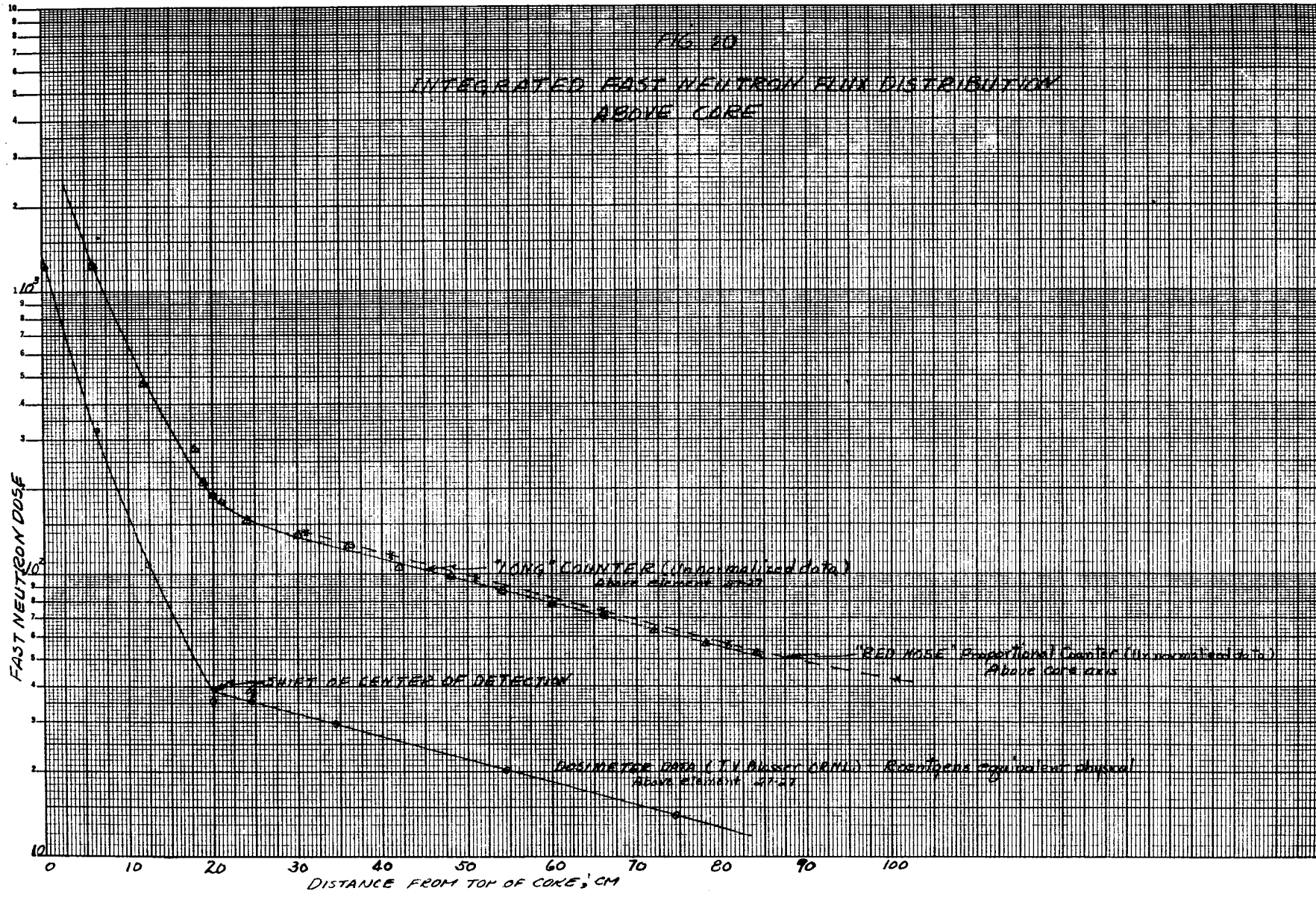
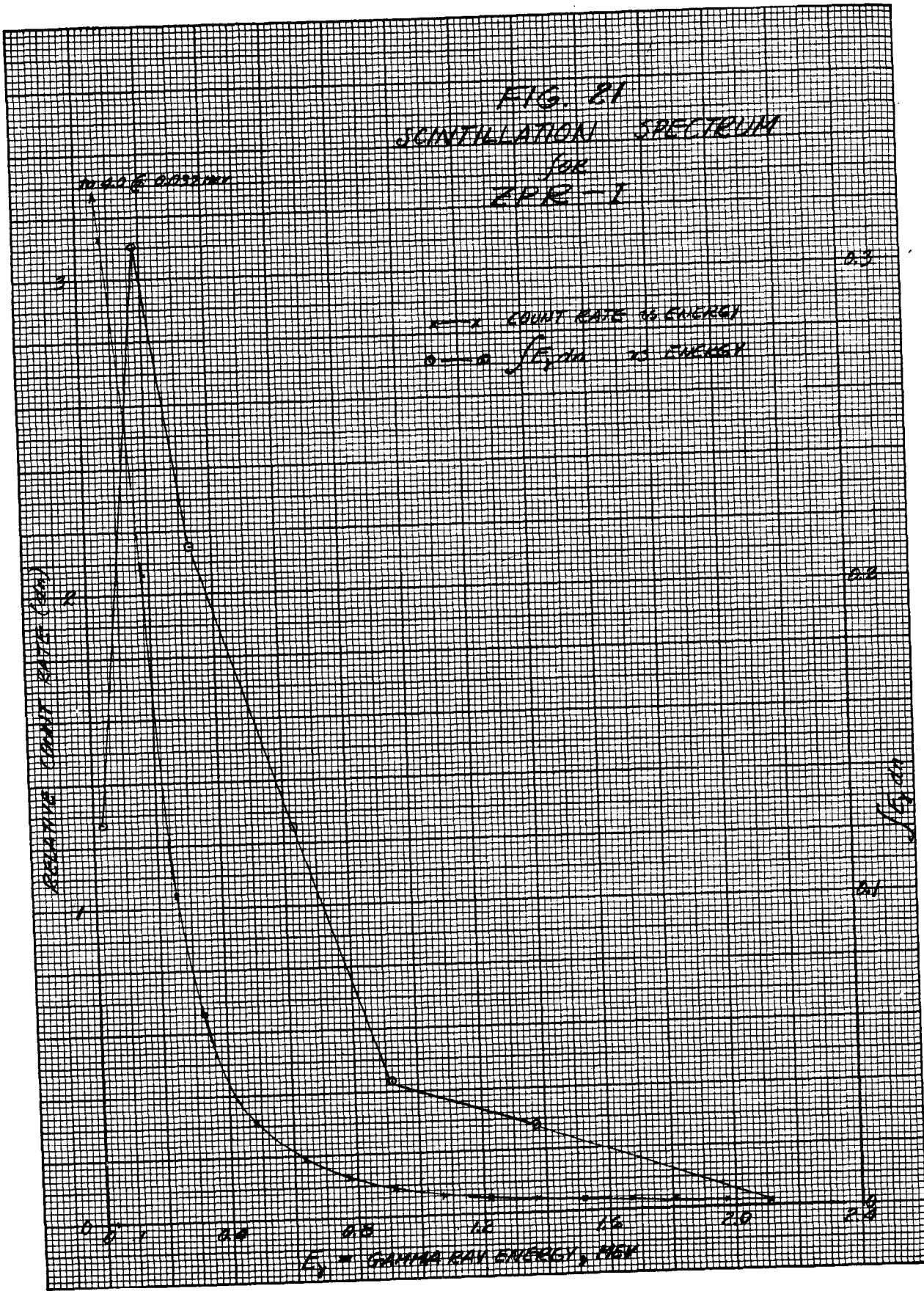


FIG. 21
SCINTILLATION SPECTRUM
for
EPR-1



THERMAL NEUTRONS

Three measurements of the thermal neutron flux were made at $x = 11''$, $y = 13''$, $z = 54''$. One measurement was made with a boron-lined chamber with and without a Li metal shell. An analogous experiment was performed in the CP-3' thermal column in a known thermal flux. The second measurement was made using a BF_3 proportional counter both on the reconstructed core and in the CP-3' thermal column. The results agreed within 10% and the ratio of energy released in the burst to energy released in the test indicated an average incidence of thermal neutrons of $1.2 \times 10^9 \text{ n/cm}^2$. A third set of measurements was made with Li loaded NTA plates resulting in an incidence of $2.3 \times 10^9 \text{ n/cm}^2$. These measurements are not treated in detail herein since the results indicated doses of only 0.6 to 1.0 rep.

PROMPT GAMMAS

A measurement of γ -flux distribution above the core along a vertical line at $x = 3''$, $y = 3''$ was obtained in two runs with the reactor operating at 4.3 watts for 30 minutes and 60 minutes, respectively. In the accidental burst, the γ 's during operation were prompt, whereas in the reconstructed experiment operation for an extended period resulted in a significant delayed contribution as indicated in Figure 22. Using these corrections, and the ratio of total energy released in burst to that in the reconstructed experiment, the prompt γ -flux distribution above the core for this location is obtained and shown in Figure 23.

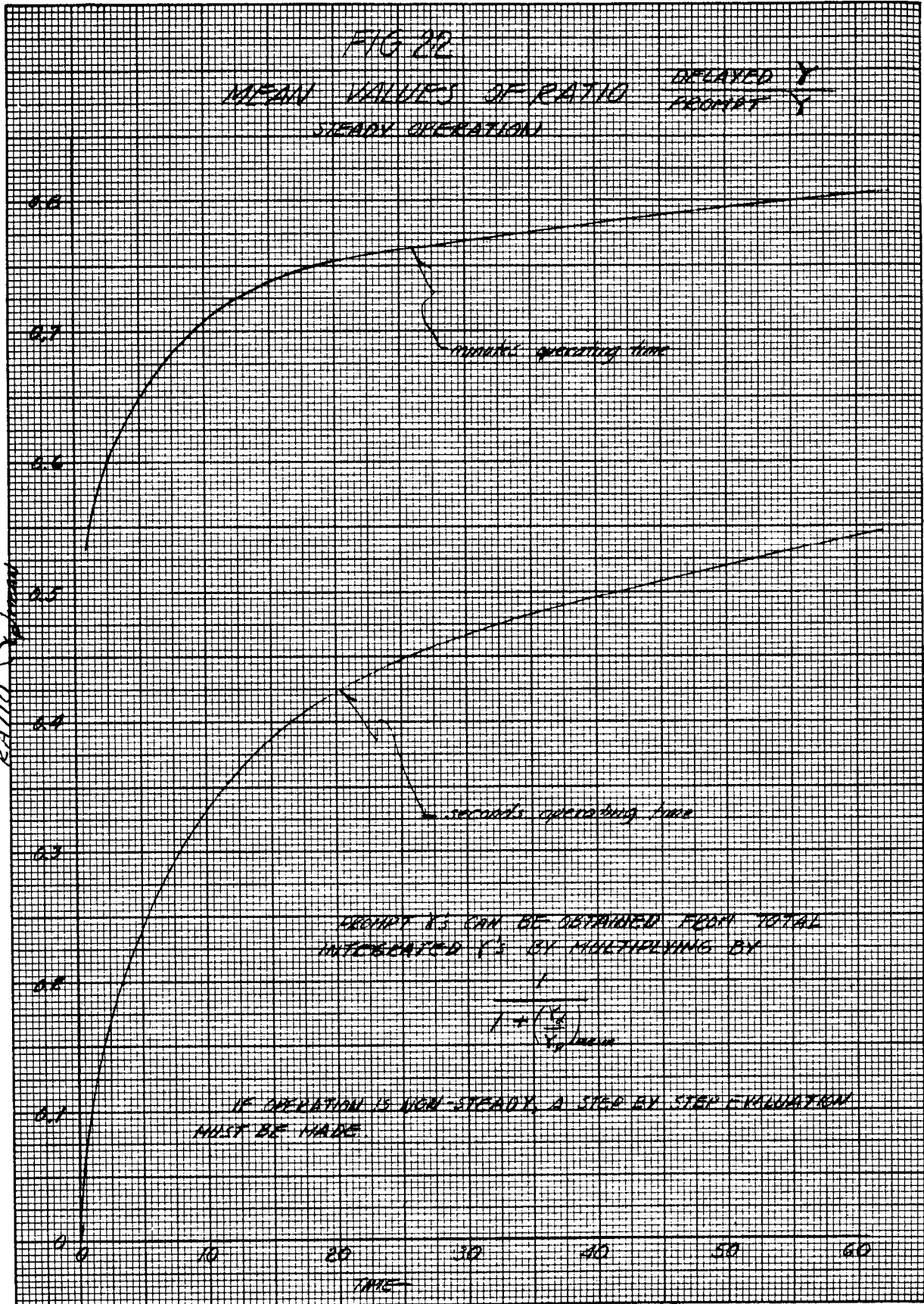
Film badges were exposed in air at $x = 11''$, $y = 13''$, $z = 54''$ and at $x = -48''$, $y = -12''$, $z = 63''$ during a four hour run at 22.6 watts and later developed. Densitometer readings showed 17.9 and 6 "badge roentgens" respective

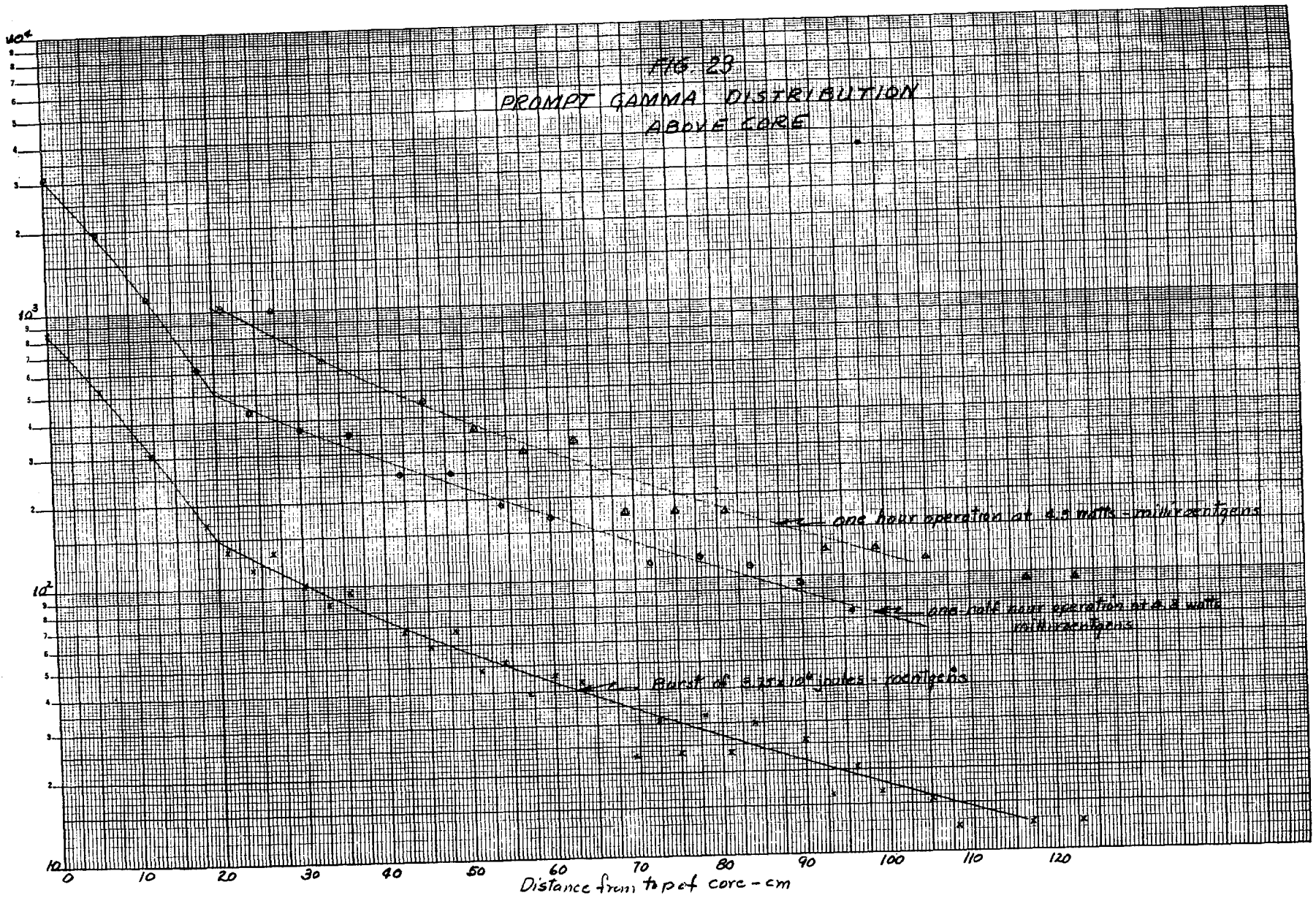
DECAY GAMMAS

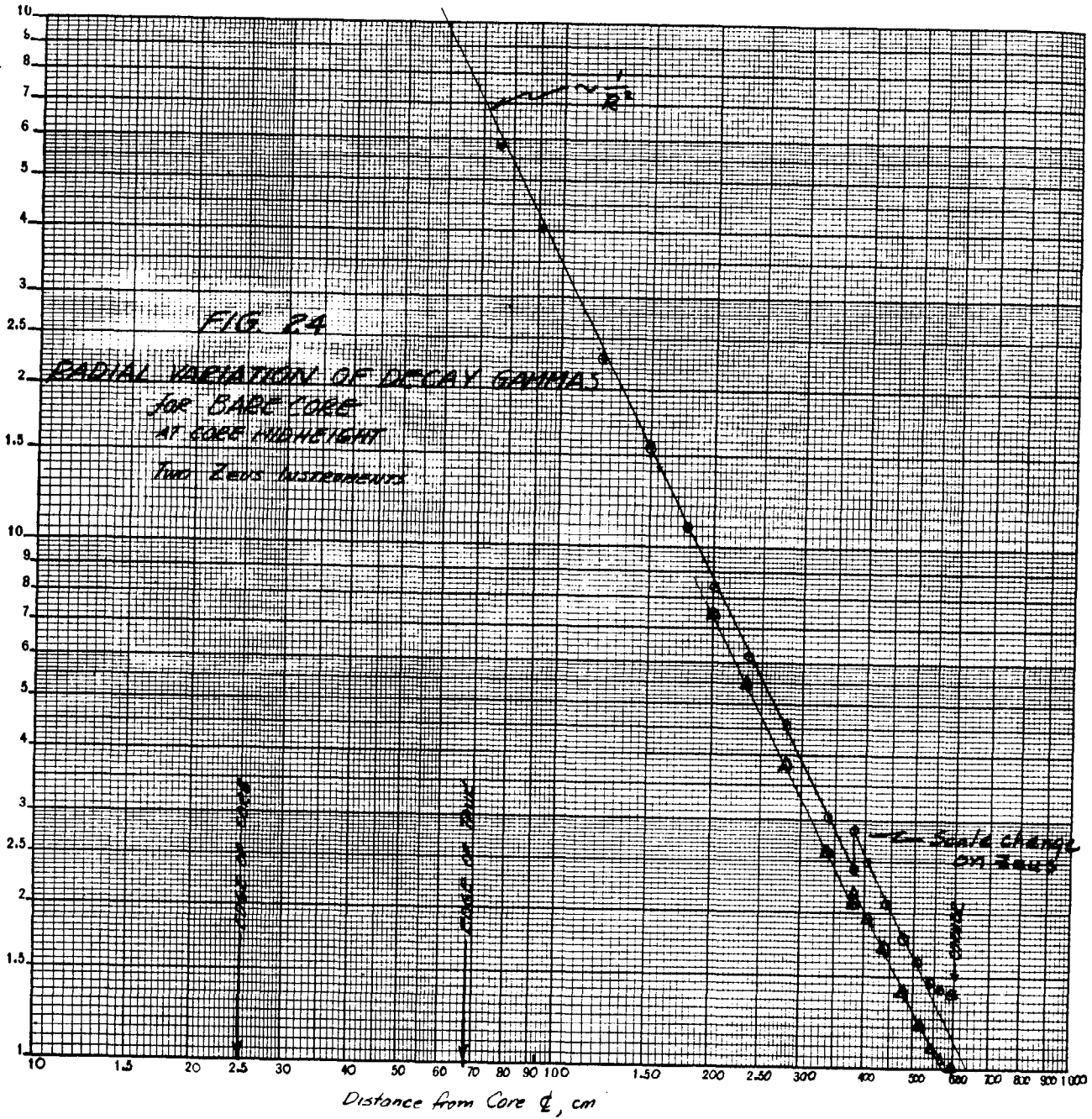
A series of γ -flux surveys were made after removing the water following a run with the reconstructed core. Three distributions of delayed γ 's were obtained. One was a radial distribution running from the edge of the tank to the SW corner of the room at $z = 0$ (origin at midplane of core). This distribution shown in Figure 24 is compared with a curve proportional to $1/R^2$ when $R = 0$ is taken at the core centerline. A second distribution was obtained above the core along the core axis. This is shown in Figure 25 compared with a $1/z^2$ curve drawn for a source at $z = 20 \text{ cm}$. The third distribution was a radial one along the line $y = x$ at $z = 134.6 \text{ cm}$ as shown in Figure 26.

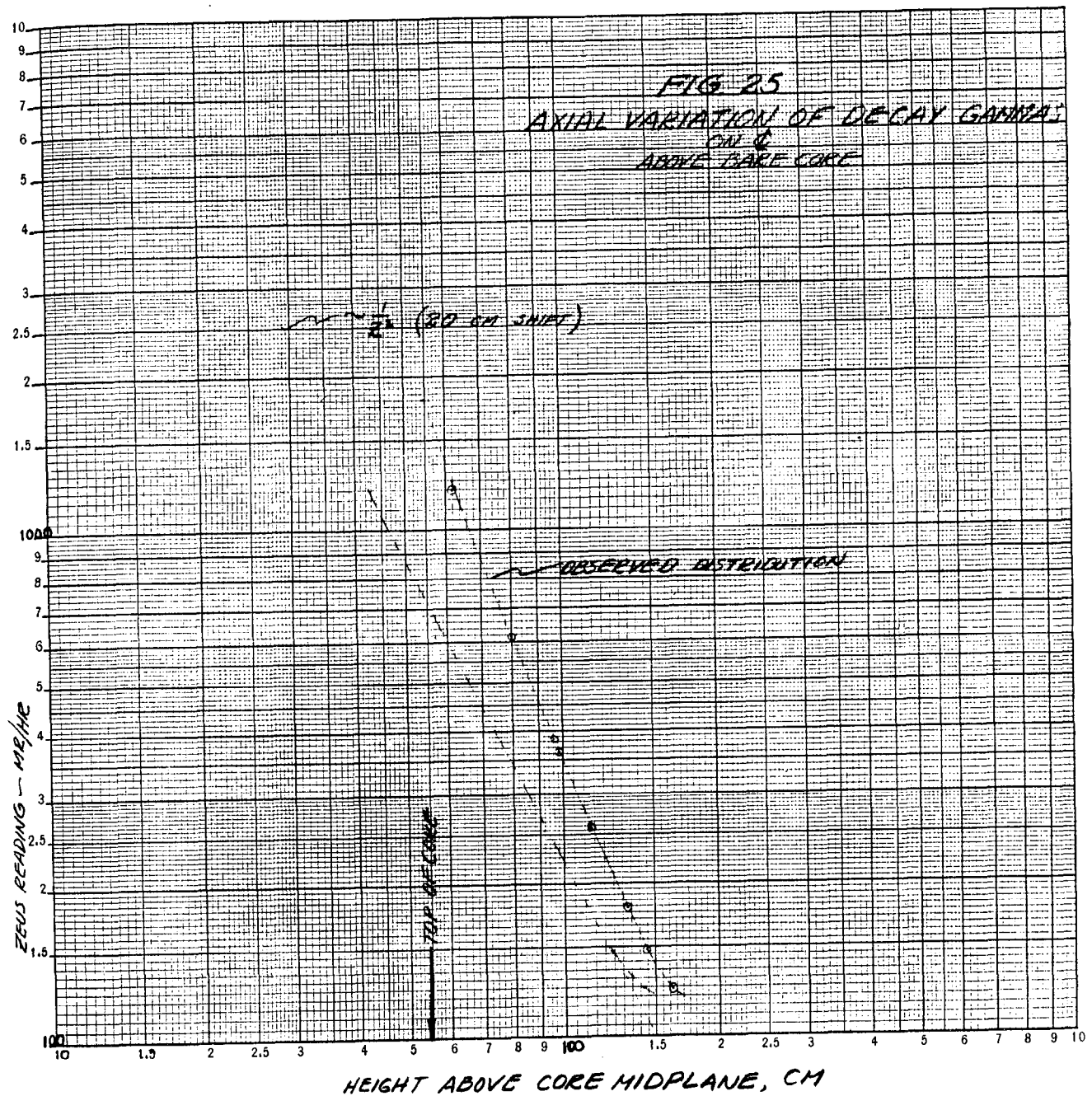
CALIBRATION OF P-V GAMMA MONITOR

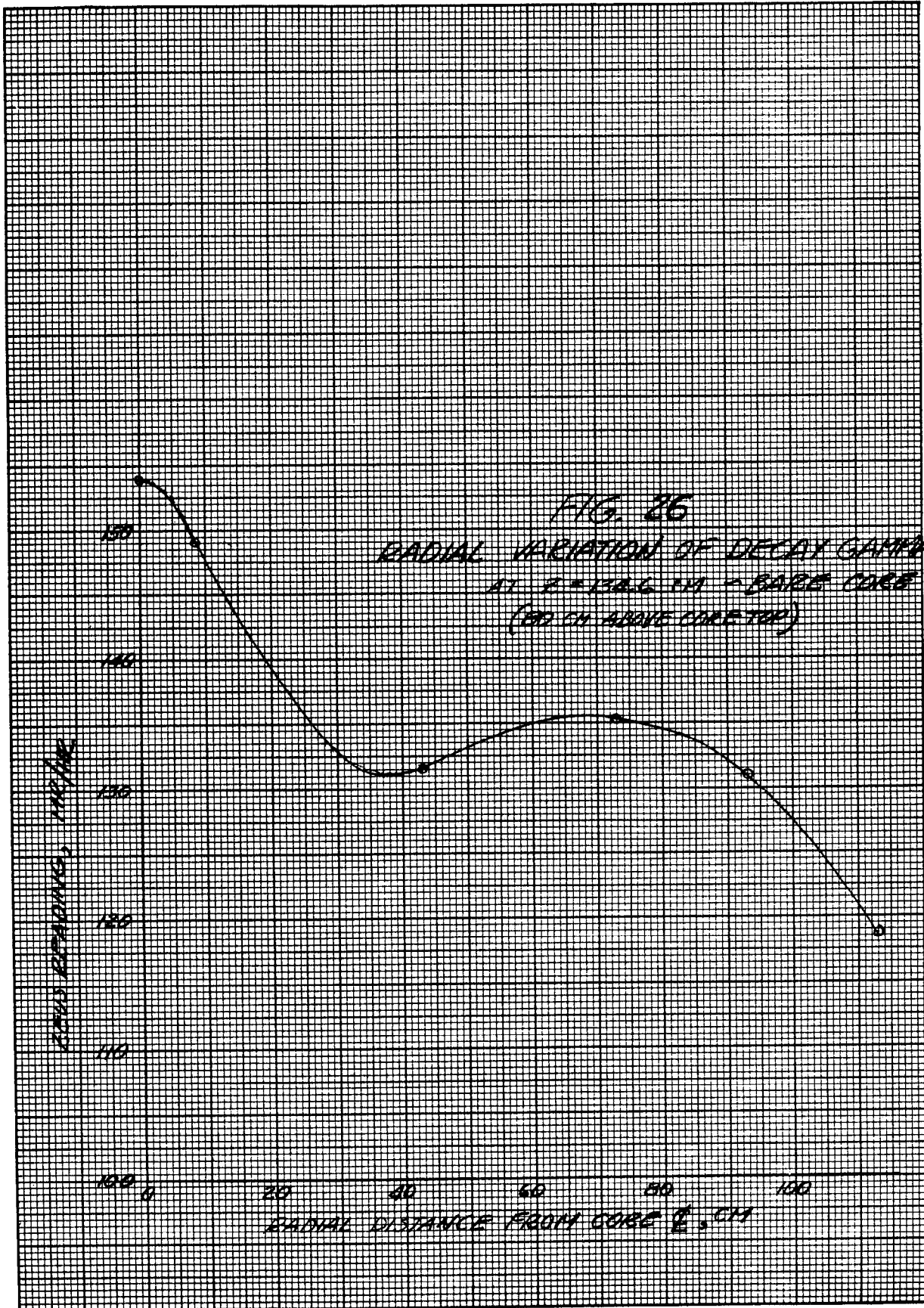
In addition to these measurements, P-V (argon-filled pressure chamber) was calibrated with the bare core (water out) after a run, using a Zeus survey meter. The intensity varied during decay by a factor of more than 100. Over











this range the factor of proportionality did not vary more than 2% and was found to be 2.63×10^{10} ($\pm 2\%$) mr/hr/amp. The same instrument was calibrated with a Co^{60} source at varying distances, using a Zeus survey meter. The inverse square law held to within 1% and a calibration 7% lower than for the bare core was obtained. This indicates that the instrument is relatively insensitive to the γ energy, since the average gamma energy for the core could be as low as 0.2 Mev as compared with 1.2 Mev for the Co^{60} source. As a result of this experiment, the readings on P-V following the burst could be related to the γ -intensity variation with time at the spatial position of the chamber.

GAMMA FLUX FIELD

The measurements made on the reconstructed core can be utilized along with those made on the accident core to establish the γ -flux field in the assembly room after $t = 0$ with respect to both time and space. The experimental data used is of three kinds: (1) decay scheme established by time recordings on P-V at one position, (2) Zeus readings near accident core as soon as access permitted, and the next day, and (3) axial and radial variations established with the reconstructed core. The readings of the first two kinds were correlated to a common time using the $t^{-1.21}$ scaling factor. The P-V readings were converted from chamber current to γ intensities using the correlation established with the bare reconstructed core and Zeus. The data of the third kind was also reduced to a common "time after scram," using decay records from P-V. This latter data gives the qualitative space variation. It was matched in magnitude with the data taken shortly after the accident where point in space coincided.

In the radial survey made from the tank wall to the SW corner of the room, the log distance - log intensity plot was a straight line of slope -2 if the zero distance was taken at the centerline of the core. Only deviations greater than 1% occurred within 40 cm of the room corner, where back-scattering was very noticeable and indicated readings were from 0% to 17% higher than predicted by inverse radius squared scheme.

In a survey made vertically above the core on its centerline, the data were found to follow the inverse distance squared scheme if the zero distance is chosen 20 cm above the reactor midplane, with a small amount of back-scattering evident above 150 cm from the midplane attributed to the massive steel components of the control rod drives and supports.

The two other principal distributions were made radially from the centerline in two places above the core (63 cm and 135 cm above the midplane). These were made to match the axial distribution and one point taken for the accident core. As one would expect, considering that the γ source distribution is everywhere like the prevailing thermal neutron flux distribution, at the time of the burst above the core the flux drops off radially until the edge of the core is reached whereupon contributions from the side of the cylinder are added. The low flux regions of the core at the "corners" manifest absorptions by the core.

Using all these data the γ flux field in the room has been reconstructed as visualized in Figure 7. The numbers are associated with a time 13.38 hours after the excursion. The dotted curves within the core show typical thermal neutron flux distributions in a vertical diametral plane passing half way between blade rod positions.

The variation with time for this delayed γ -flux field may be obtained as follows for t and t_n in seconds.

$$I_t = \left(\frac{t_n}{t}\right)^{1.21} I_n \quad 10^1 \text{ sec} < t < 10^5 \text{ sec}$$

$$I_t = 0.3311 t_n^{1.21} t^{-0.780} I_n \quad 10^0 \text{ sec} < t < 10^1 \text{ sec}$$

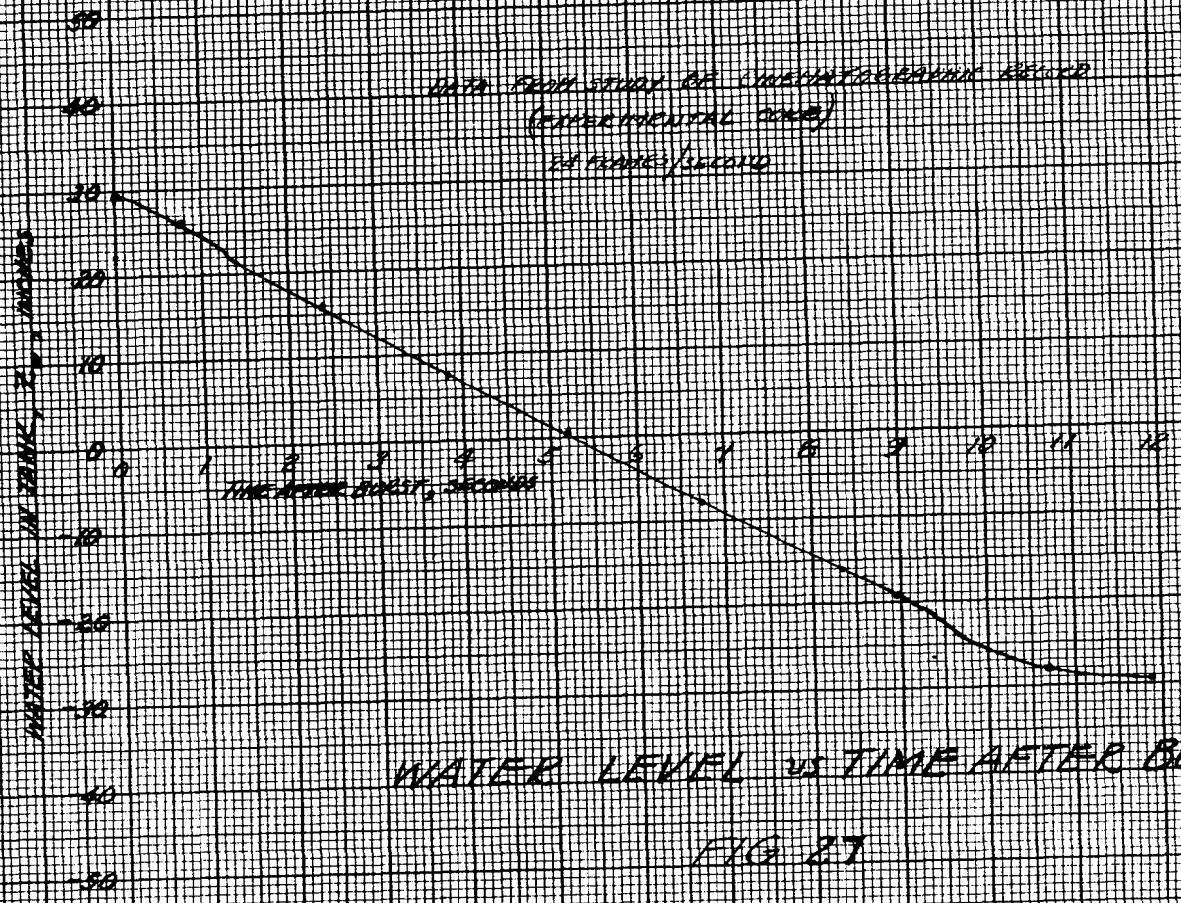
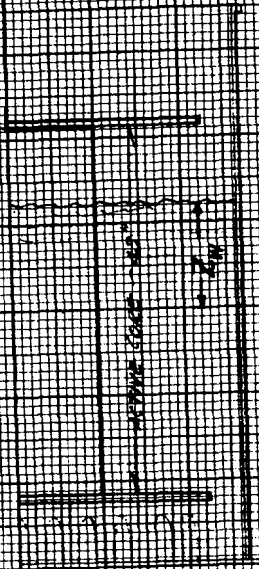
$$I_t = 0.3311 t_n^{1.21} t^{-0.311} I_n \quad 10^{-1} < t < 10^0$$

$$I_t = 0.6776 t_n^{1.21} I_n \quad 0 < t < 10^{-1}$$

Where I_n is γ -intensity at time t_n and I_t is γ -intensity at time t . This variation is based on variation of delay γ 's with time after fission for 1 fission by J. J. Taylor of WAPD.⁶

WATER DUMP

It was arranged to determine the water depth in the tank with core following a dump. Cinematographic records were obtained using 24 frames per second. From these records the location of the water surface was established in relation to time after de-energization of the electromagnetic clutch holding the dump valve closed. This derived variation of water level with time after dump is shown in Figure 27.



WATER LEVEL vs TIME AFTER BURST
FIG 27

SECTION II

SOME PHYSICS CONSIDERATIONS

F. W. Thalgott

CONDITIONS PRIOR TO EXCURSION

REACTIVITY AND REACTOR PERIOD

TOTAL ENERGY GENERATED

MECHANISM OF REACTOR SHUTDOWN

DURATION OF BURST

DELAYED NEUTRON ESTIMATES

SECTION II

SOME PHYSICS CONSIDERATIONS

F. W. Thalgott

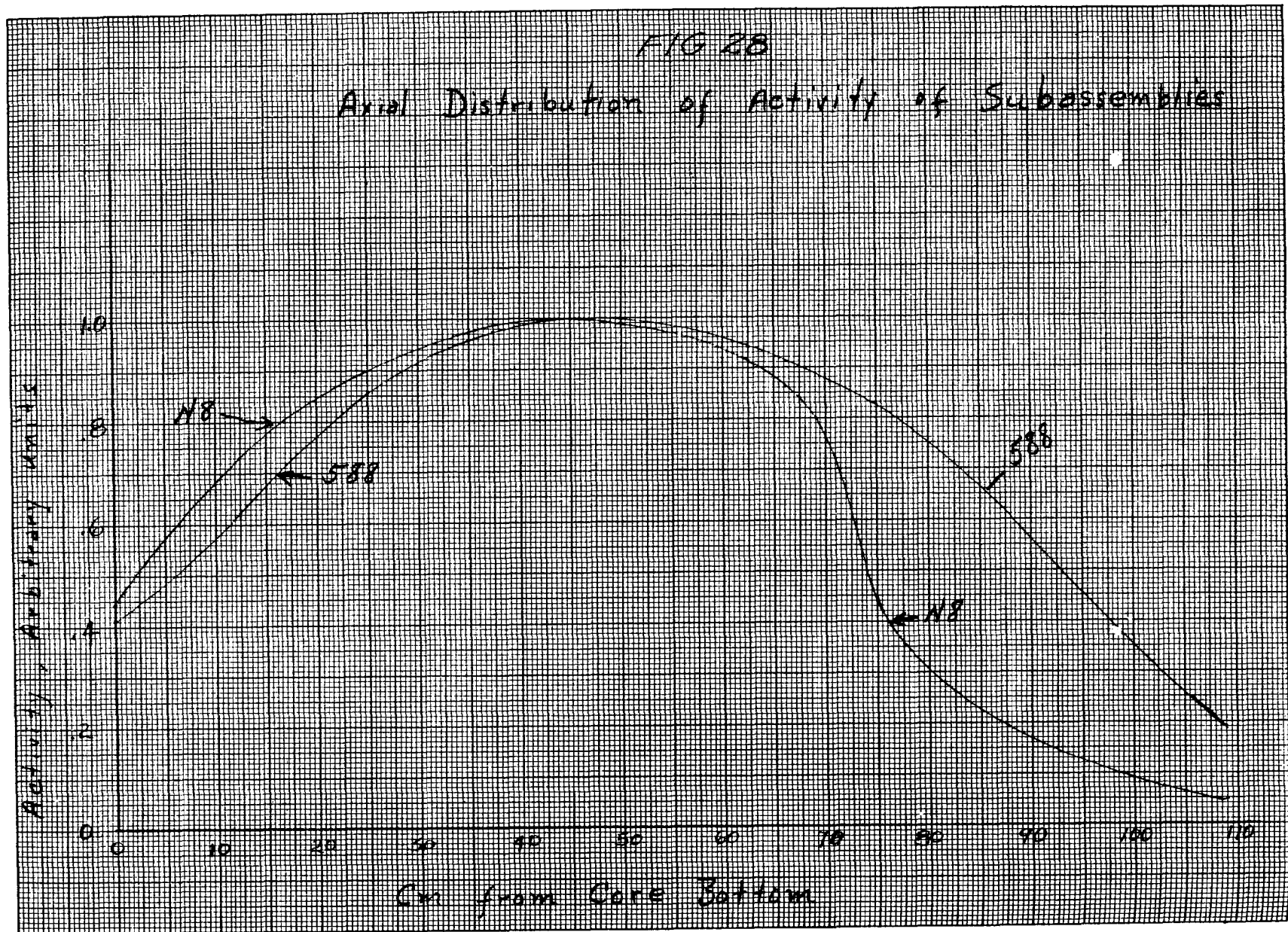
In attempting to analyze conditions in and around the reactor during and immediately following the excursion, it was necessary to establish some numbers for energy release and the shutdown mechanism using available data. These notes present calculations and considerations leading to the estimates needed. Measurements used have been presented in the preceding section.

CONDITIONS PRIOR TO EXCURSION

Something should first be said regarding the nuclear conditions of the core just before incident. The loading pattern of the core is shown in Figure 2. The four peripheral blade type safety rods were fully inserted. The tip of the cadmium-silver meat of the central cross type rod was 49.2 cm above the bottom of the core (bottom of the core defined as the lower fuel boundary). The core loading was 6.787 kg. The assembly could be made critical by withdrawing one blade type safety rod 32.5 cm. Using this calibration of the safety rod shown in Figure 2, it is seen that insertion of the safety rod from 32.5 cm to full insertion (zero cm) decreases the reactivity of the assembly by 100 inhours ($0.25\% \delta k/k$). Thus with the safety rods fully inserted the assembly was subcritical by 100 inhours or $0.25\% \delta k/k$.

REACTIVITY AND REACTOR PERIOD

The key to establishing reactivity introduced lies in determining the position of the central cross rod at the end of the excursion. The axial distribution of residual activity in fuel assembly N-8 (see Figure 2 for location) is considered the most reliable indication of maximum withdrawal of the central rod. This distribution (obtained from Figure 17a) is plotted in Figure 28 along with the distribution of activity for subassembly 588 (obtained from Figure 17b), normalized to the same maximum value for comparison. Figure 16 gives the radial distribution of fissions as derived from residual



activity measurements of individual elements of the core (see Figure 17b). The distribution for 588 is considered the nearest approach to the normal axial distribution, undisturbed by the central rod. As can be seen in Figure 17b, the distribution along element 193 is practically identical with that for 588. A comparison of the change in this normal distribution caused by the central rod, as evidenced by the distribution in N-8, with the change in the calculated distribution near a rod partially inserted in an infinite medium⁷ is shown in Figure 29. From this comparison the withdrawn position of the central rod is estimated as 75.4 ± 1.2 cm above the bottom of the core. Further evidence of the position of the central rod at the time of the burst is exhibited in Figure 30 in which the residual activity in rod #526 is compared to the distribution subsequently measured in a reconstruction of the core with the central rod located at 75.5 cm. It is seen that, although there is a marked flattening of the peak of the curve of residual activity, no vertical shifting of scale is necessary to achieve a fit of the lower portions.

A subsequent calibration of the worth of the central rod is given in Figure 19. It is seen that the worth of the central rod between 49.2 cm and 75.4 ± 1.2 cm is 735 ± 25 inhours or $1.87 \pm 0.06\%$ $\delta k/k$. Thus, subtracting 0.25% $\delta k/k$ for the initial subcriticality of the assembly we obtain $1.62 \pm 0.06\%$ $\delta k/k$ excess reactivity in the assembly with the central rod in its withdrawn position.

The macroscopic absorption cross section of the assembly for thermal (2200 m/sec) neutrons is 0.0690 cm^{-1} . Thus the lifetime of thermal neutrons in an infinite medium is 0.066×10^{-4} seconds. To account for the effect of the water reflector with its much lower absorption cross section and the rather negligible effect of slowing down time, a value of 10^{-4} seconds is probably reasonable for the actual reactor. Use of this lifetime and 1.62% excess reactivity gives a maximum reactor period of about 0.01 sec. With this period, less than 0.05 sec is required for the power to rise by the last factor of 100.

TOTAL ENERGY GENERATED

Three schemes are used to determine the energy release associated with the excursion. The first, considered most reliable, is based on fission product analyses and residual activity variation observed in core elements. Second, evidence provided by control rod rubbing shoe activation is utilized. Finally an attempt is made at calculating back for decay γ measurements made on the accident core some time after the burst. These determinations are outlined below and summarized subsequently.

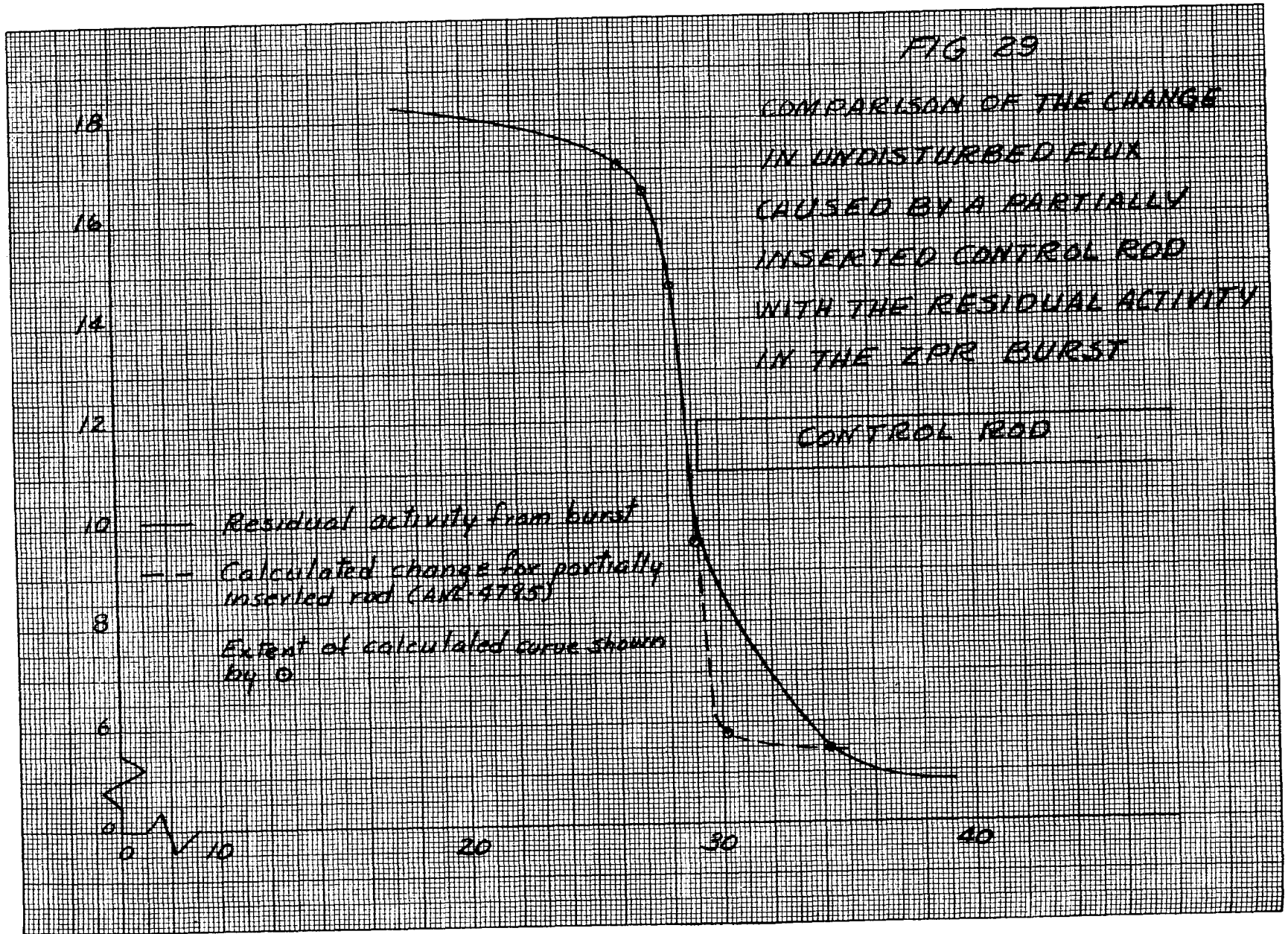
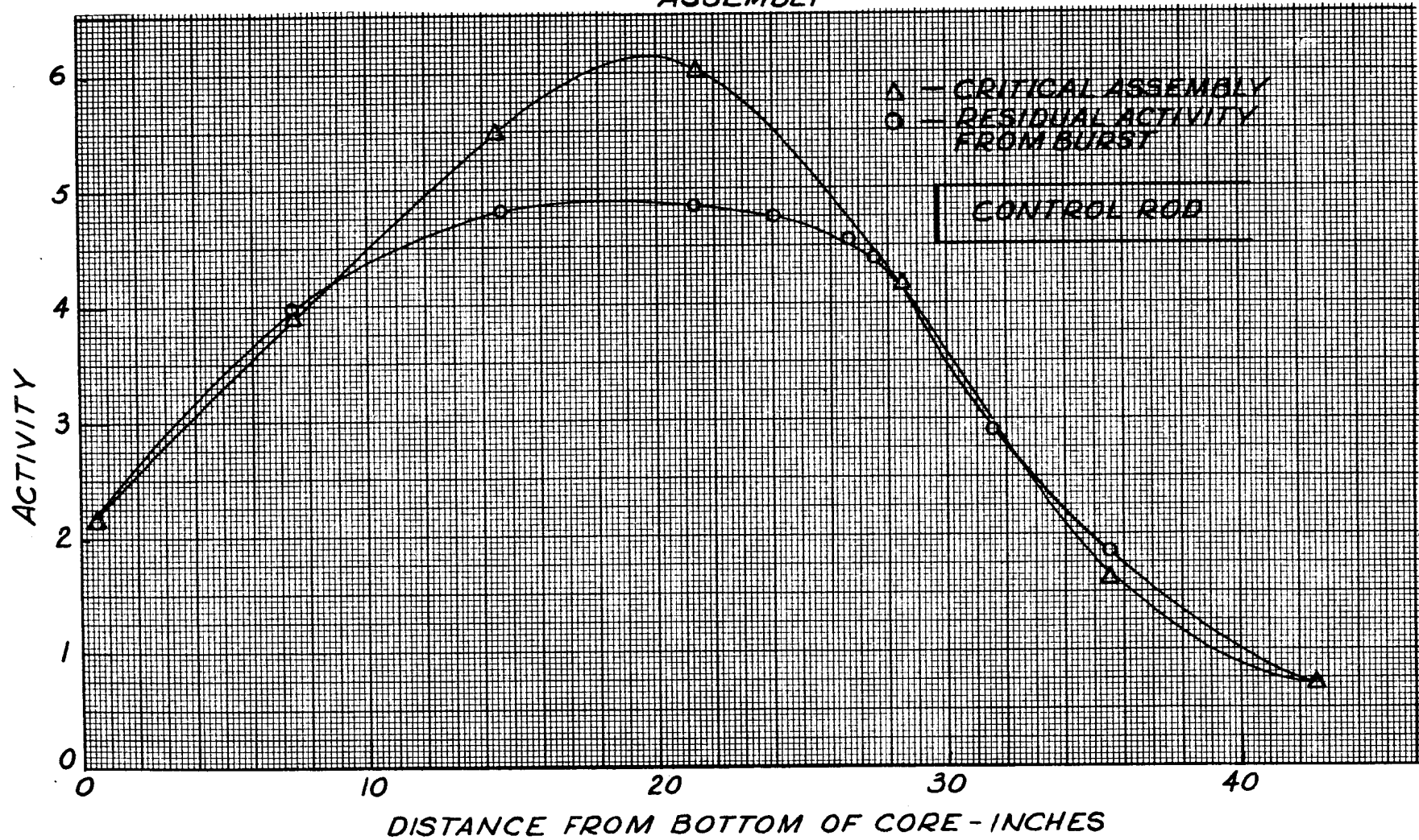


FIG. 30

COMPARISON OF RESIDUAL ACTIVITY IN FUEL
ROD #526 WITH MEASURED FLUX IN CRITICAL
ASSEMBLY



FISSION PRODUCT ANALYSES

Analyses of the fuel strip in ZPR-I for the fission product Mo^{99} give the following values for total fission density:

Subassembly N-6, 11.5 \pm 2.5 cm from top	1.01×10^{13} fissions/gm U^{235}
Subassembly N-6, 51 \pm 1 cm from top	3.33×10^{13} fissions/gm U^{235}
Subassembly 587, 54 \pm 6 cm from top	2.13×10^{13} fissions/gm U^{235}

From the survey of residual activity in various subassemblies of the core, the maximum to average ratio of power density is about 2.4 to 1, and the ratio of maximum power density to the power density at the center of subassembly N-6 is 1.3 to 1. This gives for the total number of fissions in the core:

$$\text{Total fissions} = \frac{1.3}{2.4} \times 3.33 \times 10^{13} \frac{\text{fissions}}{\text{gm U}} \times 6787 \text{ gm of U} = \underline{1.22 \times 10^{17}}$$

The ratios of fission densities observed in the three locations tabulated above agree with the residual activity ratios among these locations to 20% or better.

CONTROL ROD RUBBING SHOE ACTIVATIONS

Comparison of the Co^{60} activation in one of the stellite rubbing shoes of the ZPR-I central rod (Figure 3) with the activation of a similar shoe by a known thermal flux in the CP-2 thermal column, leads to a second determination of the power generation. The integrated thermal column flux associated with the irradiations was 1.55×10^{12} neutrons/cm² and the ratio of activation for the ZPR-I shoe to the shoe used in the CP-3 experiment was 31.6 so that the integrated flux at the position of the stellite shoe in the core is 4.9×10^{13} n/cm². This gives a fission density at this position of $4.9 \times 10^{13} \times \frac{0.6023 \times 473}{235} = 5.9 \times 10^{13}$ fissions/gm. From Figure 16 the ratio of maximum power density to density at this point is 1:0.7 hence with a maximum/average ratio of 2.4, the total number of fissions in the core would appear to be $5.9 \times 10^{13} \times 1/0.7 \times 1/2.4 \times 6787 = 2.4 \times 10^{17}$ fissions. However, some further considerations of the nature of the thermal column experiments lead to modification.

The irradiation of the stellite shoe was carried out in a beam from the thermal column of CP-3. The axis of the cross rod tip was parallel to the beam, hence the neutron path was roughly along the major axis of the stellite shoe. The activity comparison was made approximately 0.6 cm from the leading edge of the shoe. The absorption mean free path of thermal neutrons in stellite is 0.48 cm, the scattering mean free path is 2.3 cm.

Hence the point scanned could by simple theory have been subjected to a flux attenuated by a factor of 3.5. This theory assumes perfect alignment of the beam and rod tip and does not account for the complex geometry of the tip. Experimental scans of the rod tip, however, indicate an attenuation of approximately 1.4. With this latter correction applied the total fissions in the core become 1.71×10^{17} .

This is somewhat higher than that given by the Mo⁹⁹ analysis. However, it should be pointed out here that the flux gradient at the rod tip should be greater than that read from the residual activity of fuel element N-8, i.e., the ratio of flux at the shoe to maximum flux should be less than the value of 0.7. If such were the case one would obtain even closer agreements.

RESIDUAL GAMMA ACTIVITY

A number of observations of the residual activity from the core were made with survey instruments and with the argon-filled γ -sensitive pressure chamber, P-V, which is part of the normal monitoring instrumentation of ZPR-I. Later calibrations of P-V provided the mr/hr equivalent of the chamber current. All the readings were normalized to the position of P-V at a given time using a $t^{-1.21}$ decay scheme and a $1/R^2$ geometrical attenuation to obtain an average value of γ intensity of 928 mr/hr at 202 cm from the core and in the midplane at $t = 5$ hours.

The fraction of energy lost per cm^3 of air varies between 3.0×10^{-5} and 3.8×10^{-5} from 0.1 Mev to 2.0 Mev. At 1 Mev the fraction of energy lost is 3.6×10^{-5} . Hence, with $1r = 83$ ergs/gm air; air = 1.23×10^{-3} gm/ cm^3

$$1 \text{ r/hr} = \frac{83 \times 1.23 \times 10^{-3}}{3.6 \times 10^{-5} \times 1.6 \times 10^{-6} \times 3.6 \times 10^3} = 4.92 \times 10^5 \frac{\text{Mev of } \gamma \text{ flux}}{\text{cm}^2 \text{ sec}}$$

With 928 mr/hr observed at a distance of 202 cm^2 , the total energy leaving the core is

$$(4.92 \times 10^5) (0.928) (4\pi 202^2) = 2.34 \times 10^{11} \text{ Mev/sec.}$$

At times of the order of 5 hours after fission, experimental data on delay γ energy emission are best fitted by⁶

$$\text{Mev/sec fission} = 1.6 t^{-1.21}$$

At 5 hours this yields

$$\text{Mev/sec fission} = 1.14 \times 10^{-5}$$

For 1 Mev gammas, the dry ZPR-I core, (0.6 Zr, 0.11 ^{plastic-U} ~~plastic-U~~, 0.29 void, by volume) has a linear absorption coefficient of 0.214. Limits on the fraction of γ energy escaping the core may be obtained by considering the core to be a sphere of 1) 25.8 cm radius (radius of ZPR-I core); 2) 37.8 cm radius (radius of sphere of volume equal to ZPR-I core).

The fractional gamma leakages from the core, are for the conditions mentioned above, 0.145 and 0.098 respectively⁸, leading to limits of

$$1) \frac{2.34 \times 10^{11}}{1.14 \times 10^{-5} \times 0.145} = 1.41 \times 10^{17} \text{ fissions}$$

and

$$2) \frac{2.34 \times 10^{11}}{1.14 \times 10^{-5} \times 0.098} = 2.09 \times 10^{17} \text{ fissions.}$$

A better estimate of the core self shielding may be arrived at, since the γ intensity is known to follow a $1/r^2$ spatial distribution in the regions where measurements were made, and hence is equivalent to an unshielded point source of lower strength. Consider the γ flux of direction ω per unit solid angle, $d\omega$ arriving at the surface of a half space with uniform isotropic source Q_0 .

$$F d\omega = \frac{Q_0}{4\pi} d\omega \int_0^\infty dr e^{-\sigma r} = \frac{Q_0 d}{4\pi}$$

The flux incident on a surface at distance z from an emitting surface d cm by h cm is

$$F = \frac{Q_0}{4\pi\sigma} \frac{hd}{z^2}$$

i.e., at infinity the core will look like a point source of strength $Q_0 hd/\sigma$. Assuming the decay γ energy flux is constant from 0.1 to 2 Mev, and zero elsewhere⁹, the absorption coefficient σ may be expressed as¹⁰

$$\sigma(E) = 0.164 \left(\frac{2}{E}\right)^{0.789}$$

From the radial distribution of residual activity in the fuel elements, Figure 16, the ratio of activity near the surface of the core to the average

activity in the core is $0.45/0.56 = 0.802$ with the activity fairly constant near the surface. With $Q_0 = 0.8 \bar{Q}$ where \bar{Q} is the average source strength in the core, the apparent strength of a point source would be:

$$Q_{app} = \frac{0.8 \bar{Q} h d}{1.9} \int_{0.1}^2 \frac{dE}{(E)}$$

while the actual source strength would be $Q V$ where V is the volume of the core. The fraction of γ energy escaping would then be

$$P(E) = \frac{\frac{Q_0 h d}{\sigma(E)}}{Q V} = \frac{0.8 h d}{V \sigma(E)}$$

or

$$P = \int_0^{\infty} P(E) dE = \frac{0.8 h d}{1.9 V} \int_{0.1}^2 \frac{dE}{\sigma(E)}$$

With $h = 109$ cm, $d = 51.6$ cm, active volume = 213000 cm³

$$P = 0.135$$

This analysis is valid as long as the source (core) is thick as viewed from the point of measurement.

Using this fractional escape we estimate

$$\frac{2.34 \times 10^{11}}{1.14 \times 10^{-5} \times 0.135} = 1.52 \times 10^{17} \text{ fissions.}$$

SUMMARY - TOTAL ENERGY

The several estimates made above are summarized as follows.

<u>Method</u>	<u>Total Number of Fissions</u>
Fission Product Analysis	1.22×10^{17}
Control Rod Rubbing Shoe Activations	1.71×10^{17}
Residual Gamma Activity	1.52×10^{17}

Of these, the first is most closely related to the total number of fissions and accuracy is greatest. In effect the second two determinations are checks on the first. Considering this, it is felt that the total number of fissions derived from the fission product analysis is most reliable and it is used exclusively in calculations.

If one assumes 190 Mev/fission this yields 1040 watt hours or 3.75×10^6 joules for total energy.

MECHANISM OF REACTOR SHUTDOWN

Examination of the effects of fission energy release on the plastic fuel strips leads to the conclusion that the introduction of voids in the plastic was the primary means of making the reactor subcritical. Details of the mechanism leading to this conclusion are established in the following account.

As previously described, microscopic examination of a foil cut from an unirradiated ZPR-I fuel strip shows that most of the uranium oxide ($\sim 100\%$ U_3O_8) contained in the foil is disposed in particles of approximately 10 micron diameter. However, about 10^4 particles of 40 micron diameter/cc of fuel strip were found. This amounts to the fact that $1/2\%$ of the fuel is in the large particles. The heating of the small (10μ) particle group and the large (40μ) particle group are considered separately.

SMALL PARTICLES

The volume of fuel strip associated with each small particle is 13.5 times the volume of the particle, i.e., a 10μ particle embedded in a sphere ~~12.4~~³⁴ microns in diameter. An unpublished analysis by H. Greenspan of the time variation of the temperature distribution in such a sphere, with an exponentially rising heat source gives as the temperature V in the oxide, $0 \leq r \leq r_1$, for an initial temperature V_0

$$V_1(r, t) = V_0 + \frac{a}{\alpha} (e^{at} - 1)$$

$$+ e^{at} \frac{K_2}{K_1} ar_1 \frac{\left[\sqrt{\frac{a}{K_2}} (r_2 - r_1) \cosh \sqrt{\frac{a}{K_2}} (r_2 - r_1) + \left(\frac{a}{K_2} r_2 r_1 - 1 \right) \sinh \sqrt{\frac{a}{K_2}} (r_2 - r_1) \right] \sinh \sqrt{\frac{a}{K_1}} r}{\alpha r D(\sqrt{a})}$$

$$+ \frac{K_2}{K_1} ar_1 \frac{\left[\frac{(r_2 - r_1)^3}{K_2} + \frac{3(r_2 - r_1)r_2 r_1}{K_2} \right]}{\alpha \left[\frac{K_2}{K_1} r_1 \frac{(r_2 - r_1)^3 + 3(r_2 - r_1)r_2 r_1}{K_2} + \frac{r_1^4}{K_1} \right]}$$

$$+ \frac{K_2}{K_1} ar_1 \sum_{j=1}^{\infty} \frac{e^{-\lambda_j^2 t} \left[\frac{\lambda_j}{\sqrt{K_2}} (r_2 - r_1) \cos \frac{\lambda_j}{\sqrt{K_2}} (r_2 - r_1) - \left(\frac{\lambda_j^2 r_2 r_1}{K_2} + 1 \right) \sin \frac{\lambda_j}{\sqrt{K_2}} (r_2 - r_1) \right] \sin \frac{\lambda_j}{\sqrt{K_1}} r}{\lambda_j^2 (\lambda_j^2 + \alpha) \frac{d}{ds} [D(\sqrt{s})] \Big|_{s = -\lambda_j^2}} r$$

and in the plastic, $r_1 \leq r \leq r_2$, with an initial temperature V_0

$$V_2(r, t) = V_0 + \left\{ \frac{e^{at} ar_1 \left[\sinh \sqrt{\frac{a}{K_1}} r_1 - \sqrt{\frac{a}{K_1}} r_1 \cosh \sqrt{\frac{a}{K_1}} r_1 \right] \left[\sqrt{\frac{a}{K_2}} r_2 \cosh \sqrt{\frac{a}{K_2}} (r_2 - r) - \sinh \sqrt{\frac{a}{K_2}} (r_2 - r) \right]}{\alpha D(\sqrt{a})} r \right\}$$

$$- \frac{ar_1^4}{K_1}$$

$$+ \frac{\alpha \left[\frac{K_2}{K_1} r_1 \frac{(r_2 - r_1)^3 + 3(r_2 - r_1)r_2 r_1}{K_2} + \frac{r_1^4}{K_1} \right]}{\alpha \left[\frac{K_2}{K_1} r_1 \frac{(r_2 - r_1)^3 + 3(r_2 - r_1)r_2 r_1}{K_2} + \frac{r_1^4}{K_1} \right]}$$

$$+ \sum_{j=1}^{\infty} ar_1 e^{-\lambda_j^2 t} \frac{\left[\sin \frac{\lambda_j}{\sqrt{K_1}} r_1 - \frac{\lambda_j}{\sqrt{K_1}} r_1 \cos \frac{\lambda_j}{\sqrt{K_1}} r_1 \right] \left[\frac{\lambda_j}{\sqrt{K_2}} r_2 \cos \frac{\lambda_j}{\sqrt{K_2}} (r_2 - r) - \sin \frac{\lambda_j}{\sqrt{K_2}} (r_2 - r) \right]}{\lambda_j^2 (\lambda_j^2 + \alpha) \frac{d}{ds} [D(\sqrt{s})] \Big|_{s = -\lambda_j^2}} r$$

where $D(\sqrt{s}) \equiv -\frac{K_2}{K_1} \sinh \mu_1 r_1 [\mu_2 (r_2 - r_1) \cosh \mu_2 (r_2 - r_1) + (\mu_2^2 r_2 r_1 - 1) \sinh \mu_2 (r_2 - r_1)]$

$$+ [\mu_2 r_2 \cosh \mu_2 (r_2 - r_1) - \sinh \mu_2 (r_2 - r_1)] [\sinh \mu_1 r_1 - \mu_1 r_1 \cosh \mu_1 r_1]$$

with
$$\mu_k^2 = \frac{S}{\kappa_k}, \kappa_k = \frac{K_k}{\rho_k C_k}, a = \frac{Q}{\rho_1 C_1} \quad (k = 1, 2)$$

where Q = heat source, ρ = density, C = specific heat, K_k = thermal conductivity, $1/\alpha$ = period of exponential increase and where λ_j are the roots of $D(i\lambda_j) = 0$. For values of $\alpha t \sim 7$ the last two terms in each equation are negligible.

Thus, asymptotically, the solution may be considered as separable with the spatial distribution multiplied by an exponential time variation.

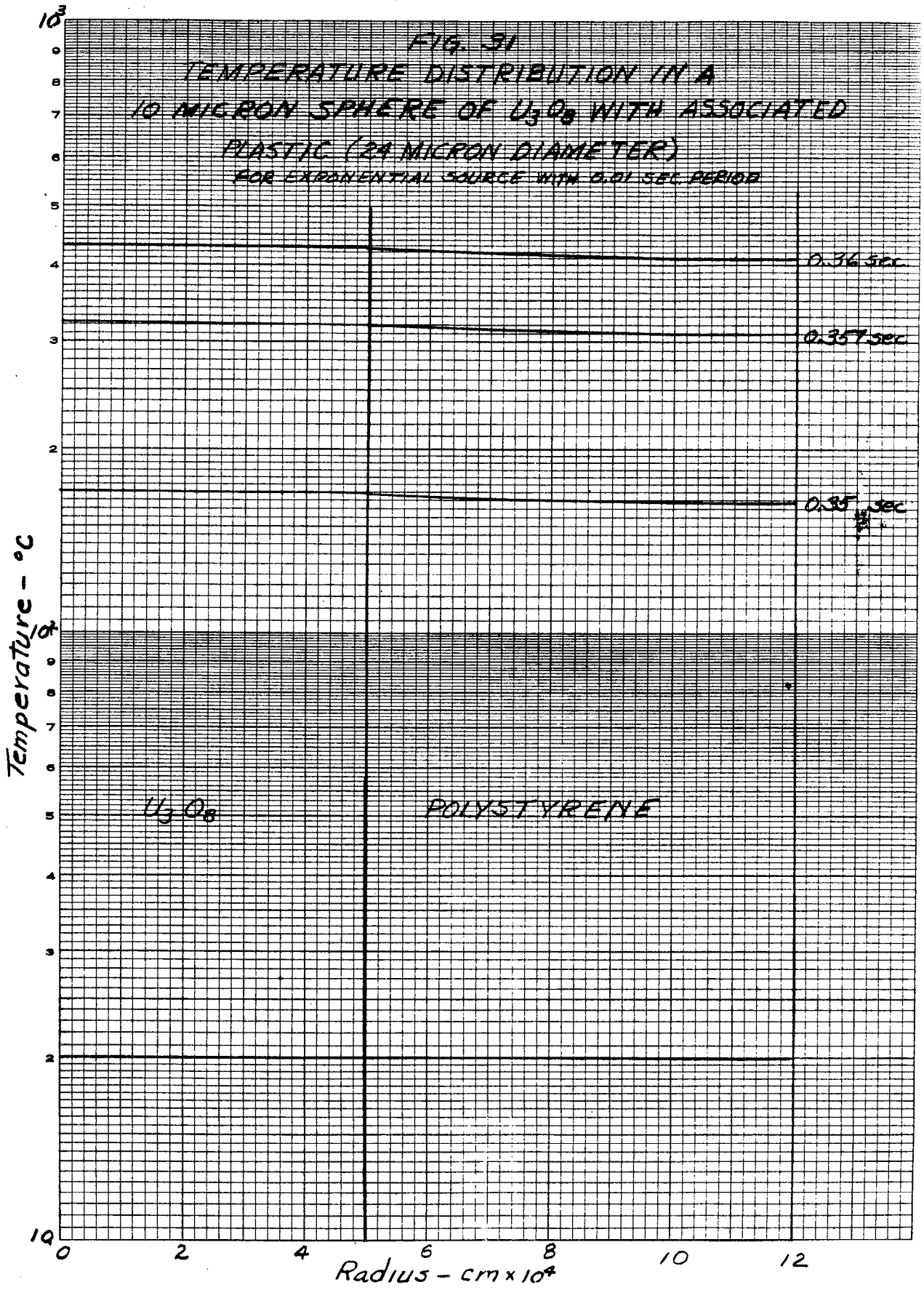
Figure 31 shows the temperature distribution resulting from the smaller particles, assuming for the oxide $\rho_1 = 7 \text{ gm/cm}^3$, $C_1 = 0.08 \text{ cal/gm}^\circ\text{C}$, $K_1 = 2 \times 10^{-3} \text{ cal/cm}^2 \text{ sec } ^\circ\text{C cm}$ and for the plastic $\rho_2 = 1.05 \text{ gm/cm}^3$, $C_2 = 0.32 \text{ cal/gm}^\circ\text{C}$, $K_2 = 4 \times 10^{-4} \text{ cal/cm}^2 \text{ sec } ^\circ\text{C cm}$ with an initial temperature of 20°C , an initial source strength of 1 fission/gm of uranium-235 rising exponentially with a period of 0.01 sec.

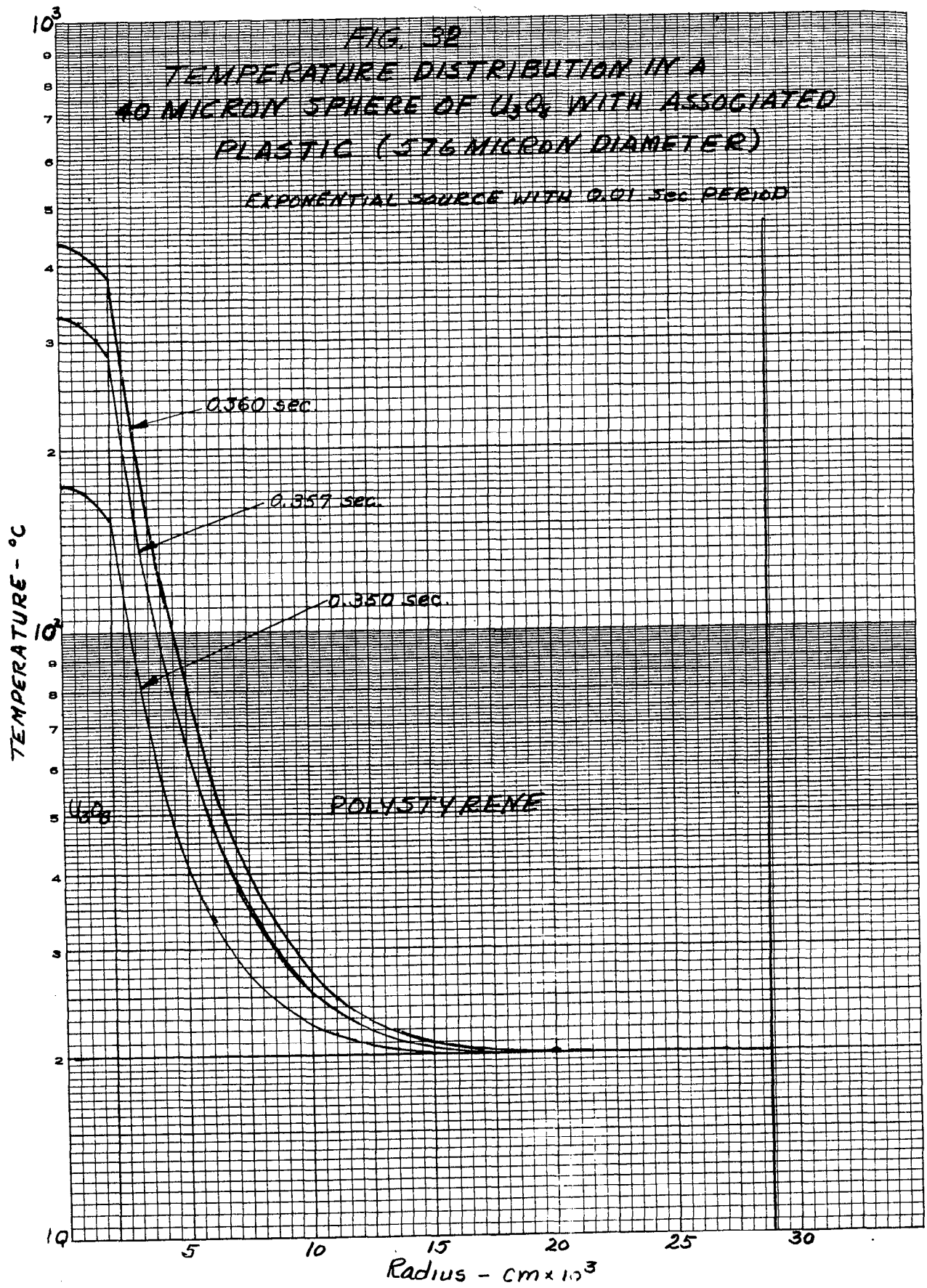
It is seen that the temperature rise is essentially uniform throughout the particle-plastic sphere, i.e., the particles are small enough and closely enough packed that the heat source may be considered uniformly distributed in this power range.

LARGE PARTICLES

The larger particles (40μ diameter) occur much less frequently. Assuming 10^4 particles per cm^3 of fuel strip, with each 40 micron particle there is associated a sphere of fuel strip material of radius 0.0288 cm. The temperature distribution in the sphere is given in Figure 32 using the same material constants as for the smaller sphere. For these particles, with associated strip material, temperatures in the oxide greatly exceed the temperature of the bulk of the strip material in the total energy range of interest, i.e., approximately 10^{17} total fissions.

Thus it is seen that the heat generation (essentially all in the smaller particles) may, as far as temperature distribution in the strip is concerned, be considered as fundamentally uniform in the strip, with perturbations created by the larger particles. From Figure 14 it seems that temperatures in the plastic immediately adjacent to larger fuel particles exceeds bulk plastic temperature by 250°C after $\sim 3 \times 10^{13}$ fissions per gram have occurred.





WATER HEATING

There remains the problem of heat conduction to the water. Five of the seven fuel strips per fuel element in the ZPR-I were glued to Zr strips, the other two were loosely held in the water channels. However for this analysis it is sufficient to consider alternate strips of fuel and water. For such a symmetrical arrangement with a uniformly distributed exponentially rising heat source in the strip, the time variation of the temperature distribution V in the strips is: $0 \leq x \leq l_1$, with an initial temperature V_0

$$V_1(x,t) = V_0 + \frac{a}{\alpha} (e^{\alpha t} - 1) - \frac{\beta a}{\alpha} e^{\alpha t} \frac{\sinh \sqrt{\frac{\alpha}{\kappa_2}} (l_2 - l_1) \cosh \sqrt{\frac{\alpha}{\kappa_1}} x}{g(\sqrt{\alpha})}$$

$$- \frac{\beta a}{\alpha} \frac{\frac{l_2 - l_1}{\sqrt{\kappa_2}}}{\frac{l_1}{\sqrt{\kappa_1}} + \beta \frac{(l_2 - l_1)}{\sqrt{\kappa_2}}} + \beta a \sum_{j=1}^{\infty} \frac{2 \sin \lambda_j \frac{l_2 - l_1}{\sqrt{\kappa_2}} \cos \frac{\lambda_j x}{\sqrt{\kappa_1}} e^{-\lambda_j^2 t}}{\lambda_j (\lambda_j^2 + \alpha) \left. \frac{d}{d\lambda} \{g(\lambda)\} \right|_{\lambda = i\lambda_j}}$$

and in the water is; $l_1 \leq x \leq l_2$

$$V_2(x,t) = V_0 + \frac{a}{\alpha} e^{\alpha t} \frac{\sinh \sqrt{\frac{\alpha}{\kappa_1}} l_1 \cosh \sqrt{\frac{\alpha}{\kappa_2}} (l_2 - x)}{g(\sqrt{\alpha})}$$

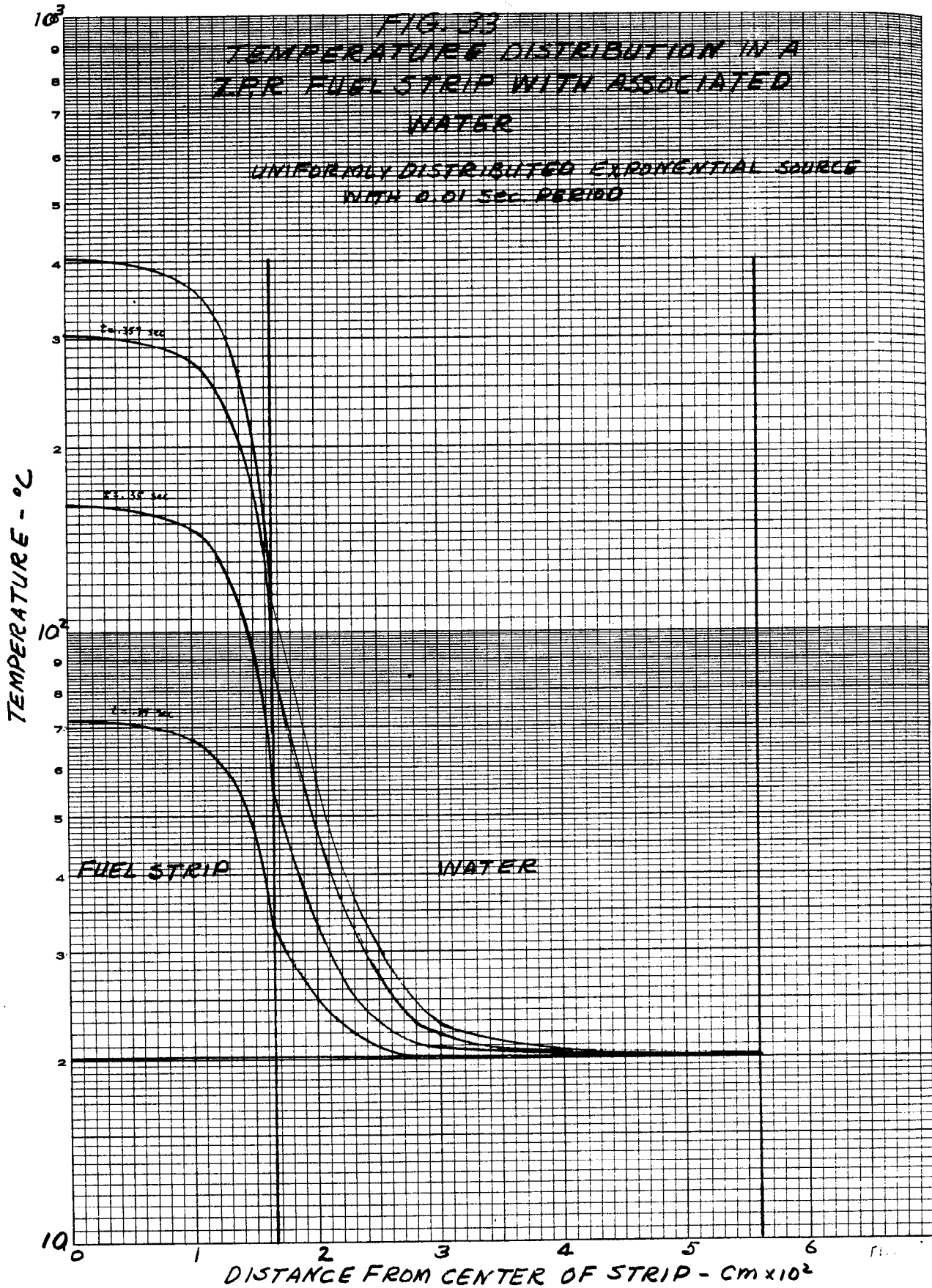
$$+ a \frac{\frac{l_1}{\sqrt{\kappa_1}}}{\frac{l_1}{\sqrt{\kappa_1}} + \frac{\beta(l_2 - l_1)}{\sqrt{\kappa_2}}} - a \sum_{j=1}^{\infty} \frac{2 \sin \lambda_j \frac{l_1}{\sqrt{\kappa_1}} \cos \frac{\lambda_j}{\sqrt{\kappa_2}} (l_2 - x) e^{-\lambda_j^2 t}}{\lambda_j (\lambda_j^2 + \alpha) \left. \frac{d}{d\lambda} \{g(\lambda)\} \right|_{\lambda = i\lambda_j}}$$

where $g(\sqrt{S}) = \sinh \mu_1 l_1 \cosh \mu_2 (l_2 - l_1) + \beta \cosh \mu_1 l_1 \sinh \mu_2 (l_2 - l_1)$

$$\mu_k^2 = \frac{S}{\kappa_k}; \kappa_k = \frac{K_k}{\rho_k C_k} (k = 1, 2); a = \frac{Q}{\rho_1 C_1}; \beta = \frac{K_2 \sqrt{\kappa_1}}{K_1 \sqrt{\kappa_2}}$$

Q = heat source, ρ = density, C = specific heat, K_k = thermal conductivity, $1/\alpha$ = period of exponential increase and where $i\lambda_j$ are roots of $g(i\lambda_j) = 0$. Again for $\alpha t \sim 7$ the last two terms are negligible.

Figure 33 shows the temperature distribution resulting in the strip and water, assuming for the strip (composite of oxide and plastic) $\rho_1 = 1.49 \text{ gm/cm}^2$, $C_1 = 0.234 \text{ cal/gm } ^\circ\text{C}$, $K_1 = 4.2 \times 10^{-4} \text{ cal/cm}^2 \text{ sec } ^\circ\text{C cm}$



and for water $\rho_2 = 1 \text{ gm/cm}^3$, $C_2 = 1 \text{ cal/gm } ^\circ\text{C}$ and $k_2 = 1.4 \text{ cal/cm}^2\text{sec } ^\circ\text{C cm}$, with an initial temperature of 20°C , an initial source strength of 1 fission/gm of uranium-235, rising exponentially with a period of 0.01 sec.

It is seen that the temperature is fairly uniform through the plastic except near the edges where it falls off very rapidly. After 3×10^{13} fissions per gram of uranium the maximum temperature of the uniformly heated plastic is $\sim 300^\circ\text{C}$ while the surface temperatures, i.e., maximum water temperature, is $\sim 90^\circ\text{C}$. If we superimpose on this distribution the effects of the larger oxide particles it is seen that plastic temperatures of $\sim 550^\circ\text{C}$ might exist adjacent to the particles with maximum water temperatures of $< 100^\circ\text{C}$.

From the above analysis the heat flow into the water may be determined and, neglecting the effects of the transient terms, is at all times less than 20% of the total heat generated.

CONCLUSIONS

The appearance of the elements taken from the core confirm the temperature calculations made for the established energy release, when correlated with known characteristics of the plastic set forth in the previous section. The experiments conducted to indicate gross behavior of fuel strip at various temperatures (Figure 15) along with the depolymerization temperatures, softening temperatures, and monomer vaporization temperatures are factors considered.

Thus it seems likely that the primary mechanism of reactor shutdown was vaporization of the plastic at local hot-spots in the fuel strip, before water temperatures were sufficient to form steam. This, of course, was followed by some steam formation as the heat stored temporarily in the plastic flowed into the water before the dump.

Lack of information concerning volume changes accompanying plastic vaporization, and the quantity of heat required to thus destructively distill polystyrene prevents direct quantitative analysis of the shutdown mechanism to determine total energy release. However, to illustrate order of magnitude of the effects, assuming expansion of the plastic by $\sim 10^3$ upon vaporization with a molar heat of disassociation equal to twice the molar heat of vaporization of water, in order to completely fill the spaces between the zirconium strips it is necessary to vaporize 0.3% of the plastic and requires 1.4% of the total energy release of 1.14×10^{17} fissions. Neglecting, then, the energy necessary to vaporize the strip we consider only the energy necessary to heat the strip to 300°C per cm^3 of strip, the quantity of heat necessary to raise the strip from 20°C to 300°C is

$$Q = \Delta t C \rho = 280(0.3493) = 97.8 \text{ cal or } 409 \text{ joules.}$$

With a U^{235} content of the strip, (7.46% U_3O_8 by volume, 93.2% enriched) of 0.412 gm/cm^3 , this corresponds to

$$\frac{409 \times 3.26 \times 10^{10}}{0.412} = 3.23 \times 10^{13} \text{ fissions/gm } U^{235} .$$

This is compared with the average of 1.8×10^{13} fissions per gram of U^{235} and a maximum value of 4.3×10^{13} fissions per gram of U^{235} .

DURATION OF BURST

An estimate of the duration of the entire burst has been made by comparing the rate of rod withdrawal for linear withdrawal, and hence rod position in time, with the energy release in the burst. The essentially linear change of reactivity (Figure 19) caused by withdrawal of the central rod was approximated by a series of step changes in reactivity. Assuming an initial fission rate of 1 fission per gram of U^{235} it is found that sufficient energy is released in the core (3×10^{13} fissions/gm U^{235}) to stop the reaction when the rod has reached 75.4 cm for a linear withdrawal from 49.2 cm to 75.4 cm in 0.7 sec. This rate of withdrawal does not seem unreasonable.

Uncertainties in the actual initial source strength and the exact energy release for shutdown reduce the validity of this comparison. However, a change in initial source strength of 10^3 will produce a change of approximately 0.07 seconds in the time for the burst, still a reasonable result.

DELAYED NEUTRON ESTIMATES

The delayed neutron contribution to the total neutron exposure would be insignificant if the geometry of the core had not changed for 10 seconds after the burst. However as the water drained from the tank, the shielding effect of the water was lost and the importance of the delayed neutron contribution relatively increased.

The delayed neutron production rate per prompt neutron is given by

$$\frac{dn}{dt} = 7.35 \times 10^{-6} \left[0.439e^{-t/79.9} + 7.00e^{-t/34.2} + 37.0e^{-t/7.9} + 132e^{-t/2.5} + 223e^{-t/0.52} \right]$$

and is plotted in Figure 34. From 1 second to 10 seconds after the burst the delayed neutron production rate varies from 2.9×10^{-3} to 1.4×10^{-4} neutrons per second per prompt neutron. An estimate of the delayed neutron dose, taking into account the effects of the water dump, and hence the changed geometry of the assembly, may be obtained from the delayed neutron production rate per prompt neutron, by comparison with the experimentally determined prompt neutron dose above the core.

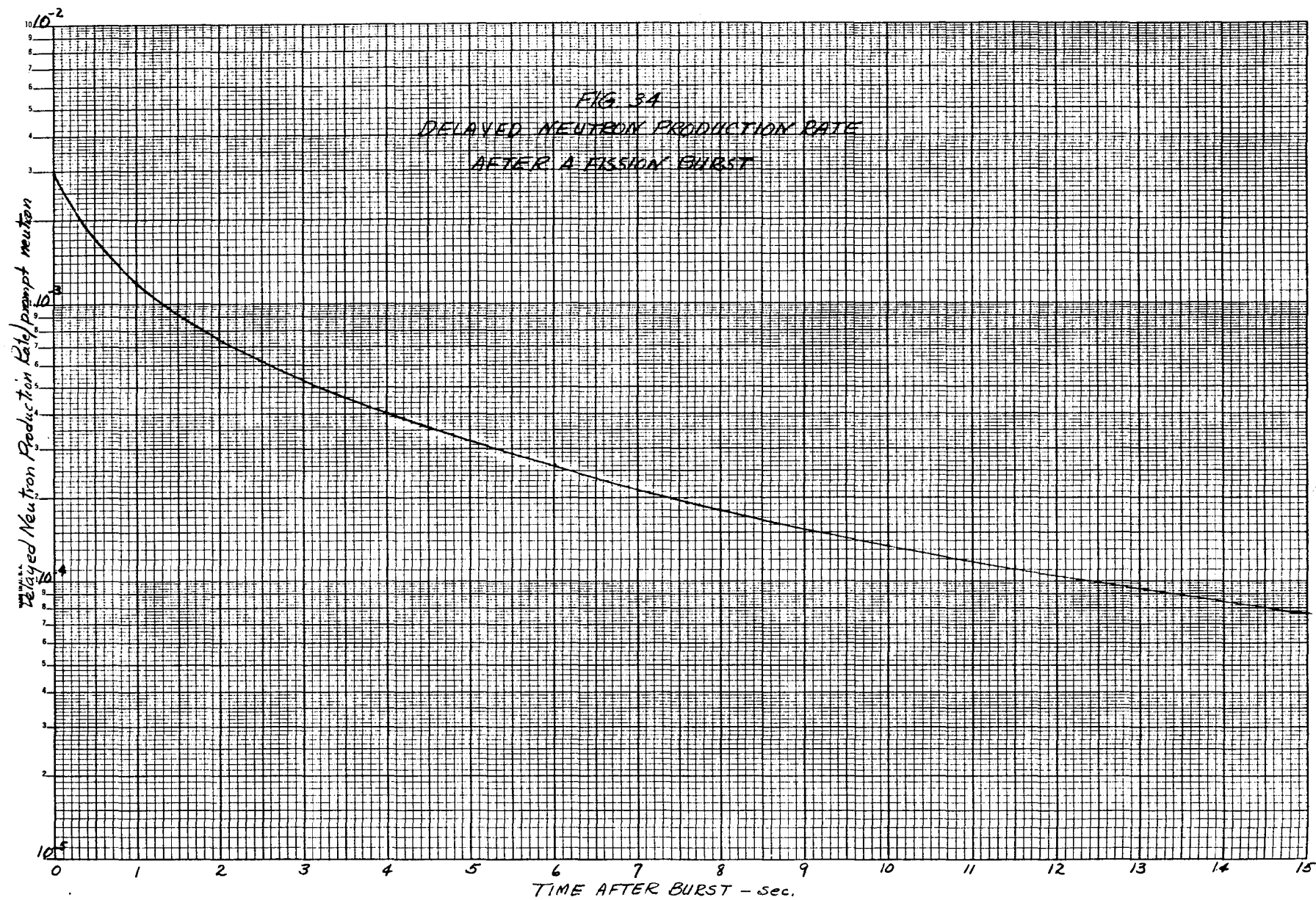
Such an estimate must take into account subcritical multiplication of delayed neutrons, increased leakage of neutrons due to expulsion of water from the core and increased leakage due to loss of reflector.

The mechanism of reactor shutdown was foaming of the plastic fuel strips and consequent expulsion of water from the core. Expulsion of 5% of the water in the core was sufficient to counteract the excess reactivity introduced into the reactor, but the energy stored in the plastic during the burst was sufficient to vaporize enough plastic to completely fill the space between zirconium strips and hence expel all of the water over much of the core.

Assuming that plastic foam completely fills the space between metal strips in the core, and that the water reflector is intact, an estimate may be obtained of the subcritical multiplication of the core after the burst. Using 20 cm reflector savings as obtained for a dry core with infinite water reflector, with an age of 508 cm^2 and a thermal diffusion area of 22.75 cm^2 , a simple two group diffusion calculation yields a multiplication of 1.86 with top reflector intact, and 1.3 with no top reflector. For lower water levels a multiplication factor of 1 is assumed.

An estimate of increased leakage above the core due to expulsion of water from the core may be obtained by using the removal concept for fast neutron self shielding and comparing the change in fractional leakage in spheres of radius equal to half-height of the core. For the undisturbed core, with a removal cross section for water of 0.14 cm^{-1} ,²² and a removal cross section for zirconium of 0.1835 cm^{-1} (3/4 of total cross section), the removal cross section of the core is 0.1662. For a sphere of radius 54.5 cm the fractional leakage is 0.088.²³ For the core with water expelled, using as the removal cross section, the cross section of plastic only, the removal cross section of the core is 0.00695, and the fractional leakage, as above, is 0.80, an increase by a factor of 9.1.

The effect of the reflector on prompt neutron intensity is shown in Figure 20, where an attenuation of 30 is shown through the reflector. Assuming the same attenuation for delayed neutrons as for prompt neutrons, loss of the top reflector will increase the leakage of delays by a factor of 30 less the geometric attenuation through distance occupied by the reflector. From Figure 25 this is estimated to be a factor of 2.5. Hence the effect of total



loss of the reflector on delayed neutron dose above the core is to increase the delayed neutron dose by a factor of 12. The height of water in the assembly as a function of time after the burst is shown in Figure 27.

Application of these factors to the production rate of delayed neutrons (Figure 34) gives as the dose rate of delayed neutrons above the core, expressed as a per cent of the prompt neutron dose:

Time Sec After Burst	Water Height from Bottom of Core	Delayed Neutron Production Rate per Prompt Neutron	Subcritical Multiplica- tion Factor	Core Leakage Factor	Reflector Factor	Dose Rate % of Prompt Dose above Core per Sec
0	129	2.9×10^{-3}	1.86	9.1	--	5.4%
1.3	109*	1×10^{-3}	1.3	9.1	12	15.5%
3	80	5.3×10^{-4}	1	9.1	12	6.3%
5	57	3×10^{-4}	1	9.1	12	3.6%
10	0	1.4×10^{-4}	1	9.1	12	1.6%

*Top of core

The delayed neutron dose rate, as a percentage of the prompt dose, above the core is shown in Figure 35.

The ratio of the dose rate at the side surface to the dose rate at the top surface of the assembly with water drained from the core is estimated as the product of the ratios of the fractional leakage from spheres of radius 25.8 cm and 54.5 cm (radius and half-height of the cylinder), the inverse ratio of the surface areas of the spheres, and the ratio of the projected areas of the side and top of the core:

$$\frac{0.90}{0.80} \times \left(\frac{54.5}{25.8}\right)^2 \times \frac{51.6 \times 109}{\pi \times (25.8)^2} = 13.5$$

Assuming the side dose rate varies as $1/r^2$ from the core centerline (see Figure 24) the ratio of dose rate at the surface of the tank to the prompt dose rate at the surface of the top reflector will be

$$13.5 \times \left(\frac{25.8}{68}\right)^2 \times \frac{2.5}{1} = 4.86$$

Before the water drains from the assembly the side reflector is 17" thick. This provides enough shielding that the delayed neutron dose rate through the water is negligible. However, as the water drops, from

FIG. 35
DELAYED NEUTRON DOSE RATE
AFTER PROMPT NEUTRON DOSE

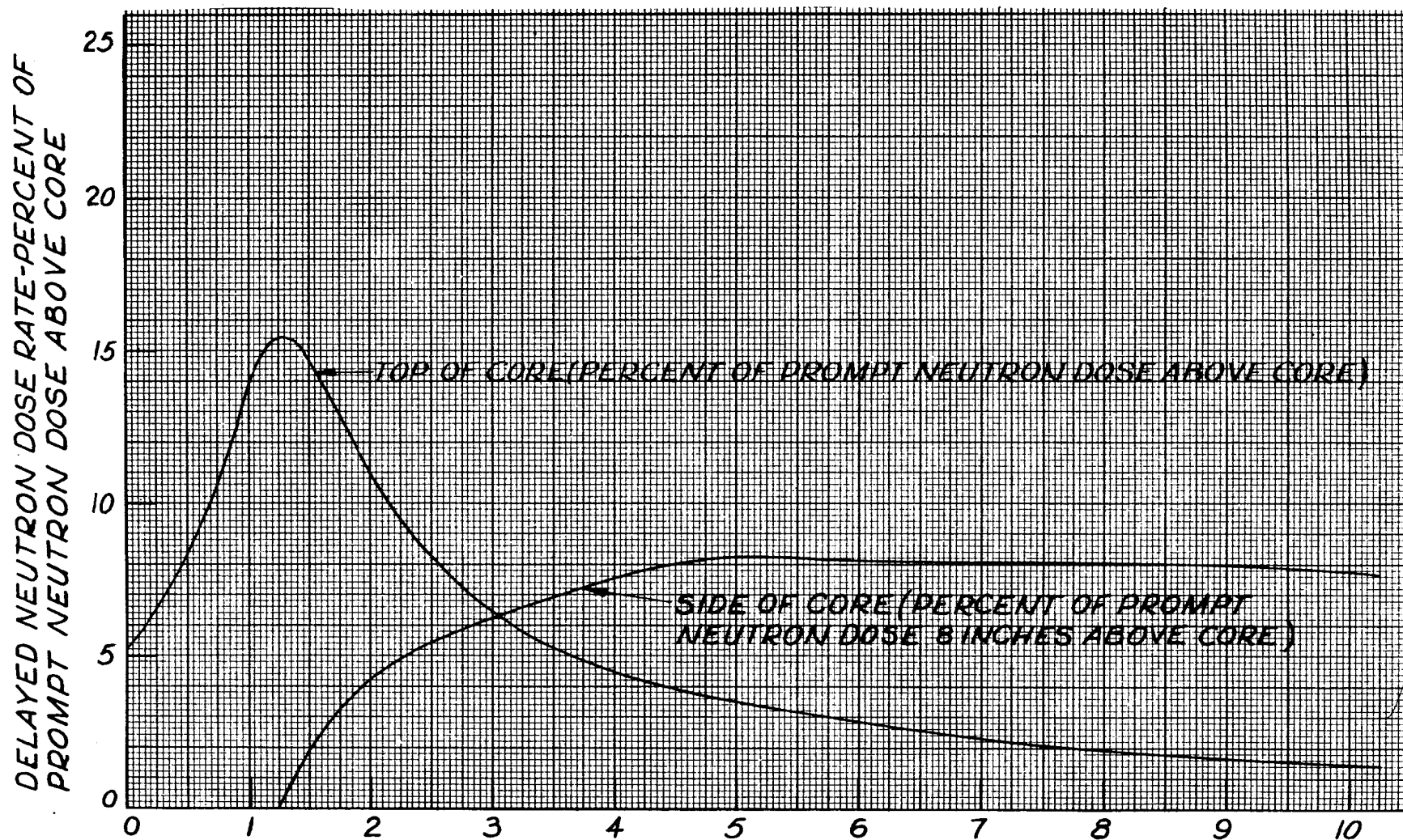


Figure 27 the fraction of the core uncovered may be calculated and hence, using the factor above, the side dose rate at the surface of the tank determined as a percentage of the prompt dose rate 8 in. above the core.

Time	Fraction of Core Uncovered	Factor on Top Dose Rate	Top Dose Rate of Prompt Dose per second	Side Dose Rate % of Prompt Dose 8 in. above Core
0	0	0	5.4	0
1	0	0	14.0	0
2	0.08115	0.394	11.1	4.37
3	0.221	1.075	6.3	6.76
4	0.349	1.695	4.5	7.62
5	0.477	2.32	3.6	8.35
6	0.593	2.88	2.8	8.05
7	0.730	3.54	2.3	8.15
8	0.837	4.06	2.0	8.12
9	0.941	4.57	1.75	8.00
10	1.00	4.86	1.6	7.77

The delayed neutron dose rate at the assembly tank surface as a percentage of the prompt neutron dose 8 in. above the core is shown in Figure 35.

Use of these dose rates, together with measured attenuation of prompt neutrons above the core, an assumption of $1/r^2$ radial attenuation of delayed neutrons outside the tank wall, and the estimated position of the persons involved in the incident as reconstructed in Figure 4, yields the individual dose rates as a function of time after the burst. Integrating the dose rates over the time of exposure yields as the delayed neutron dose:

Art - 2.0 rep

Bill - 4.2 rep

Carl - 1.0 rep

Don - 0.15 rep

SECTION III

ESTIMATE OF THE RADIATION EXPOSURES

L. D. Marinelli

MEASUREMENT OF GAMMA RADIATION INCIDENT
UPON THE FILM BADGES

ESTIMATE OF THE GAMMA RAY EXPOSURE IN ROENTGENS

ENERGY RELEASE COMPARISONS

THE NEUTRON DOSE

DISCUSSION

SECTION III

ESTIMATE OF THE RADIATION EXPOSURES

L. D. Marinelli

The Division of Radiological Physics assumed the task of estimating the exposure of the personnel involved in the incident. In the interest of accuracy it was thought preferable to accomplish this by relying on the most direct evidence available or obtainable from suitable ionization measurements, instead of attempting to calculate the dose directly from an estimated number of fissions. Most of the measurements used herein are reported in preceding sections of this report. The scheme of referencing the exposed personnel is consistent with that used previously. The approach used in making the estimates consisted of:

Measuring the equivalent radium gamma ray exposure to the film badges worn by Art, Bill, and Carl.

Estimating the gamma ray air exposure (in roentgens) incident upon Art, Bill, and Carl by taking into consideration their motion, the uncovering of the reactor core by the dumping of the water from the tank, and the wave length dependence of the film badge.

Comparison of total energy release estimates based on determined prompt γ -exposures to estimates based on fission product analysis.

Estimating the dose due to fast and slow neutrons to which the film badges worn were not significantly sensitive.

(Extension of this analysis to the case of Don must necessarily be based on calculations only, since he wore no badge.)

Each step outlined above is treated in turn. Some additional measurements made on personnel during the course of the investigation are shown in the Appendices. The upper limits of doses have been summarized in Section I.

MEASUREMENT OF GAMMA RADIATION INCIDENT
UPON THE FILM BADGES

The personnel badges, containing photographic emulsions du Pont #502 (range 0.2-10r) and #510 (range 1-35r) were darkened by the exposure beyond the readable limit of commercial densitometers. This difficulty was overcome

by comparing them to a set of #510 films from the same batch, exposed to known doses of radium gamma radiation, by the use of the following methods:

- a. Separate densitometric measurements of each emulsion layer.
- b. Relative estimate of reduced silver in the films by neutron activation analysis.
- c. Relative estimate of the reduced silver by measurement of its characteristic x-ray radiation.

Details of the methods are given in Appendix D and have been published in the open literature.¹¹ The calibration curves are reproduced in Figure 36. Results from these measurements were very consistent among themselves and showed the following exposure in equivalent gamma radiation from radium:

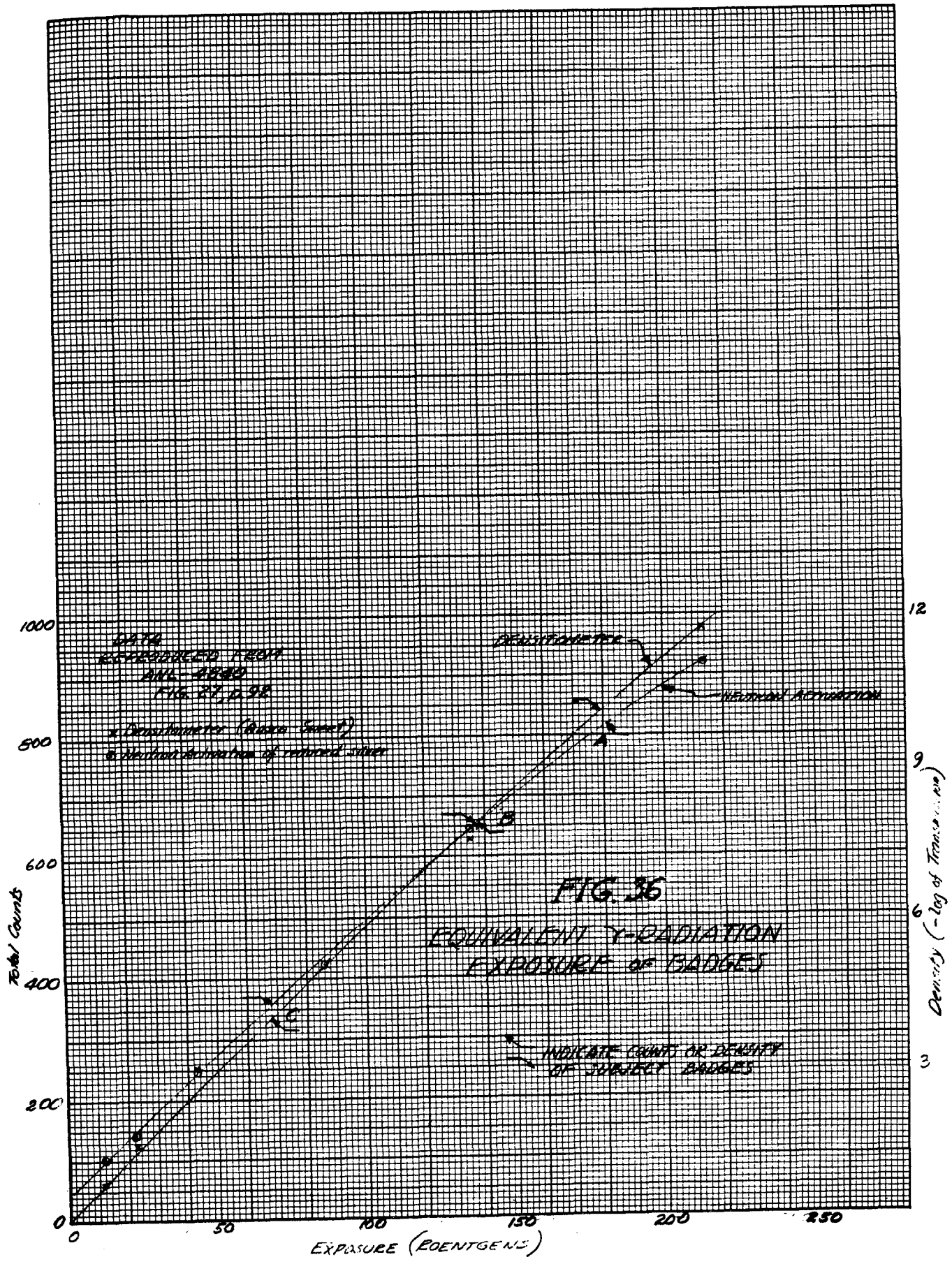
Art's badge	179-181 roentgens
Bill's badge	137-138 roentgens
Carl's badge	68- 68 roentgens

ESTIMATE OF THE GAMMA RAY EXPOSURE IN ROENTGENS

The exposure to personnel in roentgens is estimated in terms of exposure to a unidirectional beam. The estimate will refer to roentgens in air since a determination of the total body integral dose would require long term investigations not considered feasible for this incident. Although the badges can be assumed to have integrated correctly the gamma ray skin dose delivered to the upper anterior portion of the operator's trunk, they cannot be assumed to have measured the dose in roentgens in air unless calibrated against a suitable ionization chamber under the conditions of the accident; corrected further for backscatter from the operator's body; and corrected for that portion of the dose missed by the badge on account of the shielding provided by the operator's body when the latter was facing away from the reactor during part of the itinerary followed on his way out from the room.

CALIBRATION

Comparison between film badges and a suitably calibrated graphite chamber was carried out twice by simultaneous exposure to radiation from the reconstructed reactor running at 22.6 and 4.5 watts at the point which



Art's badge occupied at the time of the accident (Figure 4). Both tests yielded consistent results ($\pm 2\%$) indicating roentgens in air = equivalent badge roentgens in air/1.12.

BACKSCATTER CORRECTION

In order to estimate the contribution of the person's body to the blackening of the film, two sets of badges were exposed at Bill's badge position, one set in air and the other attached to a phantom consisting of wooden trough (40 x 50 x 30 cm) filled with water. The results were:

equivalent badge roentgens in air = equivalent roentgens of badge on personnel/1.24.

It follows therefore that:

roentgens in air = equivalent roentgens of badge on personnel/1.39.

MISSED DOSE CORRECTION

A realistic estimate of this correction can be made only by ascertaining the water level of the reactor and the location of badges as a function of time after the fission process and by estimating therefrom the dose at these locations at the proper instant. Since both Art and Bill noticed the water level in the tank at the time they crossed the exit door, and the position of the water level, as a function of time after scrambling, was determined with a high degree of accuracy by cinematographic records (Figure 27) it is possible to state that Art and Bill left the room at $t = 5$ and $t = 10$ seconds respectively. The positions of the personnel deduced from this data and later rehearsals are then essentially as indicated in Figure 4.

The dose in roentgens at these points can be calculated with some reliance by extrapolating the representation in Figure 7 of many ionization readings taken after the accident around the bare core, to 10 seconds after fission by the $t^{-1.21}$ law, and thence to 0.1 sec according to the scheme of J. J. Taylor.⁶

On the side of the tank, at the distances of interest, the inverse square law is obeyed and the bulk of the data indicates that the dose rate was 2.8 r/sec at 74.5 in. from the center of the bare core at 10 seconds after fission. The average value quoted in earlier sections (928 mr/hr at 202 cm, $t = 5$ hours) was used in this extrapolation.

As for the doses prevailing above the reactor, a reading of 1.3 r/hr at $t = 4.82 \times 10^4$ sec was obtained at an identifiable point 6 in. above the core top surface. Extrapolation of this reading for fission product decay

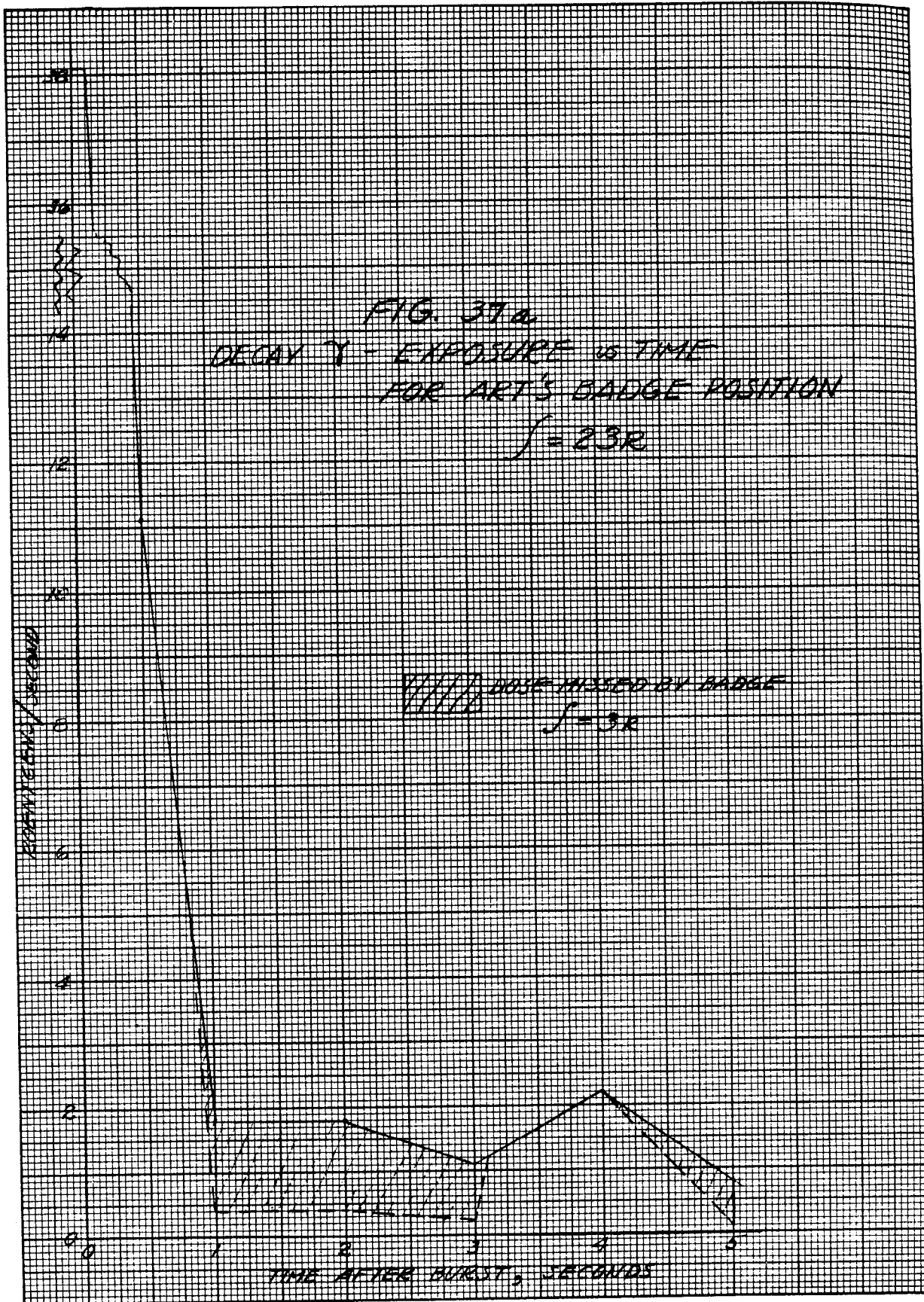
to the first ten seconds was done in a similar way, but correction for distance between the point in question and the point where Bill's badge was at time zero was based on relative geiger counter measurements taken with the reconstructed bare core and by photographic emulsion with the water up and the reactor running. It was assumed that once the operators reached the edge of the platform, the doses estimated by the readings taken at the sides of the reactor became valid. To calculate the significant dose rates while the operators were on the platform the assumption was made (Figure 4) that Bill hesitated for 2 seconds and took 2 more seconds to reach the top of the stairway walking on the platform on arc of a circle concentric with the axis of the core. Art was assumed to have taken one-half second to stand erect from the bent-over position and to have reached the stairway one-half second afterwards. Absorption by water is based on straight exponential absorption assuming an absorption coefficient $\mu = 0.06$ appropriate to the poor geometry and a monochromatic radiation of 1 Mev.¹² The variation of dose rates (in roentgens in air) for each of the personnel at their respective badge positions are shown in Figures 37 a, b, c, and d. From integration under the curves it is concluded that the unidirectional doses received at the badge positions after the runaway are 20 air roentgens for Art, 55 air roentgens for Bill, 10 for Carl, and 3.1 for Don. Furthermore the badges missed 3, 5, and 1 roentgens (air) respectively, since they turned away from the reactor while descending the stairs from the platform (Don wore no badge).

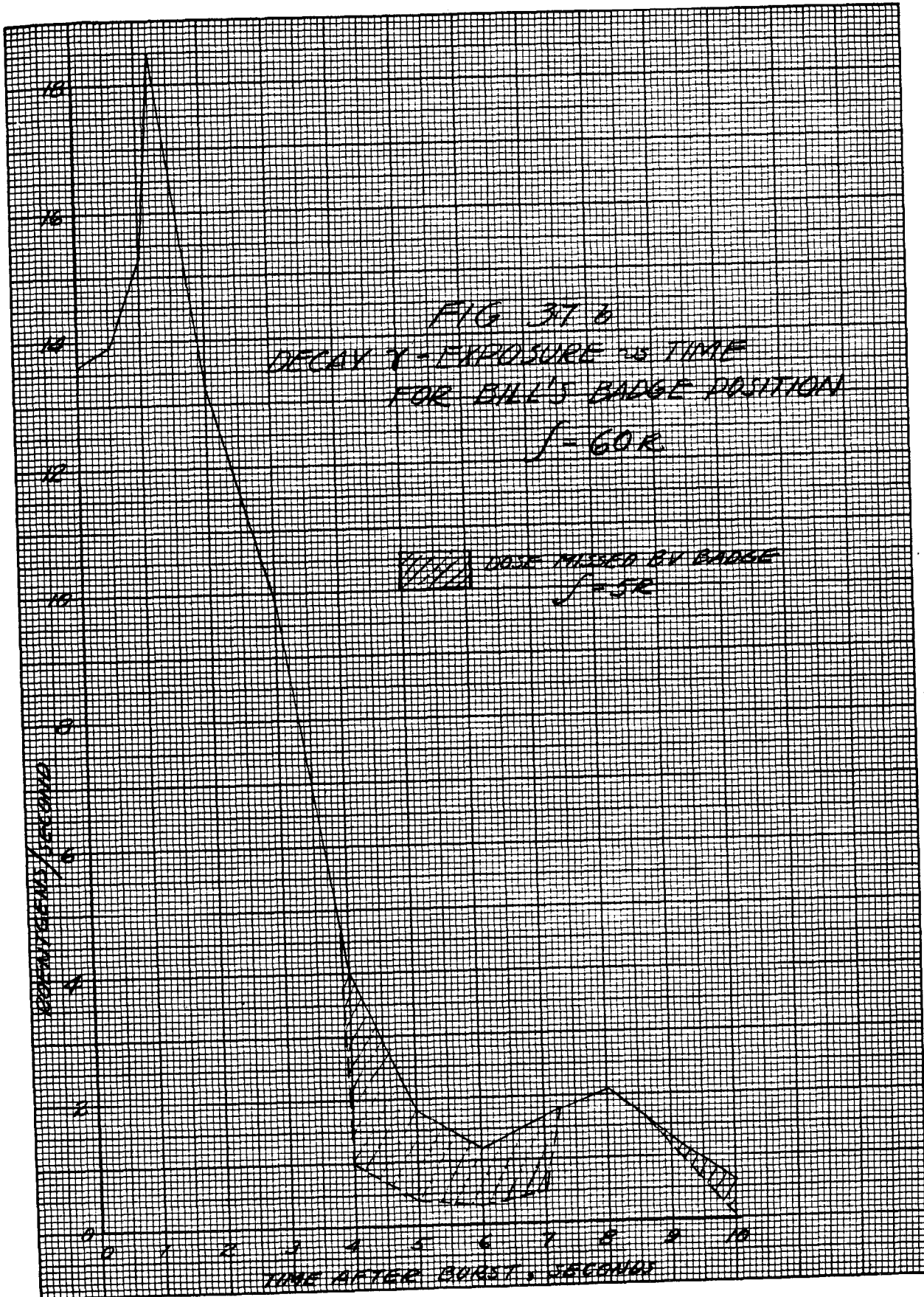
In view of the correction factors evaluated above it may be stated that the equivalent unilateral dose in air at the site of the badges is:

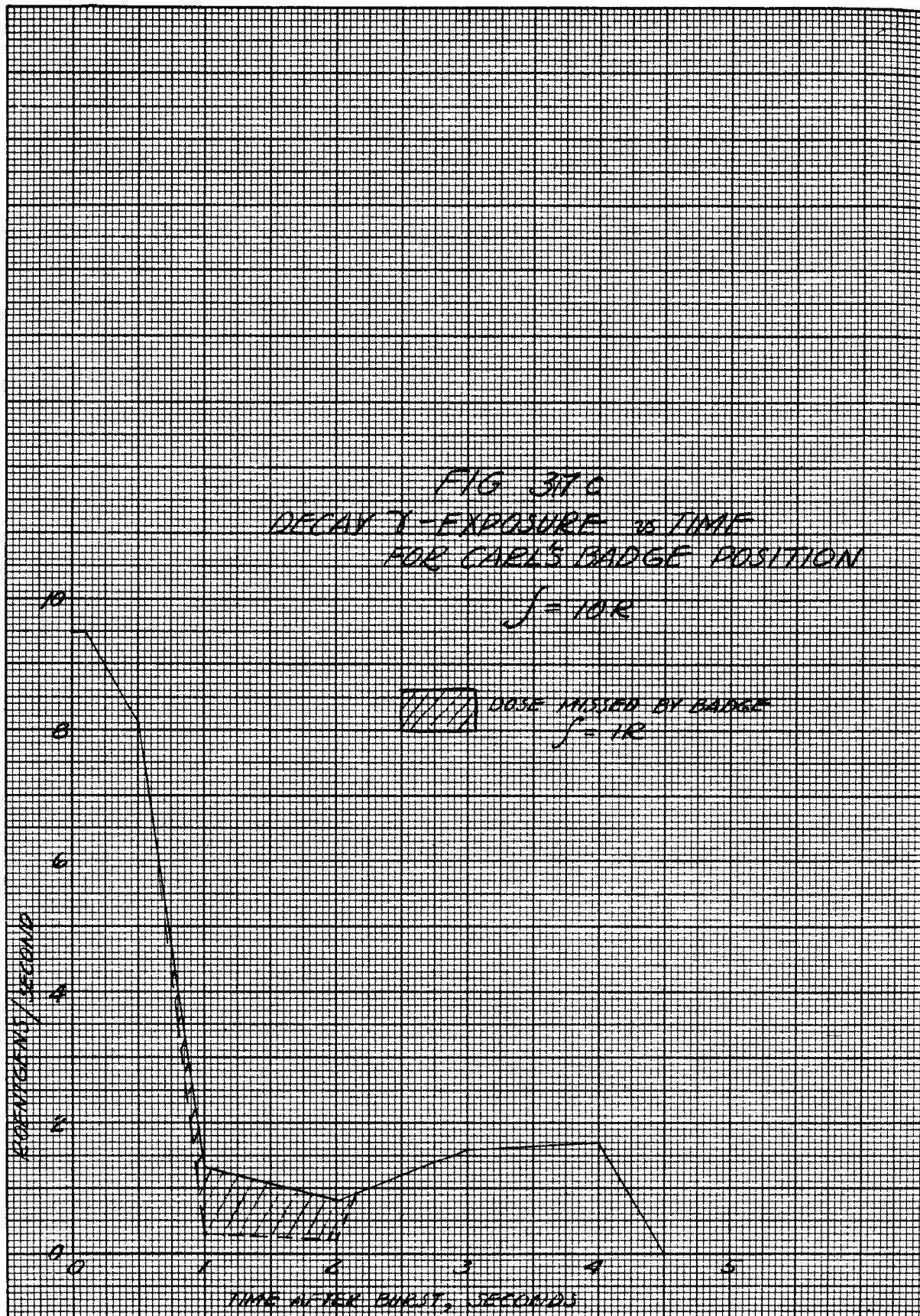
$$\begin{aligned} \text{Art} &= \frac{179}{1.39} + 3 = 132 \text{ roentgens } \pm 10\% \\ \text{Bill} &= \frac{139}{1.39} + 5 = 105 \text{ roentgens } \pm 10\% \\ \text{Carl} &= \frac{68}{1.39} + 1 = 50 \text{ roentgens } \pm 10 \end{aligned} \quad (1)$$

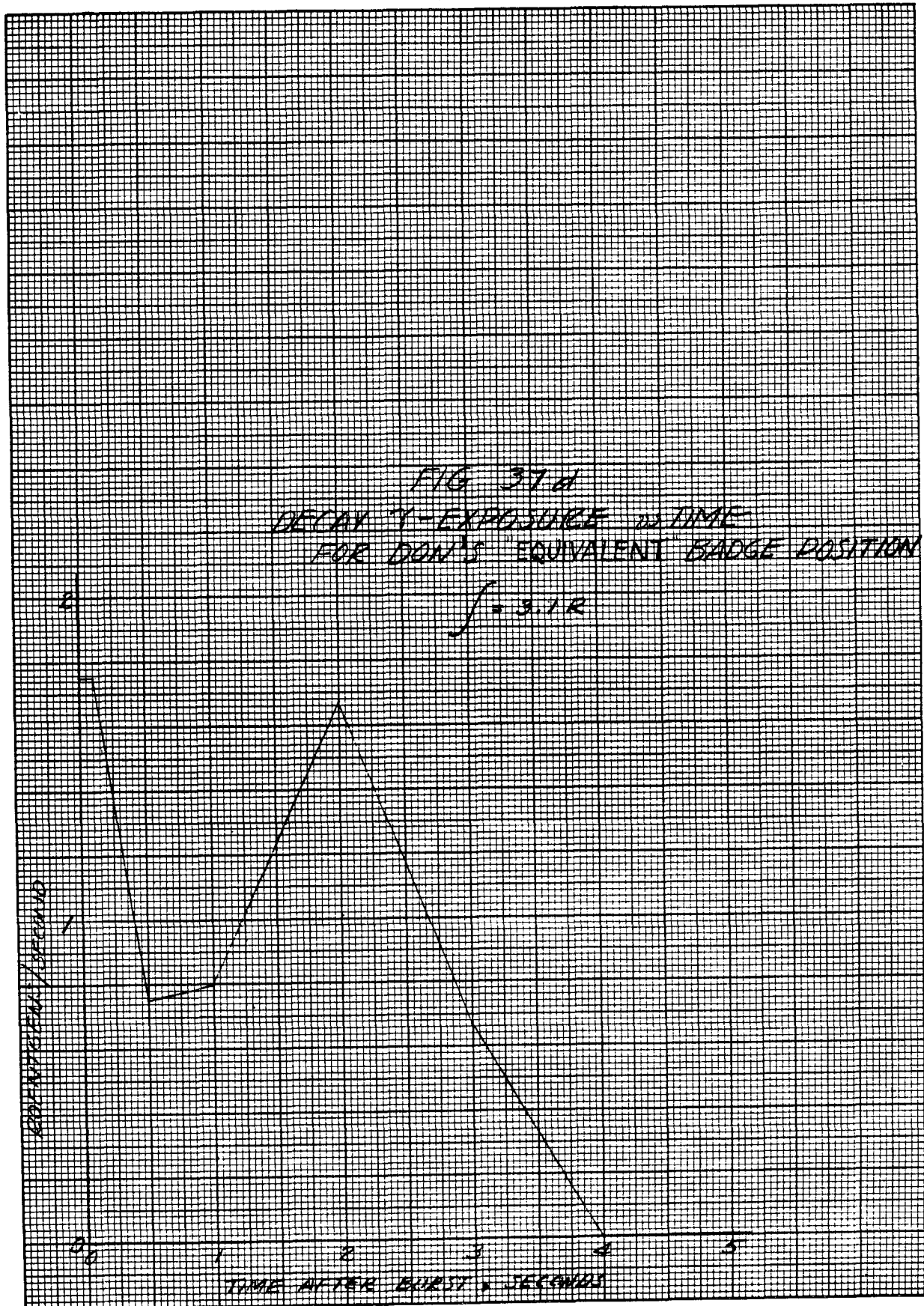
From these values the exposures due to the prompt reactions (fission plus capture gammas) at the badges can be easily calculated as:

$$\begin{aligned} \text{Art} & 132 - 23 = 109 \text{ roentgens in air} \\ \text{Bill} & 105 - 60 = 45 \text{ roentgens in air} \\ \text{Carl} & 50 - 10 = 40 \text{ roentgens in air} \end{aligned} \quad (2)$$









It should be noted in passing that although the badge readings of Bill and Carl are in the ratio $139/68 = 2.04$, the ratio of the estimated prompt exposures is only $45/40 = 1.12$. This would be expected from their essentially identical distances from the core axis at the time of the burst.

Of further interest is an approximate estimate of the equivalent dose at the lower end of the trunks of the personnel. Use is made of relative values obtained in air with the film badges while the reconstructed reactor was run at low power and with monitoring instruments around the bare core. In the case of Art, the prompt exposure is assumed uniform along his trunk since it can be considered that he was in the configuration of an arc of a circle approximately concentric with the center of the upper surface of the core. As he straightened up and reached the top of the stairs on his way out, his groin must have received radiation at the rate of about $10/6$ of the rate received by the badge, but from then on, the total exposure at both locations must have been approximately equal. Calculations thus based and similar analyses for the others yield the doses (unidirectional in air) at the groin, the average for the trunk, and the maximum for the feet are as follows:

Total γ Exposures (Unidirectional in Air) in Roentgens

	<u>Art</u>	<u>Bill</u>	<u>Carl</u>	<u>Don*</u>
At the groin	140	148	70	
Average for the trunk	136	127	60	9
Maximum for the feet	200	280	190	

*No badge - dose at trunk position is assumed maximum.

These figures should be correct to better than 20%.

ENERGY RELEASE COMPARISONS

Evaluation of the prompt dose in roentgens as in (2) above permits an attempt to estimate the energy released in the accident if valid comparisons can be made with the same reactor during operation at known power levels. Badges were exposed in air on the platform at Art's and Bill's badge positions while the reconstructed reactor was run at the constant power of 22.6 watts for four hours, a total of 90.4 watt hours. Readings were 17.9 and 6 "badge roentgens" respectively, equivalent to 16.0 and 5.36 roentgens in air respectively. Before use can be made of this value in the estimate, it is necessary to realize that, for the same number of

fissions, the badges during the 90.4 watt-hour run received a considerably greater amount of gamma radiation (due to "decay" gamma radiation from fission products) than they would have received from the "prompt" gammas alone due to the fission and capture process. The ratio of total gamma energy to prompt gamma energy is estimated as follows: Consider that the gamma production processes are fission, capture, and fission product decay. The fission γ energy is taken as 5.1 Mev/fission.¹³ Using the binding energy from the mass energy balance for U^{236} formation of 0.00730 A.M.U.¹⁴ the U^{235} capture γ energy is 6.8 Mev/capture. Assuming equal capture in H_2O and Zr and taking 2.2 Mev/capture for H_2 with 8 Mev/capture in Zr, the H_2O -Zr capture γ energy is 5.1 Mev/capture. Finally, the average decay gamma energy per fission during a uniform 4-hour run at 22.6 watts can be obtained from

$$E_{\gamma} = 5.5 \int_0^{4 \text{ hr}} d\tau \int_0^{\tau} f(t) dt = 5.0 \text{ Mev/fission}$$

where $f(t)$ is the γ -ray decay function. The application of the relative cross sections for the processes yield

<u>Process</u>	<u>Mev/Process</u>	<u>Relative Cross Section</u>	<u>Mev</u>
Fission	5.1	0.72	3.67
Capture (U^{235})	6.8	.13	.88
Capture (H_2O and Zr)	5.1	.11	.56
Decay	5.0	.72	<u>3.60</u>

Total emission = 8.71 Mev

The ratio of total emission to prompt energy is then $\frac{8.71}{8.71-3.60} = 1.71$.

Hence the readings obtained during the 90.4 watt-hour run should be divided by 1.71. By so doing one obtains $16.0/1.71 = 9.35$ roentgens and $5.36/1.71 = 3.13$ roentgens for the prompt gamma ray air doses at the badges. Calculations of the power released follows using the data from (2) thus:

From Art's badge $109 \times 90.4/9.35 = 1050$ watt-hours

From Bill's badge $45 \times 90.4/3.13 = 1300$ watt-hours

For the purpose of calculation of neutron dose to be presented, the energy release will be taken as 1050 watt-hour because the uncertainties involved in the estimate of the prompt dose from Art's badge are less than for the case of Bill. Notice should be taken, nevertheless, of the reasonable agreement between these values and the value of 1040 watt-hours obtained in the preceding section of the report based on the fission product analysis of the number of fissions. Although this agreement between entirely unrelated observations can be taken as independent evidence of the substantial correctness of the estimate of gamma ray doses, it should be noted that the accuracy of value of the power released depends directly on the value of the ratio "prompt" gamma/"prompt" + "decay" gammas. Lack of adequate basic data on both the energy and spectrum of fission gamma ray, capture gamma rays and "early" gamma rays from fission products precludes fruitful efforts to improve on the accuracy of these estimates.

THE NEUTRON DOSE

Estimates of the fast and thermal neutron dose were based on neutron measurements performed during the 90.4 watt-hour run of the reconstructed reactor and on the assumption that an energy release of 1050 watt-hours occurred. The measurements have been described previously and the results are taken from that section. The sources used to calibrate the instruments are Co⁶⁰ and Ra for gammas, and Po-Be or Po-F for neutrons. We are indebted to D. Froman of Los Alamos for making the neutron sources available.

PROMPT FAST NEUTRON DOSE ESTIMATES

The tissue and graphite ionization chambers were exposed simultaneously to gamma rays of different quality to determine the variation of their response as a function of photon energy. The ratio of the ionization recorded by the tissue chamber to that of the graphite chamber was as follows:

<u>Source</u>	<u>\bar{E}_γ</u>	<u>Tissue/Graphite</u>
Co ⁶⁰	1 Mev	0.662 ± .008
Ra	0.8 Mev	0.656 ± .002
200 KV X-Ray + 1 mm Sn \simeq	0.12	0.646 ± .002
135 KV X-Ray + No Filter \simeq	0.05	0.552 ± .004

When the chambers were similarly exposed at Art's badge position the ratio was $0.651 \pm .006$, namely, intermediate between the values obtained with filtered 200 kv X-rays and radium gamma rays. From analysis of the scintillation spectrometer results obtained at the same position (Figure 21.) it is inferred that the average value of the pulse heights equals the value that would have been obtained with a monochromatic gamma ray source of 500 kev.¹⁵ In order to allow, however, for the higher incidence of small pulses (thus weighing our neutron estimate on the high side) it has been assumed that the gamma ray spectrum from ZPR-I is equivalent to that of 200 kv machine filtered by 1 mm of Sn.

By separate experiments with Po-B sources it has been established that 1 rep of neutrons of average energy of 2.5 Mev is recorded as 0.08 "reps" by the graphite chamber and that it would be less for neutrons of lower energies such as fission neutrons. By simple analysis it can be proven that in a mixed beam of gamma rays and neutrons, the fraction of neutron reps to gamma reps is:

$$F = \frac{R_1 - R_2}{R_2 - 0.08 R_1}$$

where R_1 = Tissue/Graphite ratio in mixed beam
 R_2 = Tissue/Graphite ratio in gamma ray beam

By this means and using the stated per cent errors one arrives at an estimate of neutron dose of $(0.85 \pm 1.35)\%$ of the gamma ray dose available under the conditions of the low power run. After correcting by the 1.71 factor this becomes $(1.45 \pm 2.31)\%$. In terms of reps, we have for prompt fast neutron exposures:

Art	$0.0145 \times 109 = 1.6 \pm 2.5$ reps
Bill	$0.0145 \times 45 = 0.7 \pm 1.0$ reps
Carl	$0.0145 \times 40 = 0.6 \pm 1.0$ reps
Don	$0.0145 \times 6 = 0.1 \pm 0.1$ rep

The "Rednose" dosimeter yielded an integrated exposure of 3.2×10^9 n/cm² of energy equivalent to 2.5 Mev energy, or about 11 reps, for the prompt reaction at Art's badge. This discrepancy is percentage-wise, very large. It should be noted, however, that this instrument, to be useful, must be biased rather carefully and special precautions must be taken to insure discrimination against gamma rays. Although rough tests have been performed with this in mind, lack of clean monochromatic neutron sources has precluded the possibility of assessing whether in this instrument the counting rate is actually proportional to neutron dose and to what extent it is influenced by the overwhelming gamma radiation. The independent survey

by T. V. Blosser of the Shielding group at ORNL, using a polyethylene-ethylene proportional counter²¹ and suitable integrating circuit, yielded by suitable extrapolation 10.2 reps at Art's position, in good agreement with "Rednose." This, in a way, should be expected, because both instruments were calibrated at Oak Ridge in similar fashion; hence, the reservations mentioned above should apply also to this instrument. As to the ionization method, only the presence of very soft gamma radiation (not detectable by the aluminum covered crystal of the scintillation counter) could have masked the contribution of fast neutrons. On the other hand, the ratios R_1 and R_2 are very nearly equal, so that the difference method, considering probable errors on the ratios and a small value of the ratio of neutron dose to γ dose gives large relative errors.

The N.T.A. plates used in the experiments have been used for personnel monitoring on both sides of the Atlantic. From the number of tracks observed per cm^2 on the assumption of 1 Mev neutron energy, the neutrons incident per cm^2 upon the badge due to the prompt reaction are estimated to be 10^9 n/cm^2 . Upon acceptance of this value the estimated fast neutron dose becomes 2.4 reps for Art's badge position, within the limit set by the ionization chamber method.

DELAYED NEUTRON DOSE

An upper estimate of the delayed neutron dose contribution in the accident (core bare) can be had by assuming that not more than 90% of the delayed neutrons could have escaped from the bare core. Since the total neutron escape (with the core submerged) is of the order of 2% per fission and since the delay neutrons are about 1.8% per fission, the delayed neutron dose could not possibly have been higher than $\frac{1.8 \times 0.9}{2.0} = 80\%$ of the prompt neutron dose. More realistically, by taking into account their half life, the partial shielding contributed by the water as the tank was emptying, and the motion of the operators, this contribution is not likely to be higher than about 40% of the prompts. A detailed study by F. Thalgott in an earlier section along the lines of that made here for the decay gamma doses shows the values to be:

Art	2.0 reps
Bill	4.2 reps
Carl	1.0 rep
Don	0.15 rep

THERMAL NEUTRON DOSE

The difference in ionization readings obtained with a boron-lined chamber (placed at Art's badge position) and provided with, and devoid of, a Li metal shell was compared to the increase in ionization obtained in an analogous experiment performed at the thermal column of CP-3' at a point where the thermal flux was determined by means of gold foil activity. Simultaneous readings were taken at the same points with a BF_3 counter. The ratio of the readings at the two sites checked within 10%. The average ratio yielded 1.2×10^9 n/cm² for the prompt reaction of the accident. Another estimate was obtained from an exposure of Li loaded N.T.A. plates and a calculation of their sensitivity based on their Li content. The result is 2.3×10^9 n/cm² for the prompt reaction.

On the basis of a maximum deposition of 4.71×10^{-8} ergs/n/cm² and 1 rep = 93 ergs, the thermal neutron dose is estimated to be 0.6 - 1.0 rep for Art and hence about 0.5% of the total.

DISCUSSION

An analysis of the factors influencing the accuracy of the estimates presented above, discloses that the film badge acted as a satisfactory personnel monitoring instrument in the presence of degraded gamma rays from the fission reaction. Test of the badge with fast fission neutrons at the Biological facility attached to CP-3' showed very low sensitivity to fast neutrons. Since these were not present in relatively high proportion during the accident, the response of the badge was essentially a gamma ray response. Obviously, the presence of badges of adequate range would have considerably simplified the task of estimating exposures.

As to the variation of dose at different points of the body, much more could have been learned if more badges, or their equivalent, had been worn. While it is obvious that an array of badges is awkward, it might not be impractical to consider wearing a photographic film in the shape of a strip to be adapted to the particular circumstances of an experiment. Since this would serve the purpose of recording relative doses, the response need not be independent of energy.

The energy released could have been compared to a given power run by activation analysis. It should be noted that brass screws measured by A. Stehney's group would have served the purpose admirably were it not for the fact that the activity was relatively low and would have required for satisfactory comparison an expenditure of energy from the reconstructed

reactor wholly comparable to that released from the accident. There is little doubt, however, that the principle of placing suitable materials at appropriate distances for the purpose of monitoring a neutron producing reaction should be implemented more widely.

The wide discrepancy in the neutron measurements reflect, unfortunately, the state of the art, sadly in need of improvement, not because of the lack of interest on the part of radiological physicists, but by the lack of access to suitable monochromatic neutron testing facilities, free of gamma rays. This state of neutron dosimetry is emphasized in a recent article by H. H. Rossi.¹⁷

It is to be noticed that the activation of the body sodium does not lead to satisfactory evaluation of the neutron exposure (Appendix B). This is to be expected in the absence of information on neutron energies; nevertheless, it has proven of definite prognostic value when compared to the results of the accidents reported by Los Alamos.

In this incident as in an earlier one at Los Alamos the relation of prompt to delayed doses requires comment. Compare the prompt/delay dose ratio of Art, who left quickly with that of Bill who delayed leaving the core vicinity. It is immediately evident that had they left together, Bill's γ dose would have been 36% less. If the doses had bordered on lethality, this could have meant the difference between life and death. Time and distance contribute heavily to total dose. One should get away as fast and as far as possible from an accidentally encountered source, and stay away.

The writer of this section wishes to acknowledge the valuable cooperation of C. E. Miller and P. F. Gustafson in the performance of the dosimeter tests.

SECTION IV

CLINICAL REPORT

R. J. Hasterlik, M.D.

CASE HISTORIES

LABORATORY DATA

SUMMARY AND CONCLUSIONS

SECTION IV
CLINICAL REPORT

R. J. Hasterlik, M.D.

At approximately 3:52 P. M. on June 2, 1952, the four individuals concerned in the incident were exposed to gamma radiation and neutrons. The patients were seen ten minutes later by Dr. Earl A. Hathaway and the author, at which time there were no gross clinical findings of note. Blood pressure determinations and cardiac rates were within the normal range. Subjectively, the patients were asymptomatic except for moderate tension and apprehension. In spite of the fact that all realized that they might have been exposed to quantities of radiation in the lethal range, an observation worthy of note was their quiet, self-contained behavior.

Within the first thirty minutes after the exposure and as soon as possible after the rapid clinical evaluation, capillary and venous blood were drawn for the determination of the red and white blood cell count, hemoglobin, platelet and reticulocyte count, and smears made for the differential count of white blood cells. Ten cubic centimeters of venous blood were collected from each in a heparin containing tube for the estimation of blood Na^{24} and P^{32} activities induced by the neutron irradiation.

The patients were then transported to the Albert Merritt Billings Hospital of the University of Chicago and hospitalized on the service of Dr. Leon O. Jacobson. Since at this time the magnitude of the radiation exposure was not known, the patients were placed at absolute bed rest. All urine and fecal samples were saved for various subsequent analyses.

The radiation dosage and dose distribution in gamma and neutron rep has been presented in the section of this report written by L. C. Marinelli. As reference points, the following will serve as general indications of comparative dosages, being the average gamma exposures (as measured in air) distributed to the trunk. The reference names are shown here, although patient numbers will be used in this section.

Patient #1:	136 rep	(Art)
Patient #2:	127 rep	(Bill)
Patient #3:	60 rep	(Carl)
Patient #4:	9 rep	(Don)

There follow the case histories of the patients, the laboratory studies, and a summarization with conclusions.

CASE HISTORIESPatient #1

White male, age 31 years. On admission to the hospital the patient's temperature was 37.4°C., pulse 102, respirations 20, and blood pressure 140/80.

The patient was a well developed, well nourished white male, alert and cooperative, appearing moderately apprehensive but in no other apparent distress. The physical findings were all within normal limits except for a mild erythema of the face and neck. The patient stated that he had been exposed to sunlight over the weekend and that the erythema had been present before the exposure to ionizing radiation.

Several hours after admission, the patient had one episode of nausea accompanied by vomiting. Following emesis the nausea did not reappear and the patient ate a hearty breakfast the next morning. During the remainder of his sixteen-day hospitalization he was asymptomatic. The erythema of the face and neck subsided and at no time subsequently has there appeared erythema of the soles of the feet, the hands, or the face, the portions of the patient's body closest to the radiation source, nor has epilation occurred. The patient was discharged on the 16th day.

Following discharge from the hospital the patient rested at home for an additional week. He returned to his work at the Laboratory on the 23rd day after the radiation accident and has continued to feel well. No erythema or epilation developed, and no changes in the rate of growth of the finger or toe nails is apparent. Hematologic studies have been done at regular intervals and will continue. Another sperm count was repeated at eight weeks after the radiation exposure.

Patient #2

White male, age 30 years. On admission to the hospital the patient's temperature was 36.9°C., pulse 100, respirations 20, and blood pressure 122/70.

The patient was a well developed, well nourished white male, alert and cooperative and in no apparent distress. The physical examination revealed only findings within the limits of normal.

During hospitalization the patient remained completely asymptomatic and afebrile. His appetite was at all times good and there was no nausea or vomiting. None of the usual symptoms of "radiation sickness" were present in this patient and he was discharged from the hospital on the 16th hospital day.

This patient also returned to his duties on the 23rd day after irradiation and has remained asymptomatic and without physical findings. On July 30, 1952 he transferred his activities to another project within the AEC and is being followed by physicians there. There occurred no epilation or skin erythema.

Patient #3

White female, age 49 years. On admission to the hospital the patient's temperature was 36.0°C., pulse 82, respirations 20, and blood pressure 105/50.

The patient was a well developed, well nourished white female, alert and cooperative and in no apparent distress. The physical examination revealed only findings within the limits of normal.

On the third hospital day the patient vomited on several occasions and had four loose stools. However, these symptoms rapidly disappeared on a liquid and bland diet and did not recur. It was our clinical impression that this was a manifestation of anxiety and tension rather than a display of "radiation sickness." Otherwise, with the exception of occasional headaches, the patient remained afebrile and asymptomatic throughout her hospital stay, and she was discharged from the hospital on the 16th hospital day.

Following discharge from the hospital the patient noted the persistence of a moderate degree of fatigue and tension. She returned to her duties on July 7, 1952, 34 days after the radiation exposure and has felt well subsequently. No epilation or skin erythema was noted.

Patient #4

White male, age 29 years. On admission to the hospital, the patient's temperature was 36.8°C., pulse 80, respirations 20, and blood pressure 140/85.

The patient was a well developed, overnourished white male, alert and cooperative, and in no apparent distress. The physical examination revealed only findings within the limits of normal.

The patient remained completely asymptomatic and afebrile. He had an excellent appetite, at no time noted any subjective deviation from his usual state of well being, and was discharged from the hospital on the 16th day.

The patient has continued to be asymptomatic, felt very well, and returned to work on the 23rd day after the radiation incident. On the 15th day after exposure, fundiscopic examination revealed a very small, flame-shaped hemorrhage immediately inferior to the limbus of the optic disc in

the right eye. Repeat examination a month later demonstrated normal appearing fundi with no evidence apparent of the site of the previous hemorrhage. No generalized bleeding tendency was noted and no petechiae or suggilations were observed. Epilation and erythema were not seen. A second semen analysis was done eight weeks after the radiation exposure.

LABORATORY DATA.

During the hospitalization, the following studies were done on the patients:

Analysis of daily 24 hour urine samples for Na^{24} and P^{32} excretion; excretion of amino acids; and coproporphyrins (done by Dr. Henry Koch of the Sloan-Kettering Institute of New York City).

Analysis of daily fecal samples for coproporphyrins (by Dr. Koch) and for fission products.

Daily hematologic study of the red cell count, hemoglobin, hematocrit, white cell count and differential count, platelet count, sedimentation rate, reticulocyte count, bleeding and coagulation times.

Bone marrow biopsy done on the 11th day.

E. N. T. consultation.

Slit lamp microscopy of the refracting media of the eyes as a base line for future reference.

Psychometric and personality inventory studies done by Dr. Ward Halstead, Professor of Psychology in the Department of Medicine of the University of Chicago and utilizing his battery of tests of the integrative functions of the frontal lobes of the cerebrum.

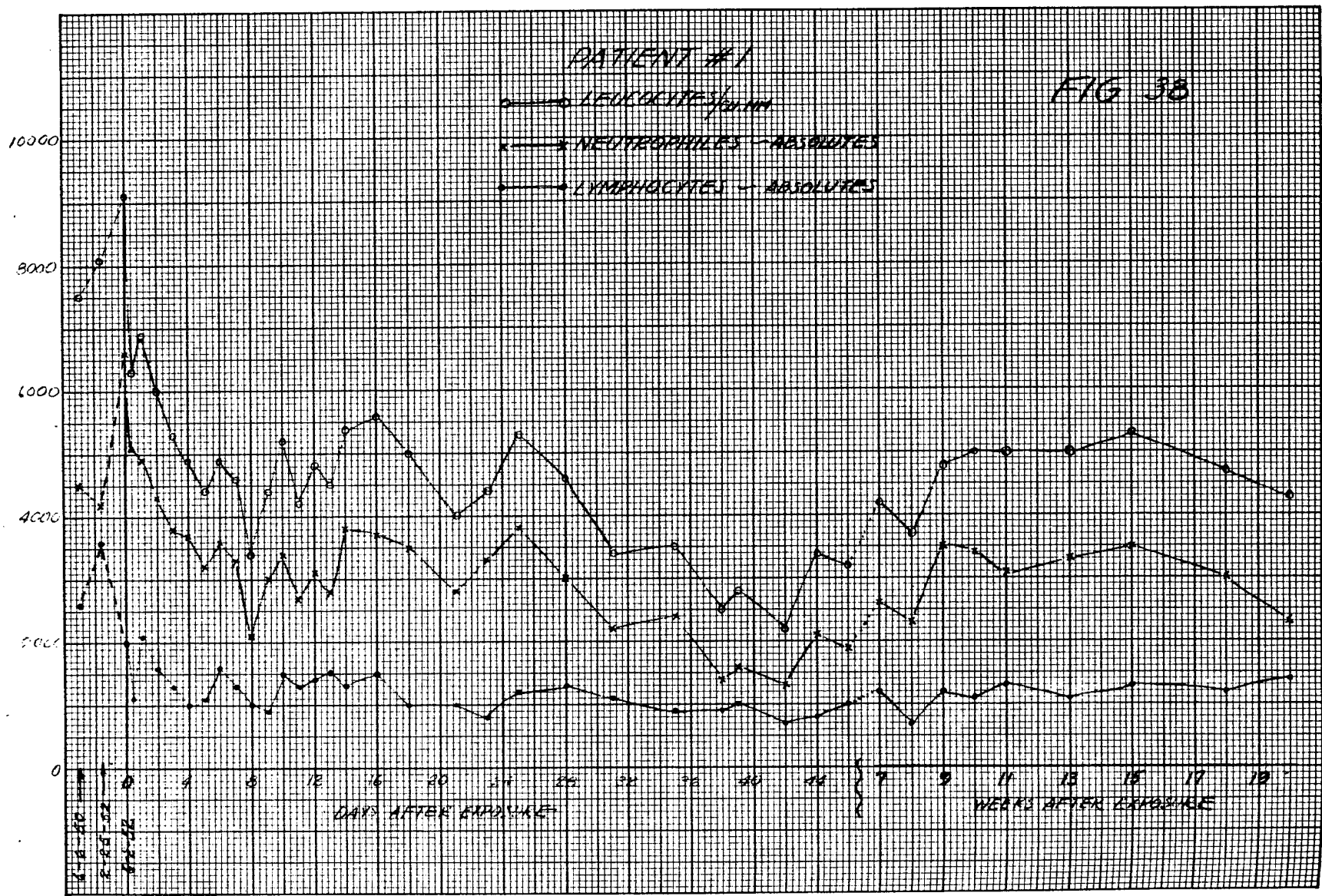
Semen examination and sperm count done on the 14th day on the male patients.

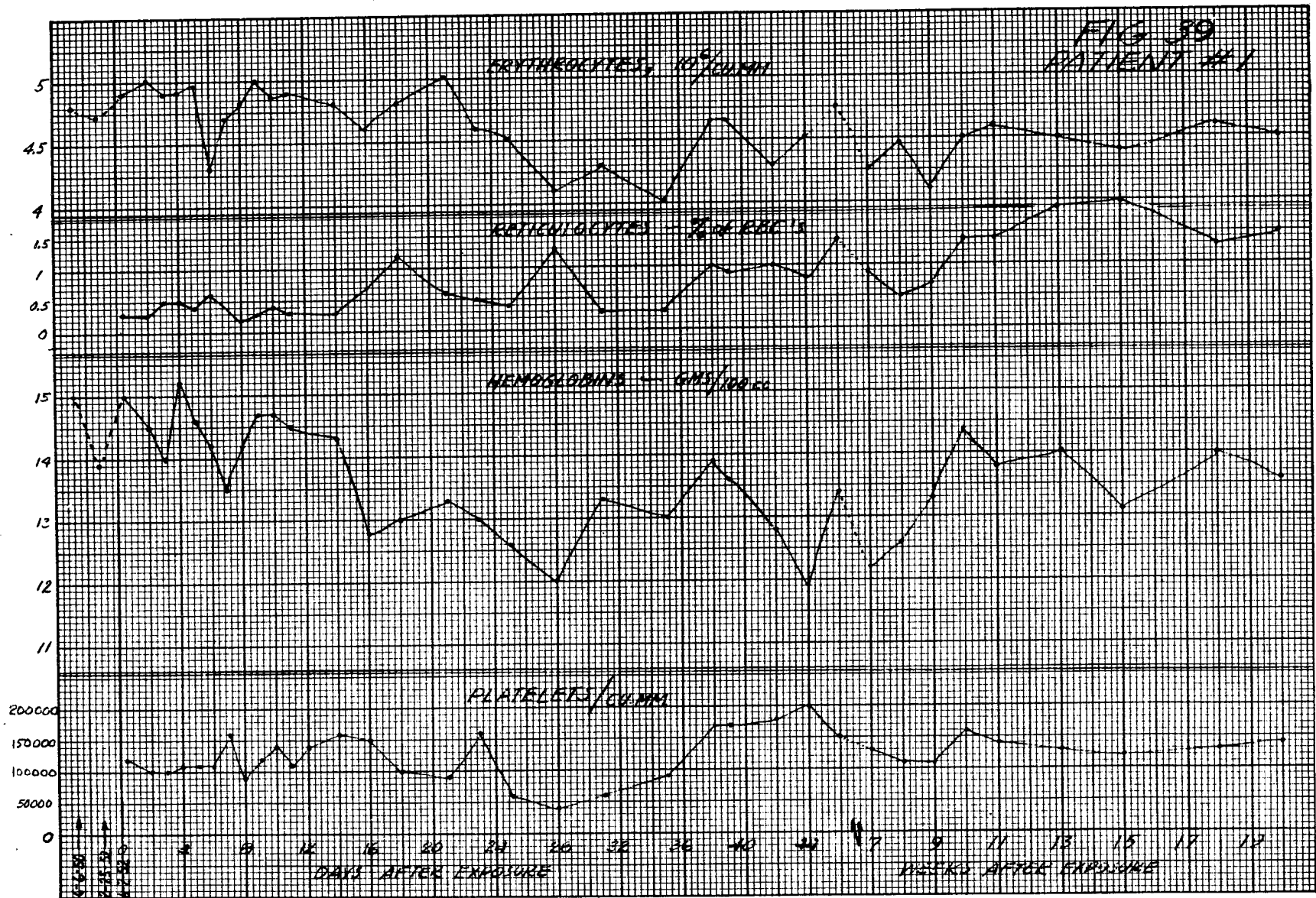
HEMATOLOGICAL STUDIES:

These studies were made by Miss Ellen Skirmont of the ANL Health Services Division and are summarized in Figures 38 thru 45 as follows:

- Figure 38 Total leukocyte counts, absolute neutrophil and lymphocyte counts with pre-radiation levels and data to 20 weeks post-radiation done on Patient #1.
- Figure 39 Erythrocyte, reticulocyte, platelet counts and hemoglobin determination with pre-radiation levels and data to 20 weeks post-radiation done on Patient #1.
- Figure 40 Total leukocyte counts, absolute neutrophil and lymphocyte counts with pre-radiation levels and data to 8 weeks post-radiation done on Patient #2.
- Figure 41 Erythrocyte, reticulocyte, platelet counts and hemoglobin determination with pre-radiation levels and data to 8 weeks post-radiation done on Patient #2.
- Figure 42 Total leukocyte counts, absolute neutrophil and lymphocyte counts with pre-radiation levels and data to 20 weeks post-radiation done on Patient #3.
- Figure 43 Erythrocyte, reticulocyte, platelet counts and hemoglobin determination with pre-radiation levels and data to 20 weeks post-radiation done on Patient #3.
- Figure 44 Total leukocyte counts, absolute neutrophil and lymphocyte counts with pre-radiation levels and data to 19 weeks post-radiation done on Patient #4.
- Figure 45 Erythrocyte, reticulocyte, platelet counts and hemoglobin determination with pre-radiation levels and data to 19 weeks post-radiation done on Patient #4.

Hematologic studies on Patient #2 subsequent to his transfer to another Laboratory are not presently available. The total white blood counts of Patients #3 and #4 have returned to the pre-irradiation levels. Patient #1 continues to have a white cell count significantly lower than the pre-irradiation levels. From the diagnostic standpoint, a white cell count done on one patient, excepting Patient #1, on any one day following irradiation was not strikingly significant from the clinical standpoint as an indicator of radiation overexposure. It is only through repeated counts in comparison with previous base line studies that the trend toward diminution of the white count becomes apparent and indicative of the overexposure. More striking have





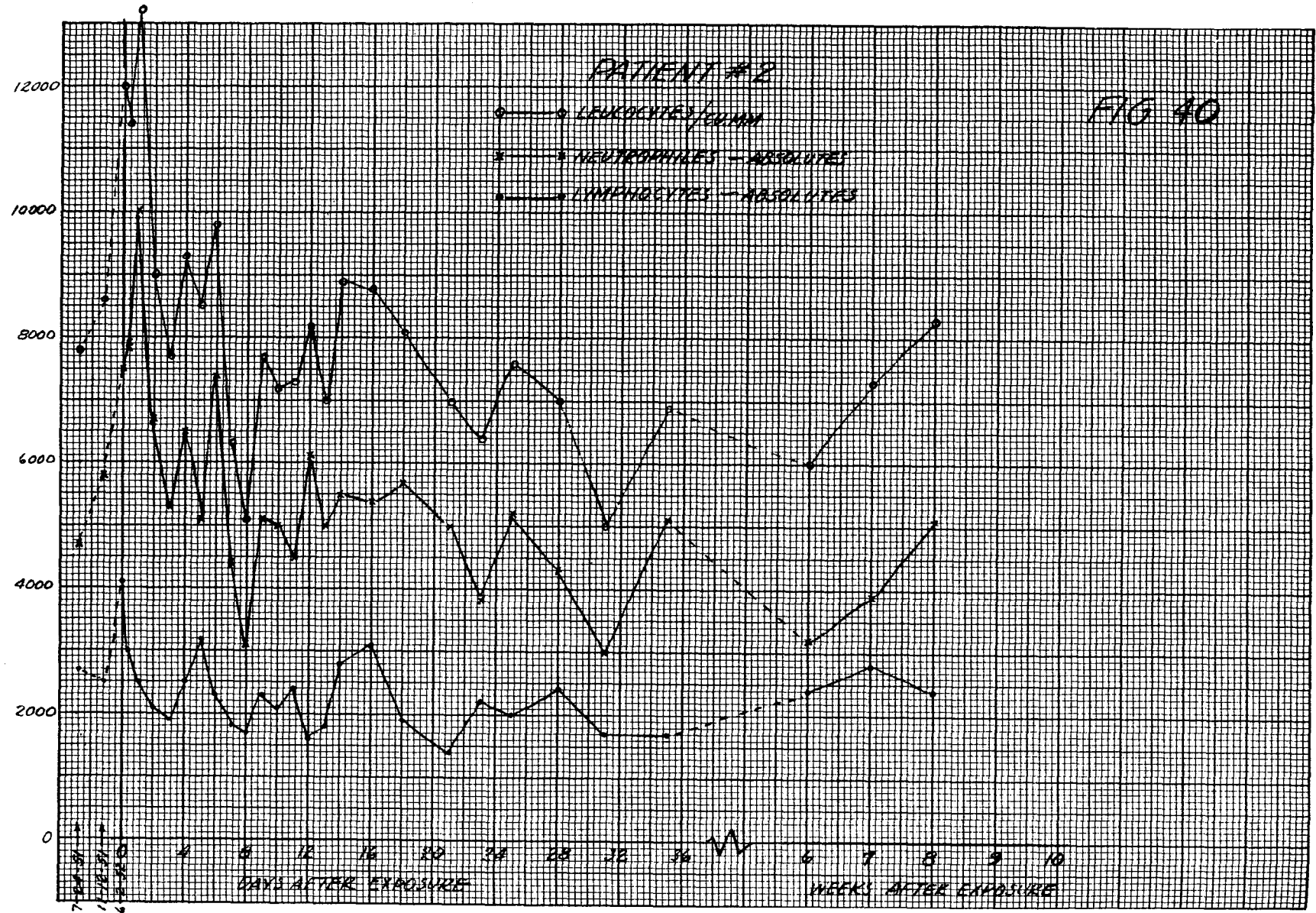
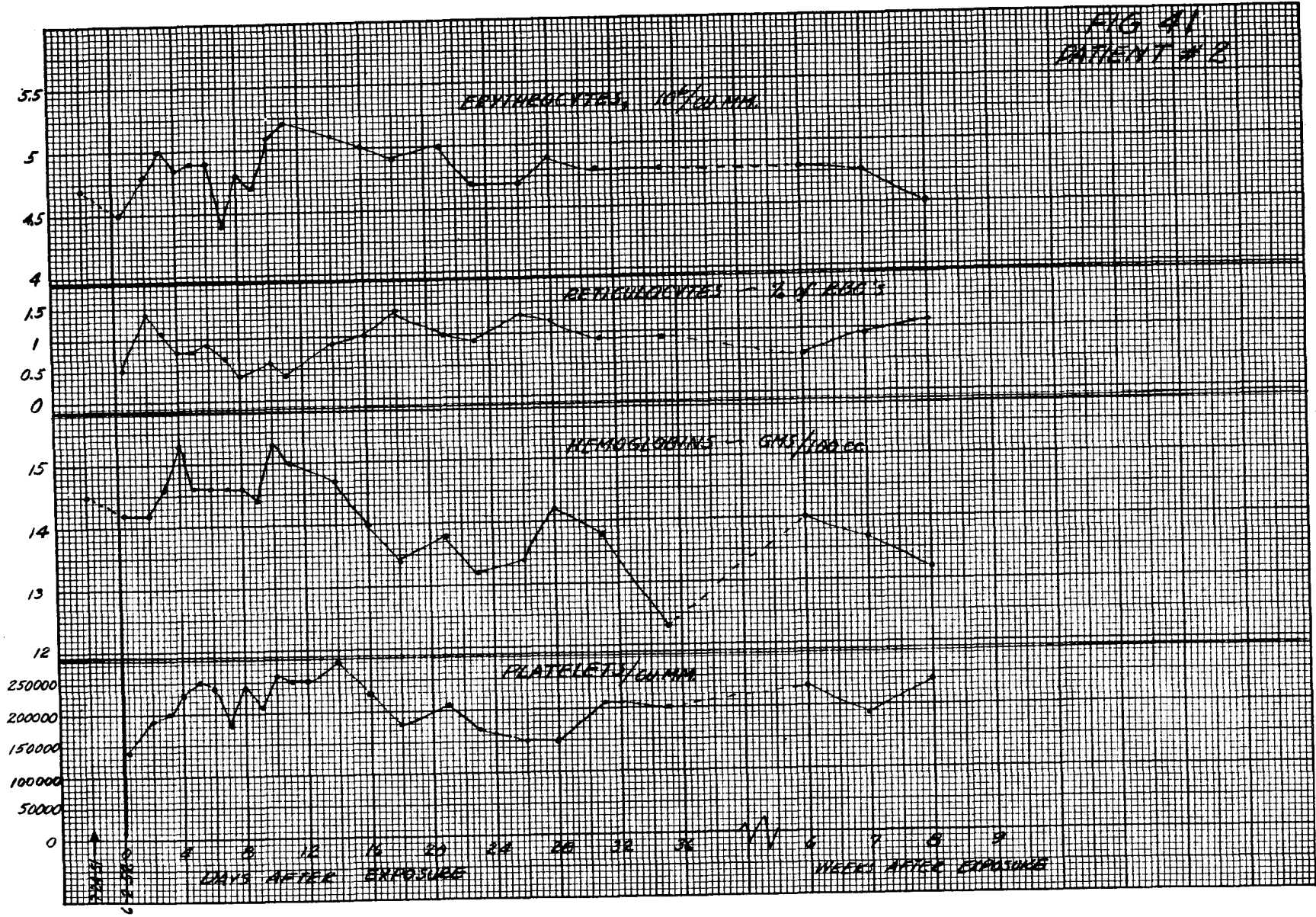


FIG 41
PATIENT # 2



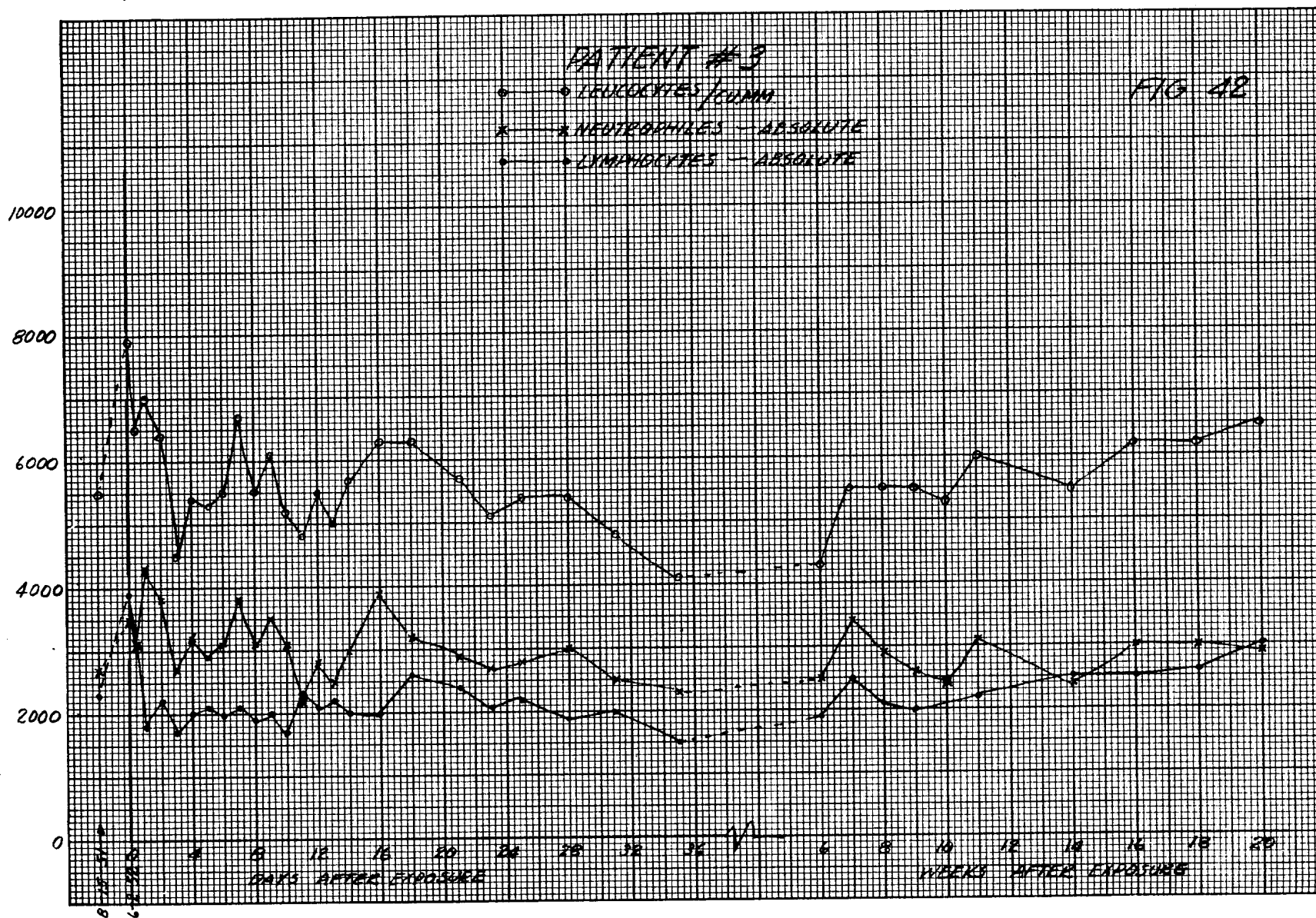
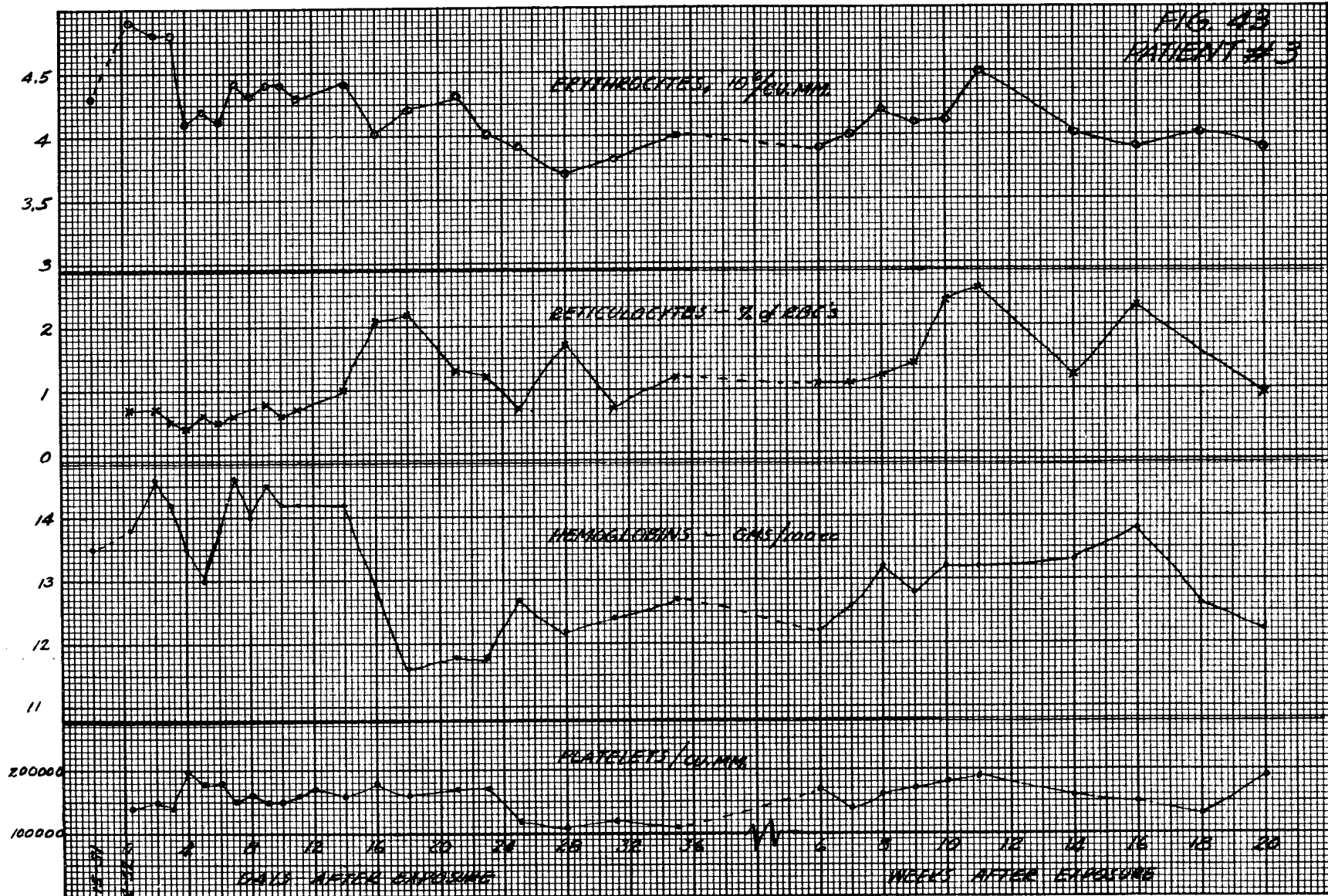
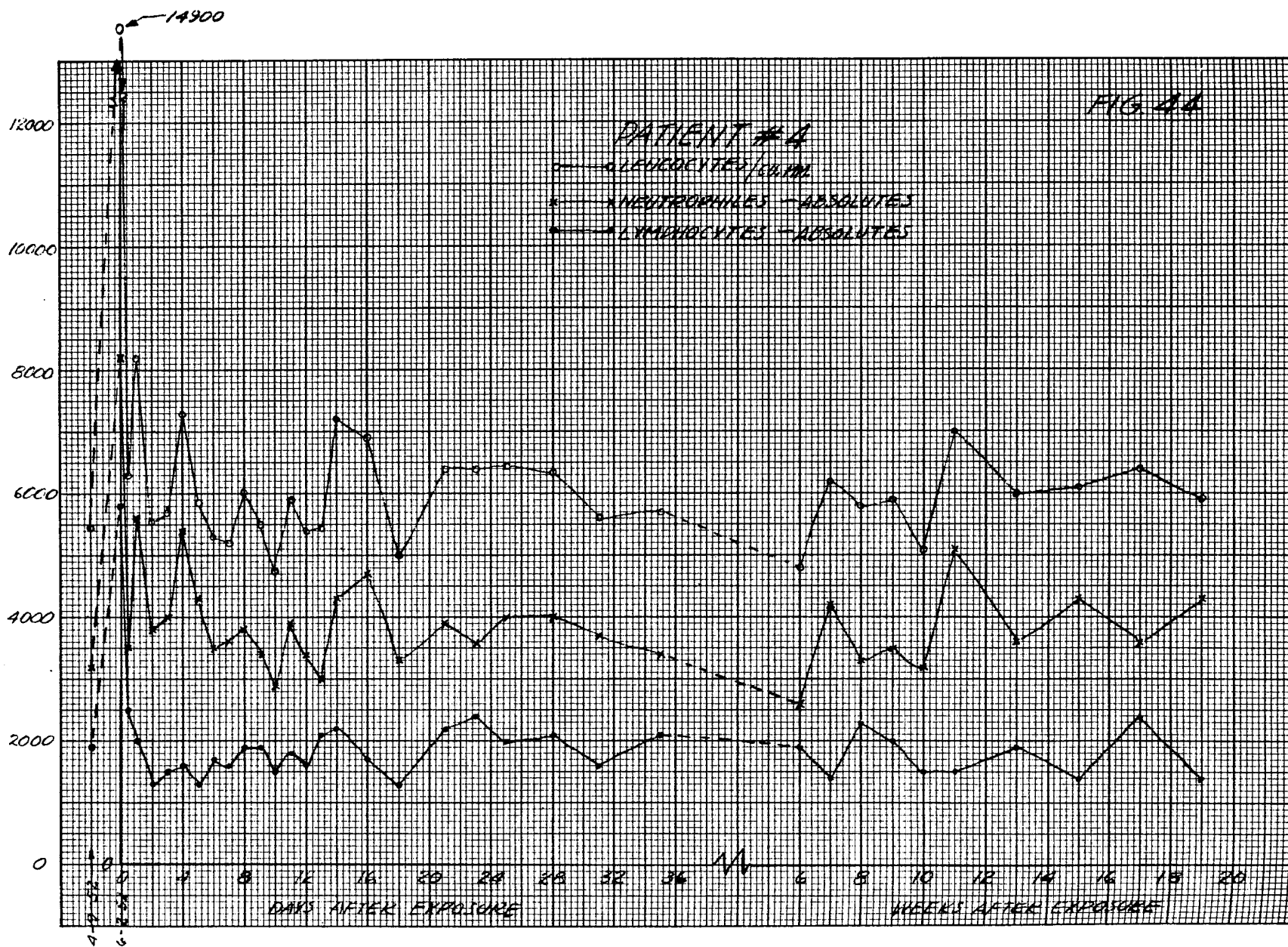
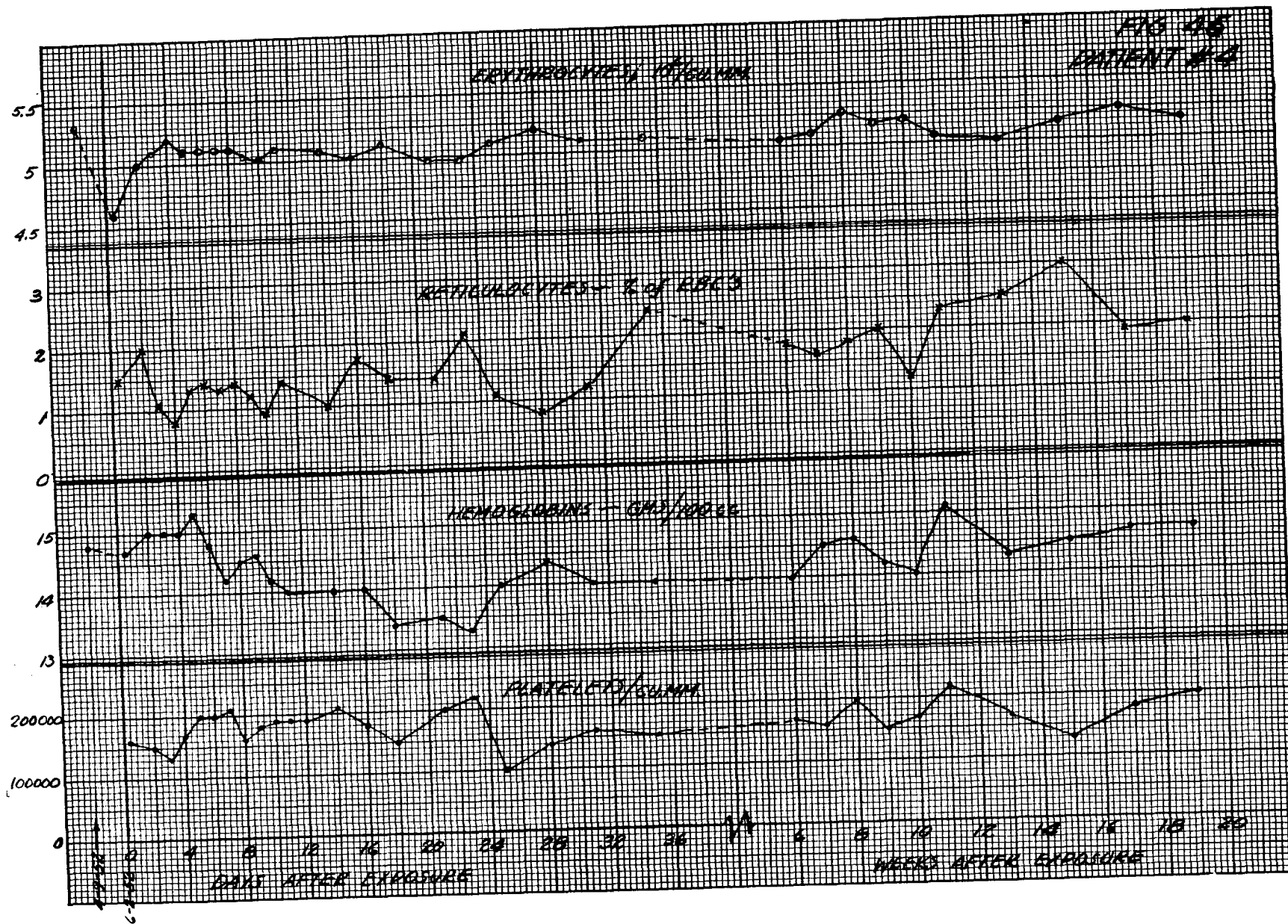


FIG. 43
PATIENT #3



8
6





been the cytologic changes observed in the white blood cells. These will be reported in detail in the open literature, and include greatly increased granularity of the cytoplasm of the lymphocytes, immature forms, cells with karyorrhexis, and the presence of inclusion bodies in the cytoplasm of the lymphocytes.

Bilobed lymphocytes were seen with the following frequency:

	<u>Total Cells Counted on Blood Smears</u>	<u>Bilobed Lymphocytes</u>
Patient #1	11,400	2
Patient #2	8,100	3
Patient #3	11,400	1
Patient #4	10,200	1
Total	41,100	7

BONE MARROW BIOPSIES:

- Patient #1 Done on the 11th day post-irradiation.
Report: Normal marrow.
- Patient #2 Done on the 14th day post-irradiation.
Report: Erythroblasts appear decreased. Will do sections for further evaluation.
- Patient #3 Done on the 11th day post-irradiation.
Report: Normal marrow.
- Patient #4 Done of the 11th day post-irradiation.
Report: Normal marrow.

AMINO ACID EXCRETION:

The work on amino acid excretion was done by Miss E. Katz of the ANL Health Services Division. The detailed findings will be published subsequently. The following is a preliminary summary of the findings.

Urinary amino acid excretion was studied utilizing paper partition chromatography. All four patients showed a consistent daily increase in the amounts of amino acids excreted following the accident. The results are in agreement with those found previously in a study of aminoaciduria in nine other workers also accidentally exposed to radiation.¹⁸

Comparison by this laboratory of paper chromatographic studies of amino acids in the urine of normal persons with values obtained by microbiological methods¹⁹ shows agreement of the two methods. Using the chromatographic method of analysis, the following amino acids are usually found in the urine of normal patients: glycine, alanine, and taurine, in amounts of approximately 0.2 mg/ml, and traces of leucine and valine (0.01 mg/ml). Although it is possible to show the presence of other normally occurring amino acids, under conditions of this work (using a 25 μ l aliquot of a 24-hour sample) only the above amino acids are found. In the case of the four patients under study, the following free amino acids have been tentatively identified:* cystine, ascorbic acid, aspartic acid, glutamic acid, serine, glycine, taurine, threonine, alanine, histidine, leucine, valine, tryptophane, and possibly proline, arginine, phenylalanine, lysine, and glutamine. Each patient did not show all of these amino acids. The quantities of amino acids excreted in excess varied from two to twenty times normal amounts.

In all cases, glycine and taurine showed the greatest excretion. There was a marked increase over normal amounts in amino acids such as cystine and glutamic acid, as well as a great increase in the number of amino acids excreted the day following the initial exposure. In all cases, abnormal excretion regarding both number and quantity of amino acids persisted as long as nine days after exposure. Three of the patients showed abnormal excretion two weeks after the accident.

In Patient #1 there was an increase in the number of amino acids excreted the day following exposure, followed by a drop in the total number and quantities of certain amino acids, but a peak in the amount of excretion was reached on the sixth day after exposure, in agreement with previous findings.¹⁸

The greatest quantity of amino acids excreted, however, was displayed by a patient who did not receive the greatest radiation exposure (Patient #3). Here also a peak was reached on the sixth day following exposure, but, in disagreement with previous findings, excretion did not match exposure. These samples, however, were only partial 24-hour samples. If one assumes equal quantities of amino acids excreted per unit time, this individual excreted greater amounts of amino acid than the amounts reported in the literature in cases of renal lesions, Wilson's disease, and severe "Lysol" burn with accompanying uremia and neurological disturbances. If, on the other hand, one assumes variable excretion, the per diem aminoaciduria exhibited by this patient would probably be less than that shown by the patient with the greatest exposure.

No new theories concerning the significance of aminoaciduria after irradiation are presented. Statements already presented¹⁸ indicate that defects in utilization of amino acids along with increased protein breakdown may be responsible for the increased excretion.

*Full studies have not yet been completed.

OPHTHALMOSCOPY:

No ocular pathology was noted in any of the patients except for a slight injection of the bulbar conjunctiva in Patient #1.

Slit lamp microscopy of the refracting media of the eyes will be repeated on all patients at six monthly intervals.

PSYCHOMETRIC STUDIES:

These will not be reported in detail in this communication except to indicate that on the 2nd or 3rd day after irradiation no impairment of frontal lobe function attributable to acute exposure to radiation was observed.

The personality profile studies yield clues which indicate that an extension of these types of studies as an aid in the selection of personnel for experiments involving such instruments as critical assemblies may be helpful in the prevention of similar serious accidents.

SEMEN STUDIES:

The studies on the effect of radiation on spermatogenesis and motility in these patients will be reported in the medical literature.

SUMMARY AND CONCLUSIONS

The clinical syndrome of "radiation sickness" was not seen in any of the patients. Except for the moderate tension state induced in these individuals during the first 24 hours by the realization that they had been exposed to unknown, and possibly lethal, quantities of radiation, they were not at any time clinically ill.

The hematologic data do not demonstrate as precipitous or as marked a drop in the absolute lymphocyte count or total white count as might be expected from animal studies or the data from the Los Alamos patients, but the rate and magnitude of fall is roughly proportional to the levels of exposure. The cytologic changes would appear to be of value as a sensitive indicator of radiation exposure in these dose ranges.

Preliminary studies on these patients, which will be extended in experimental animals, indicate that aminoaciduria may be a significantly sensitive early indicator of radiation overexposure.

It is suggested from these studies that technics be developed and employed for the proper selection of personnel in the important area of research with critical assemblies.

The complete data from these studies will be published in the open medical literature as soon as possible. This report is to be considered as incomplete and preliminary and is presented in the classified literature for the purpose of early dissemination of pertinent information to physicians and biologists concerned with these specific problems within the AEC laboratories.

The compiler of this section is indebted to the following staff members for their part in the investigation: Dr. Leon O. Jacobson, Dr. Lawrence Myers, Jr., Miss Elaine Katz, Miss Ellen Skirmont, and Dr. Earl Hathaway and their associates of the Argonne National Laboratory as well as the many members of the clinical staff and faculty of the Department of Medicine of the University of Chicago.

APPENDICES

- A. FUEL COMPONENT DESCRIPTION
- B. RADIOACTIVITY MEASUREMENTS ON WHOLE BLOOD
- C. IN VIVO MEASUREMENTS OF GAMMA RAY ACTIVITY
- D. FILM BADGE DOSES

APPENDIX AFUEL COMPONENT DESCRIPTION

The accompanying description prepared by F. C. Beyer has been excerpted from ANL-4770 for reference.

The standard fuel assembly as shown in Figure 46 has been in use since April 24, 1952. The assembly shown contains six (6) zirconium strips and seven (7) fuel strips as compared to the assemblies used previous to the above date, which contained five (5) zirconium strips and seven (7) fuel strips. The six zirconium plates are each 0.910 in. wide x 0.110 in. thick and are fastened in polystyrene end caps by polystyrene pins. The zirconium strips are uniformly spaced and occupy 60.06% of the volume of the elemental core section, which is 43 in. long and has a cross-sectional area of 1 square in. The seven fuel strips each contain on the average 3.206 grams of U²³⁵ in oxide form of -325 mesh particles (93.2% enrichment) uniformly dispersed in polystyrene. The nominal strip size is 0.013 in. x 0.85 in. x 43.00 in. Data pertaining to the standard fuel assembly is tabulated in Table A-I.

Table A-I

STANDARD FUEL ASSEMBLY

Total core volume of element	704.6 cc	
Zr volume	423.2 cc	60%
Polystyrene volume on strips	50.4 cc	7.15% } 7.71%
Uranium oxide volume	3.9 cc	
Polystyrene spacers	0.3 cc	
Water volume	226.8 cc	32.2
Weight of Zr	2742 g	
Weight of U ²³⁵	22.44 g	
Weight of polystyrene in strips	52.3 g	
Weight of mixed uranium oxides	28.5 g	
U ²³⁵ concentration	0.0318 g/cc	

Control rod assembly No. 16 is shown in Figure 47. This is the type of control rod assembly that was in the reactor on June 2, 1952. Data pertaining to this assembly is tabulated in Table A-II.

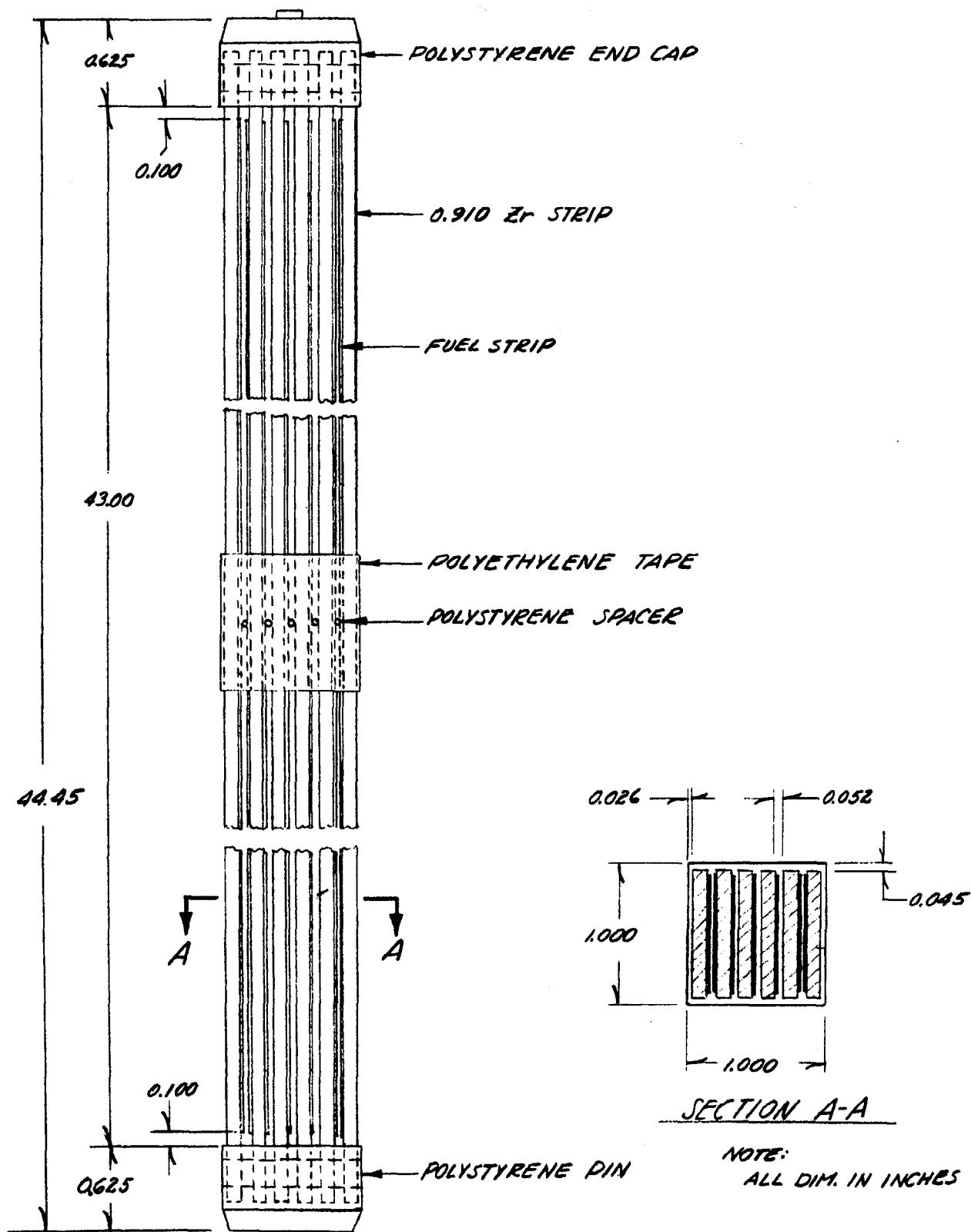


FIG 46
STANDARD FUEL ASSEMBLY

Table A-II

CONTROL ROD ASSEMBLY NO. 16

I. Zirconium Strip	
A. No. of 0.910 strips	50
B. No. of 0.710 strips	13
C. No. of 0.510 strips	2
II. Fuel Strips	
A. No. of wide strips	62
B. No. of intermediate strips	13
C. No. of narrow strips	2
D. Total weight of fuel	235 g

APPENDIX B

RADIOACTIVITY MEASUREMENTS OF WHOLE BLOOD

Two sets of measurements were made independently by A. F. Stehney of the ANL Radiological Physics Division and by Laurence S. Meyers, Jr., of the Health Services Division on whole blood samples taken from the patients. Using the disintegrations per minute per milligram of Na extrapolated to zero time the thermal neutron exposures were estimated.

A. F. Stehney

For each sample, 11 ml of whole blood were wet-ashed with HNO₃ to inorganic salts. The insoluble residue was removed by centrifugation and the supernatant was diluted to 25 ml. 20 ml aliquots were evaporated and dried on stainless steel planchets, and the remainder used for flame photometric determinations of Na and K. Decay curves were taken of the activity of each sample in order to correct for the natural K⁴⁰ content of blood. An activity of about 16 h half-life and a long-lived activity were observed for each sample. These activities were assumed to be 14.9 h-Na²⁴ and K⁴⁰ respectively for the data below in which the activities were calculated for 1600 on 6/2/52.

Subject	mg per ml		dpm per ml		dpm Na ²⁴ per mg Na	dpm K ⁴⁰ per mg K	Estimated Neutron Exposure
	Na	K	Na ²⁴	K ⁴⁰			
Art	1.8	1.7	91	3.8	51	2.3	6.7 x 10 ⁹
Bill	1.9	1.9	82	3.8	44	2.0	6.0 x 10 ⁹
Don	2.0	1.7	25	3.4	13	2.0	1.8 x 10 ⁹
Carl	1.8	1.8	20	3.0	11	1.7	1.47 x 10 ⁹

The columns headed "mg per ml" and "dpm per ml" were calculated on the basis of the original 11 ml whole blood samples, for comparison with the results of part B. Only the values of "dpm Na²⁴ per mg Na" are needed for calculating the neutron irradiation and those values are independent of possible losses of Na during the chemical processing of the blood. However, calculations indicate that 10% of the activity listed as Na²⁴ may be 12.4 h-K⁴². There are 1.5 to 2.0 beta emissions of K⁴⁰ per mg of natural K.

The neutron exposures were estimated by G. Ringo of ANL Physics Division.

L. S. Meyers, Jr.

The following results were obtained on the whole blood samples.

<u>Subject</u>	<u>Estimated dis/min/cc blood at t = 0</u>	<u>meq of Na per liter</u>	<u>dis/min/mg Na at t = 0</u>	<u>Estimated Neutron Exposure</u>
Art	110	83	57.6	5.6×10^9
Bill	76	80	41.3	4.0×10^9
Carl	25	82	13.2	1.3×10^9
Don	23	83	12.0	1.2×10^9

After being corrected for background and long-lived components, the half life of the whole blood activity was about 12 hours, indicating considerable contributions from components having a half life shorter than Na^{24} (14.8h). In making the estimate of neutron exposure, it was assumed that the average cross section was 5.0 barns and that all short-lived activity is Na^{24} . This estimate could be in error by 100%.

APPENDIX CIN VIVO MEASUREMENTS OF GAMMA RAY ACTIVITY

On June 4th and 5th the gamma ray activity of Art was measured by L. D. Marinelli at Albert Merritt Billings Hospital in a lead lined room (9 mm) of the X-Ray Therapy Department. Readings were taken with a portable scintillation counter while the patient was seated in the "Standard" chair used for determinations of this sort. The crystal was placed 64 cm above the floor and 10 cm from the center of the back of the chair. Readings from a 1.30 μc (4 P.M., June 2nd) source of Na^{24} were taken in air at distance of 25 cm distance. The ratio of the net readings from the patient to the net readings from the source were:

$$\text{June 4 (3:45 P.M.)} = \frac{191}{4620} = 0.0414$$

Average $0.0405 \pm 10\%$

$$\text{June 5 (11:36 A.M.)} = \frac{70}{1770} = 0.0396$$

Three volunteers who had ingested a known amount of Na^{24} had been measured with the same arrangement at Site B (24 hours after ingestion) and compared to the counting rate from an equal quantity of Na^{24} at 0.25 meters. The ratio of the readings, patient to aliquot, were:

$$(A) \quad (96 \text{ lb}) = 0.49$$

$$(B) \quad (155 \text{ lb}) = 0.42$$

$$(C) \quad (180 \text{ lb}) = 0.39$$

Since Art's weight is comparable to (C) the factor 0.39 applies. Thus,

$$\text{Art's content} = \frac{1.3 \times 0.0405}{0.39} = 1.35 \mu\text{c}$$

On the assumption of 105 gr of Na^{23} per 70 Kg man¹⁶ the specific activity can be calculated as:

$$\text{Na}^{24}/\text{Na}^{23} = 1.35 \times 3.7 \times 10^4 \times 60/1.2 \times 10^5 = 25 \text{ d/m/mg Na}^{23}$$

If the Na^{23} content is, instead computed according to Kleiner²⁰ (as 60 gr for a 70 Kg man) the result is

$$\text{Na}^{24}/\text{Na}^{23} = 1.35 \times 3.7 \times 10^4 \times 60/68.5 \times 10^4 = 44 \text{ d/m/mg Na}^{23}$$

in fair agreement with direct measurements from the plasma (Appendix B). No further elaboration of this result is possible because two other considerable factors enter into our estimation. One is the effect of K^{42} (probably small since both activation cross section and disintegration scheme militate against our counting it) and the other, more important, due to the fact that, under the conditions of neutron activation, Na^{24} is not distributed in manner identical to that following complete diffusion of ingested Na^{24} . In the latter case deposition in the bone is uniform whereas in the former bone activation could be located preponderately at the front of the body. This fact would tend to make our readings low, as is indeed the case.

No measurable activity was found in the thyroid since the short-lived gaseous fission products ingested by inhalation and transferred to the thyroid had all decayed. Early thyroid measurements on several personnel at Building 316 showed the presence of the short-lived iodine.

On the basis of the observations it is estimated that at the time of the accident the net count, under the conditions of test, would have been 1810 c/m. In view of the estimate of the thermal exposure (10^9 n/cm²) and of the maximum permissible level (2.8×10^8 for 40 hr week), it is obvious that a single exposure to thermal neutrons of as little as 0.1 the weekly m.p.l. could be easily detected if precautions are taken to minimize the effect of background activity in the crystal. It seems, therefore, that personnel monitoring of thermal neutron exposure by this means is feasible since the sensitivity of the set-up could be greatly improved.

APPENDIX D

FILM BADGE DOSES

The film badge doses were estimated by I. B. Berlmann, H. F. Lucas, and H. A. May using two methods. Although this work has been reported in the open literature,¹¹ it seems useful to reproduce it here in more detail.

DENSITOMETRIC METHOD

The film badges worn by three individuals involved in the incident were given a normal processing: Development in duPont concentrated liquid developer for 5 min. at $(18 \pm 1/4)^\circ\text{C}$; Photographic densities were exhibited well beyond the range employed by the film badge group for routine monitoring. It was evident that special methods would have to be employed to obtain any information from them.

A series of calibration films were exposed and processed, to determine the response of the monitoring film to filtered 250 kv X-rays and to the gamma and neutron flux from a 0.93 gm Ra-Be source, in the exposure range 10 roentgens to 500 roentgens. It was found that the duPont type 508 sensitive films reached a maximum density of 3.4 - 3.6. No reversal was apparent over this exposure range. Since the three unknown films of this emulsion all read around density 3.5, no information could be obtained from them.

The duPont type 510 insensitive films develop a much greater density, quickly exceeding a density of 6, which is the maximum readable with the Ansco-Sweet densitometer. Readings in this range, however, suggested that if we could extend the range of density determination by a factor of two, we should be able to determine exposures to approximately 200 roentgens, and thus possibly read one or more of the unknowns.

The fact that these films are coated with emulsion on both sides of the film base suggested a means of extending their range. A simple device was constructed to allow a small, well defined circular area of the emulsion to be removed, without damaging the rest of the film. This was done by softening the emulsion at the unprotected spot with NaOH, approximately 1N, at a temperature of from 50 to 75°C. The emulsion could then be loosened from the film base by swabbing with a small bristle brush or cotton swab, then washed and dried. A spot of emulsion approximately 4.5 mm in diameter was removed in this manner from each side of the film, at adjacent but not overlapping spots. The total density is then the sum of densitometer readings for each emulsion layer, less a small correction for the film base.

A calibration was prepared (Figure 36) which shows a relationship between exposure and density that is linear with exposure to at least 200r. Agreement between X-ray and radium gamma calibration is somewhat poorer than expected, with evidence of some as yet undetermined error in the X-ray calibration. For this reason only the gamma calibration data is shown.

The photographic blackening of the three disaster films, worn by Art, Bill and Carl was determined to be equivalent to that produced by radium gamma dosages of 181r, 137r and 68r, respectively.

NEUTRON ACTIVATION METHOD

An additional method has been developed for determining the amount of radiation received by du Pont film #510, the "insensitive" emulsion of the pair used in the film badge packet #552. At low levels, density 3.0, the densitometer is a very satisfactory instrument for reading films, but it is not effective for use on film with densities >6.0 due to high exposure. As a result of the new method, determination of radiation exposure is limited only by the "film qualities," i.e., among other things that the curve of density vs exposure is not too flat, and not by the reading instrument. This report clearly demonstrates the method's usefulness to densities greater than 11.8. The new method is based on the fact that the silver content of exposed and developed film can be determined by neutron activation. It is well established that the silver which remains on developed film is function of radiation exposure.

Ag^{107} has a high cross section to slow neutrons, and after activation has a short half-life 2.3 m Ag^{108} . This combination of high cross section and short half-life is very convenient. It allows short irradiation times which result in a high counting rate with essentially no increase in the background of the film due to impurities present in the film.

The procedure, as developed, is quite straightforward although extreme care is necessary to produce exactly the same conditions during activation and counting of each sample. Each film was inserted individually into the Argonne Standard Graphite Pile using Ra-Be source #38, each in the same position as the ones previous. Each film remained in the pile for (600 ± 2) seconds. The time used to remove the film from the source and place it in the counter was (80 ± 1) seconds. Each film was then counted for 900 seconds. This is almost six half-lives and gives the maximum number of counts obtainable. The background of the similarly treated blank film was subtracted and net number of counts was recorded.

The data obtained from a series of standard films is plotted in Figure 36. From 10 rep to 150 rep the curve is a straight line on a linear plot and from 150 rep to 300 rep the curve is a straight line on a logarithmic

plot. Using larger exposures more points on the curve are under investigation so as to establish the nature and useful range of the curve more fully.

In terms of an equivalent blackening of the film by gamma radiation (~ 0.8 Mev), as determined by using the foregoing method on the du Pont #510 emulsion from the Argonne standard type film badges worn by the operators, we find the following exposures:

Carl 68 rep \pm 8 rep

Bill 139 rep \pm 11 rep

Art 178 rep \pm 12 rep

REFERENCES

1. Brittan, R. O. and Associates, Experiments on Zero Power Reactor (ZPR-I), ANL-4684, August 24, 1951.
2. Brittan, R. O., Experiments on Zero Power Reactor I - Part II, ANL-4770, (in preparation).
3. Rossi and Staub, "Ionization Chambers and Counters," McGraw-Hill Book Company, 1949, pp. 192-197.
4. Rossi, H. H. and Failla, G., "Medical Physics," Yearbook Publishers Inc., Chicago, 1950, 2, p. 603.
5. Hurst, G. S., Ritchie, R. H., and Wilson, H. N., A Count Rate Method of Measuring Fast Neutron Tissue Dose, Rev. Sci. Instr. 22, No. 12, p. 981 (1951).
6. Taylor, J. J., Core Removal Shielding, WAPD-RM-59, June 21, 1951, p. 6.
7. Quarterly Report, December, 1951, January and February, 1952, Naval Reactor Program, ANL-4795.
8. Neustadt, M. and Cohen, E. R., Reactor Self Shielding, NAA-SR-12, April 20, 1950, p. 39.
9. Young, G. and Blizard, E. P., Gamma Rays from Fission and Fission Products, ORNL-420, November 17, 1949.
10. Snyder, W. S. and Powell, J. L., Absorption of γ -Rays, ORNL-421, March 14, 1950.
11. Division of Biological and Medical Research Quarterly Report for May, June, July, 1952, ANL-4840, p. 91.
12. Motz, J. W., Gamma-Ray Spectra of the Los Alamos Reactors, Phys. Rev. 86, 753 (1952).
13. Deutch, M. and Rotblatt, J., Investigation of Fission Gamma Rays, AECD-3179, 1944.
14. Metropolis, N. and Reitwiesner, W., Table of Atomic Masses, NP-1980, March 1950.

15. Prestwick, G. D., Colvin, T. H., and Hine, G. J., Average Energy of Secondary Electrons in Anthracene Dust, *Phys. Rev.* 87, 1030 (1952).
16. Recommendations of the International Committee on Radioactive Protection and of the International Committee on Radioactive Units, National Bureau of Standards Handbook No. 47, (1951).
17. Rossi, H. H., Status of Neutron Dosimetry, *Nucleonics* 10, No. 9, 26, September 1952.
18. Hempleman, L. H., et al, The Acute Radiation Syndrome, A Study of Nine Cases and a Review of the Problems, *Annals of Internal Medicine* 36, 439, 1952, Part I.
19. Harper, H. A., et al, Concentrations of Nineteen Amino Acids on Plasma and Urine of Fasting Normal Males, *Proc. Soc. Exptl. Biol. Med.* 80, 786, 1952.
20. Kleiner, I. S., *Human Biochemistry*, C. V. Mobsy Co., St Louis, 1945, p. 26.
21. Hurst, G. S., *Ra-Det*, Vol. 2, No. 4, p. 43 (1949).
22. Taylor, J. J., Submarine Thermal Reactor Shield Design, WAPD-23, January 1951, p. 32.
23. Naustadt, M. and Cohen, R., Reactor Self Shielding, NAA-SR-112, April 20, 1951, p. 16.